



Norwegian University of  
Science and Technology

# Development of a Multifunctional Snow Production Unit for Granåsen Ski Arena

**Sondre Bergtun Auganæs**  
**Synne Våge Opheim**

Master of Science in Engineering and ICT

Submission date: June 2018

Supervisor: Knut Einar Aasland, MTP

Co-supervisor: Bernhard Haver Vagle, SIAT

Norwegian University of Science and Technology  
Department of Mechanical and Industrial Engineering



# Preface

This master thesis was performed at the Department of Mechanical and Industrial Engineering (MTP) at NTNU during the spring 2018, and is written in cooperation with Centre for Sport Facilities and Technology (SIAT). The thesis addresses the development process of a multi-functional snow production unit for Granåsen Ski Arena, in connection with the upcoming development of the facility.

This thesis uses results from Auganæs & Opheim (2017), which was a pre-study for the master thesis. It should be mentioned that parts of the method description and snow theory is taken directly from the pre-study. The pre-study is available at MTP, NTNU.

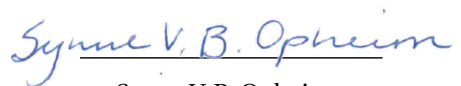
We would like to thank our academic supervisor Professor Knut Einar Aasland for great guidance during the work. Special thanks also to our co-supervisor from SIAT, Researcher Bernhard Haver Vagle, for his dedication to the project as well as helpful discussions and advice. Thanks to Pär Bengtsson from Skistar Åre, and the operators at Granåsen Arena, for welcoming us and for sharing their insights and experience with snowmaking.

Last, but not least, we would like to thank our friends and families for the encouragement and support they have provided through five years of engineering studies.

Trondheim, 05.06.2018



Sondre B. Auganæs



Synne V. B. Opheim

## Abstract

Through the last decades, climate changes have drastically affected the winters in Norway. The implications of the climate changes are shorter winter seasons with increased temperatures, which makes snow production more relevant than ever before. One of the most important arenas for cross-country skiing in Trøndelag is Granåsen Ski Arena. This arena is essential for both recreational sports as well as international sports events. In Granåsen Ski Arena, the snow is usually produced in big piles and moved into the tracks afterward. This process is both time and energy consuming. For Granåsen Ski Arena to satisfy the future snow demands a new production system is needed. From the efficiency issues, the idea of the new, multifunctional and automated snow production unit located along the track arose. In this thesis, the development process of such a unit is started.

Automated snow production units exist today, but few are designed for narrow cross-country tracks. The focus of the development process has been to increase the efficiency of the snow-making unit; by introducing automatic adjustment of the snow production, according to input data from weather stations. This approach offers the possibility of increasing the percentage of produced snow that fall within the tracks.

To be able to optimize the unit for narrow cross-country tracks, a model of the snow spray from lances is developed and used to test and refine concepts. Each sprayed water droplet has a size and an initial velocity. Euler's method is used to estimate the path and landing position of each droplet in different wind conditions. Analyses from this model show that adjustment of snow production is expedient at wind speeds up to about  $5\text{ m/s}$ . It also shows that a solution with fixed nozzles can obtain the same hit rates as a more complex solution with mobile nozzles.

Based on the results from prototyping with the analytic model, as well as interviews with experts, a design of a comprehensive, physical prototype has been proposed. The design has fixed nozzles at  $7\text{ m}$  height, divided into four horizontal orientations and two vertical steps. A guide to which nozzles should be used, depending on wind direction and wet-bulb temperature, has been proposed.

## Sammendrag

Gjennom de siste tiårene har klimaendringer påvirket vintrene i Norge. Implikasjonene av disse klimaendringene er kortere og varmere vintre, noe som gjør snøproduksjon mer relevant enn noen gang. Granåsen Skiarena er én av de viktigste skiarenaene i Trøndelag. Arenaen er viktig for all trening; fra rekreasjon til toppidrett. I Granåsen Skiarena blir snø vanligvis produsert til snølager eller i store, sentraliserte hauger. Deretter blir snøen kjørt ut i løypenettet. Denne prosessen er både tid- og energikrevende. For at Granåsen Skiarena skal kunne tilfredsstille framtidig snøbehov trengs et nytt snøproduksjonsanlegg. Fra effektivitetsproblemene har idéen om en multifunksjonell snølanse oppstått. I denne masteroppgaven er utviklingsprosessen for en slik lanse påbegynt.

Automatiserte snølanser eksisterer i dag, men få av disse er designet med tanke på smale langrennsløyper. Fokuset i utviklingsprosessen har vært å øke effektiviteten ved å introdusere automatisert justering av produksjonen med input fra værstasjoner. Denne tilnærmingen gjør det mulig å øke andelen av den produserte snøen som treffer i løypen.

For å kunne optimalisere enheten som utvikles for de smale langrennsløypene har det blitt utviklet en modell av snø fra lanser. Hver dråpe i modellen har en størrelse, en startposisjon og -hastighet. Eulers metode anvendes for finne ut hvordan hver dråpe beveger seg og hvor de lander, i ulike vindforhold. Analyser fra modellen viser at det er hensiktsmessig å justere snøproduksjon etter vind for hastigheter opp til ca.  $5\text{ m/s}$ . Analysene viser også at man kan oppnå så godt som like god treffprosent med fastmonterte dyser, som med en mer kompleks løsning med mobile dyser.

Basert på analysene er det utviklet et design av en omfattende, fysisk prototype. Denne prototypen har dyser på en høyde på  $7\text{ m}$ . Dysene er delt inn i fire horisontale steg og to vertikale steg. Hvilke steg som bør brukes avhenger av vind og våtkuletemperatur.



# Contents

Preface . . . . .	i
Abstract . . . . .	ii
Sammendrag . . . . .	iii
Nomenclature . . . . .	x
List of Figures . . . . .	xiv
List of Tables . . . . .	xviii
<b>1 Introduction</b>	<b>1</b>
1.1 Objectives . . . . .	2
1.2 Approach . . . . .	2
1.3 Limitation of Scope . . . . .	2
1.4 Outline of Thesis . . . . .	3
<b>2 Method</b>	<b>5</b>
2.1 The Product Development Methodology . . . . .	5
2.1.1 Concept Development . . . . .	6
2.1.2 Structure and Design . . . . .	7
2.2 Prototyping . . . . .	7
<b>3 Snow Theory</b>	<b>9</b>
3.1 Natural Snow . . . . .	9
3.2 Artificial Snow . . . . .	9
3.2.1 Thermal Balance . . . . .	11
3.2.2 Nuclei . . . . .	12
3.2.3 Air time . . . . .	12
3.3 Droplet size . . . . .	13
3.4 Snow Production . . . . .	13
3.4.1 Fan Guns . . . . .	14
3.4.2 Lances . . . . .	15
3.4.3 Nozzles in snow making . . . . .	15

<b>4</b>	<b>Modelling of Snow Movement</b>	<b>17</b>
4.1	Introduction . . . . .	17
4.2	Theoretical Background . . . . .	17
4.2.1	Aerodynamic Forces . . . . .	17
4.3	Problem Analysis . . . . .	19
4.3.1	Wind . . . . .	20
4.3.2	Droplet Movement . . . . .	21
4.4	Euler's Method . . . . .	22
4.4.1	Error Using Euler's Method . . . . .	23
4.5	The Drag Coefficient . . . . .	24
4.6	Implementation . . . . .	24
4.7	Important Parameters . . . . .	26
4.7.1	Droplet Speed . . . . .	26
4.7.2	Droplet Size . . . . .	26
4.7.3	Fan Angle . . . . .	26
4.7.4	Constants . . . . .	27
4.8	Discussion . . . . .	28
4.8.1	Comparison to Physical Experiments . . . . .	28
4.8.2	Weaknesses . . . . .	28
4.8.3	Strengths . . . . .	29
<b>5</b>	<b>Concept generation</b>	<b>31</b>
5.1	Exploration . . . . .	31
5.2	Concepts . . . . .	34
5.2.1	Concept 1 . . . . .	34
5.2.2	Concept 2 . . . . .	35
5.2.3	Concept 3 . . . . .	36
5.2.4	Concept 4 . . . . .	37
5.2.5	Concept 5 . . . . .	38
<b>6</b>	<b>Concept Testing and Evaluation</b>	<b>39</b>
6.1	Analytic Prototyping of the Concepts . . . . .	39
6.1.1	Concept 1 . . . . .	41
6.1.2	Concept 2 . . . . .	42



6.1.3	Concept 3	43
6.1.4	Concept 4	44
6.1.5	Concept 5	45
6.2	Feedback from Operators at Granåsen and Åre	46
6.2.1	Concept 1	46
6.2.2	Concept 2	46
6.2.3	Concept 3	47
6.2.4	Concept 4	47
6.2.5	Concept 5	47
<b>7</b>	<b>Concept selection</b>	<b>49</b>
7.1	Concept scoring	49
7.1.1	Rating the Concepts	50
7.1.2	Ranking the Concepts	51
<b>8</b>	<b>Concept Refinement</b>	<b>53</b>
8.1	Rotation of Nozzles (Horizontal Angle)	53
8.2	Tilting of Nozzles (Vertical Angle)	57
<b>9</b>	<b>Structure and Design</b>	<b>59</b>
9.1	Pipe Dimensions	59
9.2	Standard for Wind Load	60
9.3	Jet Discharge Propulsion	61
9.4	Global Design by Hand Calculations	61
9.4.1	Governing Equations	62
9.4.2	Load Cases	64
9.4.3	Case 1	65
9.4.4	Case 2	69
9.4.5	Deflection	70
9.4.6	Stresses in the Mast Openings	71
9.4.7	Stresses in Weld	72
9.4.8	Summary of Stress Calculations	74
9.5	Finite element analysis	75
9.5.1	Boundary Conditions	75
9.5.2	Loads	76

9.5.3 Mesh . . . . . 77

9.6 Comparison of FEA and Hand Calculations . . . . . 78

9.7 Materials Selection . . . . . 79

    9.7.1 Aluminium . . . . . 80

    9.7.2 Steel . . . . . 80

9.8 Part List and CAD drawings . . . . . 80

**10 Remote Control System 85**

    10.1 Control System . . . . . 85

    10.2 Recommendations for Controlling Algorithms . . . . . 86

        10.2.1 Temperature . . . . . 87

        10.2.2 Wind Strength and Direction . . . . . 87

**11 Result 91**

    11.1 Integration of the Unit in Granåsen . . . . . 91

        11.1.1 Distance Between the Units . . . . . 95

**12 Conclusion, Discussion and Suggestions for Further Work 97**

    12.1 Conclusion . . . . . 97

    12.2 Discussion . . . . . 98

    12.3 Suggestions for Further Work . . . . . 99

**Bibliography 100**

**A Report from Interviews at Granåsen 105**

    A.1 Adjustment Possibilities . . . . . 105

    A.2 Operation and Maintenance . . . . . 105

    A.3 Design . . . . . 106

**B Report from Interview in Åre 107**

**C MATLAB code 111**

**D Comparison of The Analytic Model to the Master Thesis of Shea (1999) 119**

**E Concept testing 123**

**F Nozzle Data 129**

**G Machine Drawings**

**133**

**H Light Armature from LADELYS**

**139**



# Nomenclature

## Roman Letters

A	Area; Cross-sectional area	$m^2$
$\vec{A}$	Axial force	N
a	Weld thickness	m
$a_\infty$	Freestream speed of sound	$\frac{m}{s}$
$C_D$	Drag coefficient	-
$C_L$	Lift coefficient	-
c	Chord; shape coefficient	m; -
$c_e$	Terrain factor	-
$\vec{d}$	Drag	N
d	Diameter	m
E	Elastic modulus	Pa
$f_s$	Safety factor	-
G	Shear modulus	Pa
$\vec{G}$	Weight	N
h	Step size	s
I	Second area moment of inertia	$m^4$
J	Polar area moment of inertia	$m^4$
k	Raw rating of concept	-
$\vec{L}$	Lift	N
M	Moment	Nm
$\dot{m}$	Mass flow rate	$\frac{kg}{s}$
n	Counting number	-
Q	Volume flow rate	$\frac{m^3}{s}$
$\vec{N}$	Normal force	N
p	Pressure	Pa
q	Wind pressure	N/m <sup>2</sup>

$R_{p0.2}$	Yield strength	$Pa$
$\vec{R}$	Aerodynamic resultant force	$N$
$r$	Radius	$m$
$S$	Reference area	$m^2$
$S_j$	Concept score	-
$s$	Surface	$m^2$
$T$	Torque	$Nm$
$t$	Time; Thickness	$s; m$
$\vec{u}$	Position	$m$
$V$	Shear	$N$
$\vec{V}_\infty$	Freestream Velocity	$\frac{m}{s}$
$\vec{v}$	Velocity	$\frac{m}{s}$
$\vec{G}$	Weight	$N$
$w$	Weight of criterion	%

## Abbreviations

ANSI	American National Standards Institute
GHG	Green house gas
IPM	Institute for Product development and Materials
ODE	Ordinary Differential Equation
Re	Reynold's number
RP	Raspberry Pi
SIAT	Centre for Sport Facilities and Technology (Senter for idrettsanlegg og teknologi)

## Greek Letters

$\gamma$	Shear strain	-
$\gamma_m$	Material dependent safety factor	-
$\delta$	Deflection	$mm$
$\epsilon$	Normal strain	-

$\Theta$	Circle segment angle	rad
$\theta$	Angular displacement	rad
$\mu$	Dynamic viscosity; expected value	$\frac{kg}{m \cdot s}$ ; -
$\rho$	Density	$\frac{kg}{m^3}$
$\sigma$	Normal stress; standard deviation	<i>MPa</i> ; -
$\sigma_y$	Yield stress	<i>MPa</i>





# List of Figures

2.1	Product development model by Ulrich and Eppinger . . . . .	5
2.2	The IPM process model . . . . .	5
3.1	Pressure-temperature phase diagram for $H_2O$ . . . . .	10
3.2	Temperature of a water droplet during snow production . . . . .	11
3.3	Snowmaking chart . . . . .	12
3.4	Freeze time vs. fall time for droplets falling from $10m$ . . . . .	13
3.5	Lateral movement of droplets . . . . .	14
3.6	Illustration of nozzle setup . . . . .	16
4.1	Aerodynamic pressure and shear stress on a body . . . . .	18
4.2	Aerodynamic resultant force on a body, decomposed . . . . .	19
4.3	Simplification of the wind . . . . .	20
4.4	Droplet free body diagram . . . . .	21
4.5	$C_D$ plotted versus $Re$ . . . . .	25
4.6	Landing projection, uniform droplet distribution . . . . .	27
4.7	Landing projection, normal droplet distribution . . . . .	27
5.1	Sketch of Concept 1 . . . . .	34
5.2	CAD model of Concept 1 . . . . .	34
5.3	Sketch of Concept 2 . . . . .	35
5.4	CAD model of Concept 2 . . . . .	35
5.5	Sketch of Concept 3 . . . . .	36
5.6	CAD drawing of Concept 3 . . . . .	36
5.7	Sketch of Concept 4 . . . . .	37
5.8	CAD drawing of Concept 4 . . . . .	37
5.9	Sketch of Concept 5 . . . . .	38
5.10	CAD Drawing of Concept 5 . . . . .	38
6.1	Reference coordinate system for nozzle and wind orientation . . . . .	40

6.2	Example simulation: Simulation 17	41
6.3	Example simulation: Simulation 22	42
6.4	Example simulation: Simulation 23	43
6.5	Example simulation: Simulation 1	44
6.6	Example simulation: Simulation 11	45
8.1	Hit rates, 0 <i>m/s</i> wind	54
8.2	Hit rates, 1 <i>m/s</i> wind oriented 0°	55
8.3	Hit rates, 1 <i>m/s</i> wind oriented 45°	55
8.4	Hit rates, 1 <i>m/s</i> wind along the track	56
8.5	Hit rates, 5 <i>m/s</i> wind along the track	56
8.6	Nozzle configuration	56
8.7	Hit rates with vertical nozzle tilting	57
9.1	Cross-sectional area of the unit	62
9.2	Simplified geometry of the mast	63
9.3	Bending moment caused by the weight of the light armature	65
9.4	Dimensions and moments of inertia at point 1 and 2	65
9.5	Load Case 1	66
9.6	Moment and torque diagrams for Load Case 1	67
9.7	Material element for Case 1, point A and C	67
9.8	Load Case 2	69
9.9	Weld thickness	73
9.10	Structural constraints	75
9.11	Simulation model	76
9.12	Simulation model with cut in bottom section	76
9.13	FEA model with 5 <i>mm</i> local mesh size	77
9.14	FEA model with 25 <i>mm</i> local mesh size	77
9.15	FEA model with cut and 5 <i>mm</i> local mesh size	78
9.16	FEA model with cut and 50 <i>mm</i> local mesh size	78
9.17	Maximum deflection	79
9.18	Maximum stress with cut	79
9.19	Nozzle arrangement	82
9.20	Pipe arrangement inside the mast	82

9.21 Valve placement within the mast in bottom section . . . . .	83
9.22 Solenoid valve arrangement with corresponding pipes . . . . .	83
10.1 The lance head of the Viking V2 lance . . . . .	86
10.2 Hit rates for the 45° nozzles 0,5m/s varying wind . . . . .	87
10.3 Hit rates for the 45° nozzles at 5m/s varying wind . . . . .	88
10.4 Hit rates for the 80° nozzles at 0,5m/s varying wind . . . . .	88
10.5 Hit rates for all nozzles at 0,5m/s varying wind . . . . .	89
10.6 Map showing at which wind angles the different nozzles should be used . . . . .	90
11.1 Final design of unit . . . . .	92
11.2 Final design of unit . . . . .	93
E1 Overview of NF nozzles . . . . .	129
E2 Drop size distribution NF15 . . . . .	130
E3 Drop size distribution NF30 . . . . .	131
E4 Overview of air atomizing nozzles . . . . .	132



# List of Tables

4.1	Physical constants used in the analytic model . . . . .	28
5.3	Result from brainstorming . . . . .	31
5.1	User requirements from the pre-study . . . . .	32
5.2	Product requirements from the pre-study . . . . .	33
6.1	Fixed test parameters for concept testing . . . . .	40
6.2	Learning Outcome, Concept 1 . . . . .	41
6.3	Learning Outcome, Concept 2 . . . . .	42
6.4	Learning Outcome, Concept 3 . . . . .	43
6.5	Learning Outcome, Concept 4 . . . . .	44
6.6	Learning Outcome, Concept 5 . . . . .	45
6.7	Feedback on Concept 1 . . . . .	46
6.8	Feedback on Concept 2 . . . . .	46
6.9	Feedback on Concept 3 . . . . .	47
6.10	Feedback on Concept 4 . . . . .	47
6.11	Feedback on Concept 5 . . . . .	47
7.1	Selection Criteria . . . . .	49
7.2	Description of the Rating Scores . . . . .	50
7.3	Concept Scoring . . . . .	50
8.1	Hit rate classification . . . . .	53
9.1	Snow production stages . . . . .	60
9.2	Pipe selection . . . . .	60
9.3	Summary of stress calculations . . . . .	74
9.4	Resulting Von Mises stress for each element size . . . . .	77
9.5	Resulting Von Mises stress for each element size . . . . .	78
9.6	Comparison of results . . . . .	78
9.7	Material properties . . . . .	80

9.8 Part list . . . . . 81

11.1 Product Specification . . . . . 94

B.1 Learnings from the field trip to Åre . . . . . 107

# 1 Introduction

Skiing has been a part of the Norwegian identity for hundreds of years and could be considered an important Norwegian value. In sports, skiing disciplines are where Norway as a nation traditionally reach the best international results. Moreover, skiing is a popular form of exercise among the average population and is therefore important to public health. For these reasons, cross-country skiing is considered to be the Norwegian national sport. It is therefore essential to secure skiing conditions that are both of high quality, available and appealing to people.

The climate changes have affected the winter seasons through the last decades. Increased global temperatures lead to less natural snow, which makes artificial snow production more relevant than ever before. The Norwegian Ski Federation has recognized that ski resorts that can provide artificial snow are necessary for keeping skiing as a national sport in Norway. Therefore, an increased focus on new technology and solutions is essential to improve snow production for the future.

To function as a modern area for recreational and elite sports, new and innovative solutions are needed. Trondheim Municipality has decided to spend 900 MNOK to develop Granåsen Arena (Trondheim Municipality (2017)). Highly prioritized focus areas for the development plans are reduction of Greenhouse Gas (GHG) emissions and energy consumption (Langedal (2017)). Since snowmaking is considered an energy consuming process, it has a potential for significant improvements. One of the means to address these issues is to develop a combined snow production unit and light mast. With such solution, the snow production can be distributed without moving mobile snow production units.

Few manufacturers make snow production units targeting cross-country facilities. The marked is smaller and sets other demands to the equipment, which makes room for customized solutions. By understanding the physical process of artificial snow production, the quality can be improved. Adapting production parameters dynamically using automated weather stations improves the quality and minimizes the amount of energy required (Fauve & Rhyner (2004)). Therefore, the development of a multifunctional snow production unit, which is tailor-made for Granåsen Ski Arena, has been started.

## 1.1 Objectives

The objective of this thesis is to develop a design proposition for the multifunctional snow-making unit. This includes:

1. To give an overview of important parameters concerning artificial snow production.
2. To design an analytic prototype to enable decision making.
3. To explore possible solutions. This has been done by generating feasible concepts.
4. To evaluate the concepts through expert interviews and by the use of the analytic prototype.
5. To select the most promising concept and refine it.
6. To create a detailed design and select parts that are designed according to the requirements.
7. To make a proposal for further work.

## 1.2 Approach

This Master Thesis continues the work that was started in the pre-study (Auganæs & Opheim (2017)). Through the pre-study, the product development model of Institute of Product Development and Materials (IPM) has served as a foundation, with some input from the model of Ulrich & Eppinger (2012). The work done in this thesis has continued to follow these same guidelines.

The development model is a stage-gate model, which is divided into five phases. Between each phase, there is a milestone/gate. This master thesis began with the third phase, which is Concept Development. After that followed the fourth phase, which is Structure and Design.

## 1.3 Limitation of Scope

The results from the analytic analyses done in the thesis are not fixed. They should serve as an estimate; appropriate for early phase decision making. Any assumptions made to simplify the



model has been stated. A physical prototype has not been considered given the available time and resources.

The unit that has been designed should be considered a comprehensive prototype and not the final solution. Only the isolated unit, from the ground and above, has been considered. It is assumed that the unit will be facilitated (within reason). The focus has been on the nozzle configuration and adjustment possibilities for the snow production, as lighting involves little newness. However, the interaction between the lighting and the snow production has been considered.

This thesis does not go into detail about cost analysis. There has not been done any calculations regarding the economic and environmental benefits from a solution with multifunctional lances compared to a solution with mobile fan guns or snow storages.

## 1.4 Outline of Thesis

**Chapter 2** gives a brief introduction to the Product Development Methodologies on which this thesis is based.

**Chapter 3** gives a summary of important factors to consider when making artificial snow.

**Chapter 4** presents an analytic prototype that has been designed to enable decision making in the Product Development Process. The presentation of the model includes background theory, a brief description of the implementation in MATLAB, and a discussion of strengths and weaknesses.

**Chapter 5** presents the five generated concepts.

**Chapter 6** presents results from the testing of each of the concepts from Chapter 5. Testing was done analytically with the analytic prototype from Chapter 4. Evaluation was done based on learning and interviews in Granåsen Arena and Skistar Åre.

**Chapter 7** describes how the most promising concept was chosen. This involved rating and ranking of the concepts.

**Chapter 8** describes how the chosen concept was refined to increase the performance. This involved finding the best possible orientation of the nozzles.

**Chapter 9** presents the selection of parts and strength calculations of the unit by hand and by Finite Element Analysis (FEA).

**Chapter 10** describes how the unit could be controlled based on input from weather stations.

**Chapter 11** presents illustrations of the final design, with the belonging product specifications.

**Chapter 12** comprises the conclusion, discussion and suggestions for further work.

## 2 Method

This chapter is a revised chapter from the pre-study (Auganæs & Opheim (2017)), with descriptions of how the steps have been executed.

### 2.1 The Product Development Methodology

The model of Ulrich & Eppinger (2012) provides a step-by-step approach as seen in Figure 2.1. This model gives an easily understandable overview of the project and process. Ulrich & Eppinger (2012) define product development as the set of activities beginning with the perception of a market opportunity and ending in the production, sale, and delivery of a product. In this project, the model is used as a supplement to the IPM model, seen in Figure 2.2.

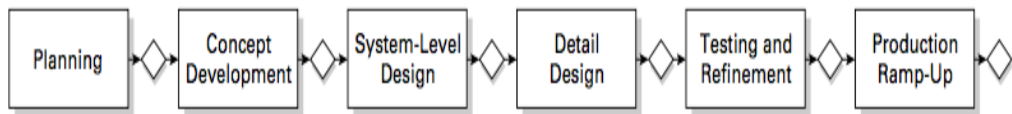


Figure 2.1: Product development model by Ulrich & Eppinger (2012)

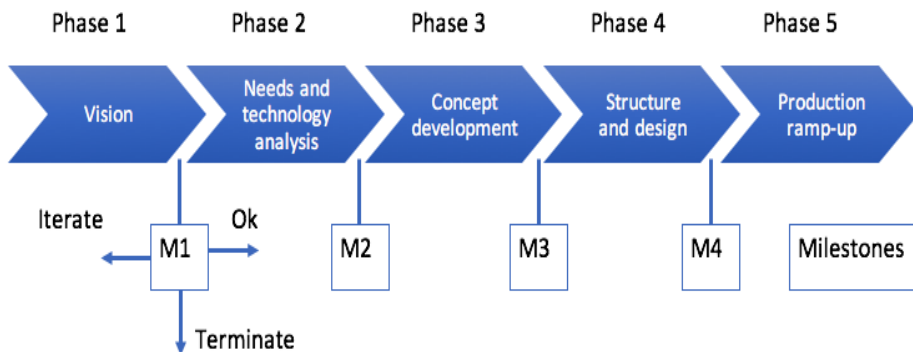


Figure 2.2: The IPM process model (Hildre (2004)).

Both models follow a stage-gate principle. Stage-gate entails control of the work that has been done after each phase. At the gates, the project members decide if they should move to the next

phase, if they need to iterate further or if the project should be terminated (Hildre (2004)). The advantage of the stage-gate principle is often increased development speed. However, stage-gate models provide less room for iterations, especially in the late process phases. Sommer et al. (2015) claims the combination of agile development and stage-gate approaches creates a healthy tension between fixed planning and iterative problem-solving. As new information was obtained evenly during the work and not just in the first phases. Trying to adapt to the new learning, also in Phase 4, has been important.

Phases 1 and 2 were completed in the pre-study (Auganæs & Opheim (2017)). Through a literature review on snowmaking and interviews with experts, information on snowmaking was gathered. This laid the foundation for the following phases.

### 2.1.1 Concept Development

The concept development is a front-end process with many interrelated activities. In practice, the front-end activities may be overlapped in time and iterations are often necessary. Ulrich & Eppinger (2012) present three steps of concept development:

**Concept generation** begins with a set of customer needs and target specifications. The concept generation results in a set of product concepts from which the team will make a final selection. A product concept is an approximate description of the technology, working principles, and form of the product.

**Concept selection** is the process of evaluating the concepts with respect to customer needs and other criteria, comparing the relative strengths and weaknesses of the concepts, and selecting one or more concepts for further investigation, testing, or development.

**Concept testing** is to test if the artifact meets the customer needs and verify the design.

The concepts presented in this thesis were created by combining technology from existing solutions with input from experts. The performance of all concepts was tested with the analytic model, while more practical concerns were evaluated with feedback from the operators at Granåsen Ski Arena.

### 2.1.2 Structure and Design

The result of the Structure and Design-phase is an approximate geometric layout of the product, descriptions of the major chunks, and documentation of the critical interactions among the chunks. A detailed design should include computer drawings describing the geometry of each part. Material selection, production cost, and performance should be estimated.

## 2.2 Prototyping

A common practice is to use prototypes to represent different parts of the design and explore different options. Prototyping is done to validate and verify assumptions, calculations, and decisions during the development. A prototype can also reduce the risk of unnecessary iterations. These unnecessary iterations will cost time and money.

Ulrich & Eppinger (2012) claims prototypes are used for learning, communication, integration, and milestones:

**Learning:** Prototypes used for learning should answer how well it meets the customers' needs.

The question "Will it work?" should be answered. Various designs could be tested to learn if they work or not.

**Communication:** It is often beneficial to communicate through prototypes with people outside the development team. A three-dimensional representation is much easier to understand than a verbal description or a sketch (Ulrich & Eppinger (2012)). When the customer understands the concept, it is easier for him/her to give better feedback.

**Integration:** By integration of different components in a prototype, one can test if the product works as expected. Sub-functions can work alone, but if the combination interferes with the overall function, evaluation and re-design are needed. Physical integration in a comprehensive prototype is a good method to detect future problems (Ulrich & Eppinger (2012)).

**Milestones:** Milestones prototypes provide tangible goals and demonstrate progress. Sometimes milestones are used to show required functions to the customer before allowing the project to proceed.

The approach to prototyping in this thesis is to use analytic prototyping. Economy and time have not allowed physical prototyping. Analytic prototyping is mainly used in Phase 3 and Phase 4, but also for communication. It is expected that Phases 2, 3 and 4 have to be iterated before the unit is ready for Phase 5. These iterations are in accordance with the agile approach to the IPM process model.

# 3 Snow Theory

This chapter is a revised chapter from the pre-study (Auganæs & Opheim (2017)). Knowledge of snow, both natural and artificial, is essential to understand the snow production process and some of the technical requirements that will affect the design. Snow, both natural and artificial, consist of clusters of ice crystals. The formed ice crystals can take different shapes depending on temperature and humidity in the atmosphere where the snow is created.

## 3.1 Natural Snow

Snow crystals are formed when water vapor in the atmosphere, usually in clouds, transforms directly into solid ice without going through the liquid phase, and the ice crystals cling together. Looking at the phase diagram of water in Figure 3.1, this transformation happens along the sublimation line where both temperature and pressure are low. The phase transformation consist of two phases: *nucleation* and *growth*. Nucleation of a given material involves the appearance of tiny particles, or nuclei of the new phase (often consisting of only a few hundred atoms), which are capable of growing. During the growth stage, these particles increase in size until the equilibrium fraction of the phases is reached (Callister & Rethwisch (2007)). One of the necessary conditions for a solidification transformation is that the temperature is below the equilibrium solidification temperature. However, this is not sufficient for the phase transformation to happen. When water is divided into small drops, the statistical probability that it will freeze at a given temperature becomes smaller since there are fewer water molecules available to form a nucleus that is capable of growth (Curry & Webster (1998)). Snow is made when water vapor is solidified onto the nucleus. If a nucleus grows to become a big enough particle, it will start falling through the air.

## 3.2 Artificial Snow

Artificial snow production consists of two main stages: (1) Generating water droplets and (2) freezing of the droplets. Small droplets are made when water and air at high pressure are mixed

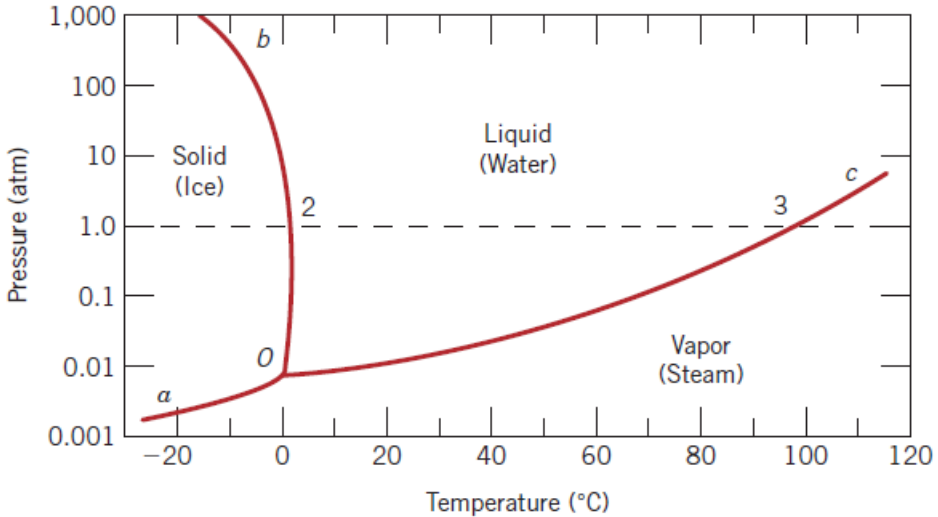


Figure 3.1: Pressure-temperature phase diagram for  $H_2O$ . Intersection of the dashed horizontal line at 1 atm pressure with the solid-liquid phase boundary (point 2) corresponds to the melting point at this pressure ( $T = 0^\circ C$ ). Similarly, point 3, the intersection with the liquid-vapor boundary, represents the boiling point ( $T = 100^\circ C$ ). The sublimation line is the boundary curve from  $a$  to the triple point,  $O$  (Callister & Rethwisch (2007)).

and atomized through a nozzle. The pressure difference from the water to the atmospheric air cause turbulence that brakes the water jet and creates droplets.

For the water to freeze in the air, certain conditions must be present: Air temperature; humidity; distance from nozzle to ground; and nuclei that can catalyze the phase transformation of the droplets. The droplets will freeze from the outside and inwards. This is what causes the structural difference between natural snow and artificial snow. Artificial snow has the advantage of withstanding longer periods of warm weather. The round grains of machine-made snow gives a structure which is close-packed, which accordingly results in a higher density compared to natural snow (Linzén (2016)). Gjerland, M and Olsen, G.Ø (2014) claims that  $10cm^3$  of artificial snow equals  $40cm^3$  of natural snow.

In general, three factors control the freezing of droplets in artificial snow production (Gjerland, M and Olsen, G.Ø (2014)):

1. **Thermal balance**, which is the ration between the wet-bulb temperature and the volume of water that should freeze.
2. Sufficient amounts of **nuclei** in the water, to start the solidification process of the water droplets.



3. The water droplets need adequate **air time** to be able to freeze.

These points are reflected in Figure 3.2.

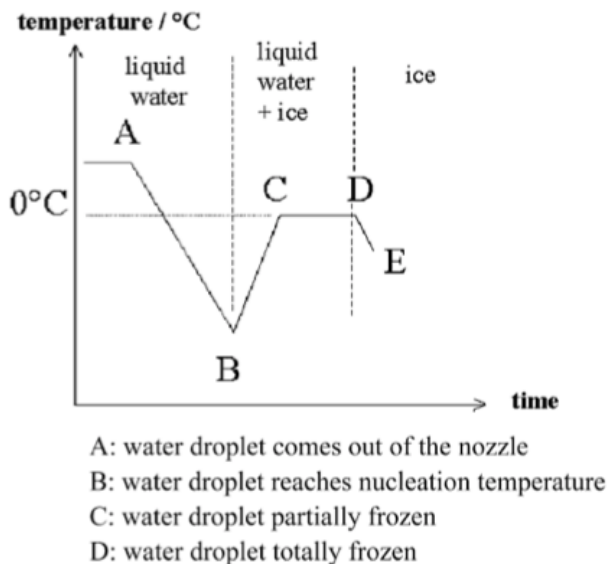


Figure 3.2: Temperature of a water droplet during snow production (Fauve & Rhyner (2004))

### 3.2.1 Thermal Balance

The *wet bulb* temperature  $T_{wb}$  is important in order to explain the relationship between temperature, humidity, and snow production. Wet-bulb temperature is dependent on relative humidity and conventional air temperature (dry-bulb). Relative humidity is a measure of the amount of water vapor in the air, expressed as a percentage of the total amount contained in saturated air at a given temperature and pressure. More specifically, wet-bulb temperature is "the temperature a parcel of air would have if it were cooled adiabatically (at constant pressure) to saturation by the evaporation of water into it, with the latent heat being supplied by the parcel" (Dunlop (2008)). Figure 3.3 shows the wet-bulb temperature for corresponding humidity and dry-bulb temperature. The different colors illustrate how the specified wet-bulb temperature affects the snow quality.

Good Snow Quality					Poor Snow Quality					No Snowmaking								
Temp C	Humidity																	
	10%	15%	20%	25%	30%	35%	40%	45%	50%	55%	60%	65%	70%	75%	80%	85%	90%	95%
-9	-12	-12	-12	-12	-12	-12	-12	-11	-11	-11	-11	-11	-11	-10	-10	-10	-9	-9
-8	-12	-11	-11	-11	-11	-11	-11	-10	-10	-10	-10	-9	-9	-9	-9	-9	-8	-8
-7	-10	-10	-10	-9	-9	-9	-9	-9	-9	-8	-8	-8	-8	-7	-7	-7	-7	-7
-6	-10	-9	-9	-9	-9	-9	-8	-8	-8	-8	-8	-8	-7	-7	-7	-6	-6	
-5	-9	-9	-8	-8	-8	-8	-7	-7	-7	-7	-7	-6	-6	-6	-6	-5	-5	
-4	-8	-8	-8	-8	-8	-7	-7	-7	-7	-7	-6	-6	-6	-6	-5	-5	-5	
-3	-7	-7	-7	-7	-6	-6	-6	-6	-5	-5	-5	-4	-4	-4	-3	-3	-3	
-2	-7	-7	-6	-6	-6	-6	-5	-5	-5	-4	-4	-4	-3	-3	-3	-3	-2	
-1	-6	-6	-5	-5	-4	-4	-4	-3	-3	-3	-3	-2	-2	-2	-2	-1	-1	
0	-5	-5	-4	-4	-4	-4	-3	-3	-3	-3	-2	-2	-2	-1	-1	-1	0	
1	-5	-4	-4	-4	-3	-3	-3	-3	-2	-2	-2	-2	-1	-1	-1	0	0	
2	-4	-3	-3	-3	-2	-2	-2	-1	-1	-1	-1	0	1	1	1	2	2	
3	-3	-3	-2	-2	-2	-2	-1	-1	-1	0	0	1	1	1	2	2	3	
4	-2	-2	-1	-1	-1	0	0	1	1	1	2	2	2	3	3	4	4	

Figure 3.3: Snowmaking chart, showing wet-bulb temperatures for corresponding humidity and dry-bulb temperature. When plotting the dry-bulb temperature versus humidity, the wet-bulb temperature is shown where they meet. The chart illustrates how the snow quality varies with different wet-bulb temperatures. Below  $-7^{\circ}C$  wet-bulb temperature gives good snow quality (dry and light).  $-3^{\circ}C$  to  $-6^{\circ}C$  gives poor snow quality (wet and dense). (Snowathome (2017))

### 3.2.2 Nuclei

As illustrated in Figure 3.2 the water need to reach nucleation temperature to start the freezing process. Freezing nuclei can be ice particles, or other solid particles, in the water. Distilled water starts to freeze at  $-40^{\circ}C$ , while water containing other particles (e.g., added proteins or "dirt" from the water source) can freeze at  $-3^{\circ}C$  (Gjerland, M and Olsen, G.Ø (2014)). When the nucleation temperature is reached, then the droplets start to freeze and release heat. The temperature then increases before the whole droplet is frozen, and the temperature decreases again (Fauve & Rhyner (2004)).

### 3.2.3 Air time

For the droplets to freeze, they need sufficient time in the air. The parameters affecting this is the height the droplets are released from, outlet speed and size of the droplet. Larger droplets will have larger weight, and will therefore fall to the ground faster. The wind can also affect the air time.

Figure 3.4 presents falling time and freezing time versus droplet size. The brown line shows the falling time from 10m for different droplet sizes falling. The other lines represent the freezing

time for droplets at different wet-bulb temperatures. The blue line corresponds to a wet-bulb temperature of  $-4^{\circ}\text{C}$ , the red to  $-9^{\circ}\text{C}$  and the green to  $-16^{\circ}\text{C}$ . The blue line crosses the brown line at a droplet diameter of approximately  $350\mu\text{m}$ . This means that droplets with diameter  $d$  larger than  $350\mu\text{m}$  will not freeze completely at a wet-bulb temperature of  $-4^{\circ}\text{C}$ .

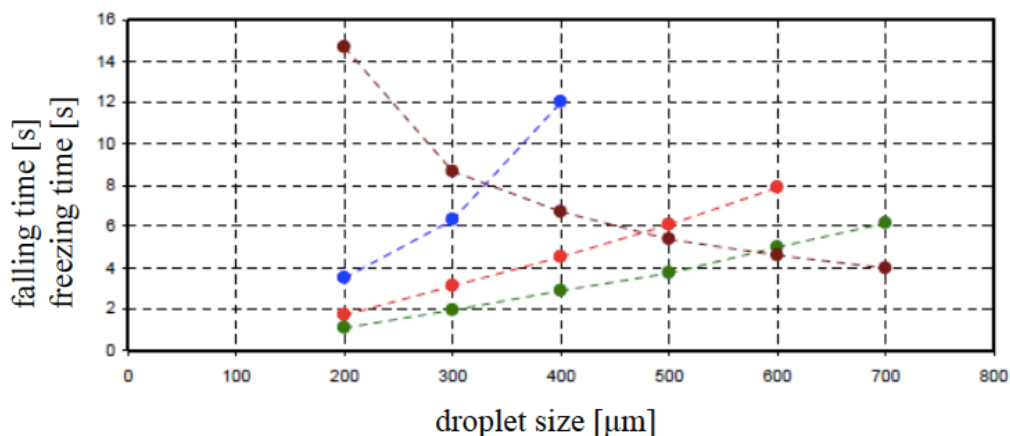


Figure 3.4: Freeze time vs. fall time for droplets falling from  $10\text{m}$  at different wet-bulb temperatures (Wolfsperger et al. (2018))

### 3.3 Droplet size

The size of the nozzle orifice and the water pressure are the main parameters controlling the droplet size. A smaller orifice diameter will cause smaller droplets. Smaller droplets will have less momentum leaving the nozzle, causing decreased throw length. Another factor concerning the droplet size is the amount of drift. Ideally, all of the produced snow should fall down within the tracks. Larger droplets will be less affected by the wind than smaller drops. Figure 3.5 shows the lateral movement of different droplet sizes in 1MPH wind ( $\approx 0,45\text{m/s}$ ). With a fall of  $6\text{m}$ , a droplet with  $d = 200\mu\text{m}$  would drift approximately three meters. Droplets with  $d = 120\mu\text{m}$  or smaller would disappear.

### 3.4 Snow Production

The decision of the type of snow guns, and when and where to produce snow are influenced by many factors: local conditions; snow demand; economy; and experience. Moreover, the snow

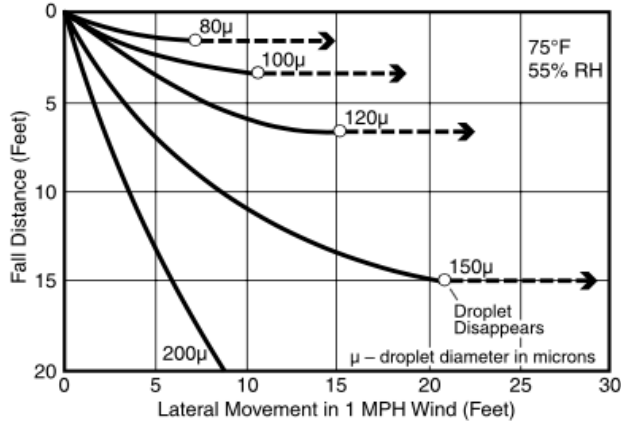


Figure 3.5: Chart showing how the lateral movement of droplets depends on fall distance and size of water droplets in 1MPH wind (Hoffman & Solseng (2014)).

production does not only depend on the type of snow gun, but also the infrastructure around the guns.

One common practice is to produce a sturdy ground layer of snow to be covered by natural snow and then produce more snow for selected parts of the course/slope to maintain snow depth and quality. Vulnerable areas where the snow requires extra maintenance could be: Tracks that are frequently exposed to the sun; at the top of steep hills (or in the hills) where skiers slow down using snowplowing technique; areas exposed to wind; et cetera. Sometimes, it could also be beneficial to produce snow in piles when the conditions are present, that may be distributed later on.

Today there are two main types of snowmaking machines on the market. These are fan based machines (fan guns) and high-pressure tower based machines (lances). They both follow the principles of snowmaking that were presented in section 3.2.

### 3.4.1 Fan Guns

Fan guns use a fan to blow the water-air mix up to 60m. This leads to high production rates and makes them less sensitive to wind. High-pressure air is made on the unit by a compressor. Therefore, proximity to a direct power outlet is necessary. Because of the high production rate snow guns are often used to produce snow in big piles, which is then transported into the tracks. More adjustment possibilities can also lead to snow production at marginal tempera-

tures. Because of a large number of parts, fan guns need more maintenance over time than lances.

### **3.4.2 Lances**

Lances use high-pressure air to atomize the water into fine droplets in the nozzle. The height of the lance is important to let the droplets be able to freeze before it reaches the ground. This again makes snow from lances more fragile in windy areas, as it can be blown away from the tracks. Lances need to be connected to a piping system of high-pressure water and air. The high-pressure air could be produced by local compressors or by pipelines from a stationary compressor unit. When installing such a piping system, there are several options as to how they can be installed along the tracks. They can either be placed above the ground, at frost-free depth or somewhere in between. This decision is often made based on economic concerns. The lances are often placed stationary to produce snow at strategic spots along the tracks. Because of the low weight, they are easier to move. Lances often involve lower investment costs compared to fan guns (Aas & Vagle (2017)).

### **3.4.3 Nozzles in snow making**

The nozzle design on lances often consists of an air atomizing nozzle together with a water nozzle, as shown in Figure 3.6. The air atomizing nozzle (nucleator) mixes water and air to produce very small droplets that freeze fast. These particles become the nuclei when they interact with the larger water droplets from the water nozzles (Bete (2017)).

The nucleator nozzles are usually either internal mix or external mix. Internal mix set-up mixes liquid and air within the nozzle. The streams are not independent, meaning that a change in air flow will affect the liquid flow. The internal mix is able to produce finer atomized droplets (Bete (2017)). When the air and liquid exit the nozzle independently and mix outside the nozzle, it is called external mix set-up. In this solution, the air and liquid flow can be controlled independently.

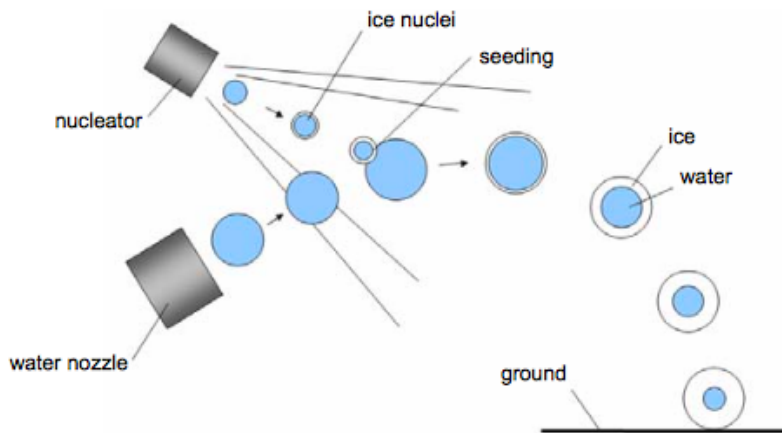


Figure 3.6: Illustration of nozzle setup. The figure illustrates how the water droplets from the water nozzle are nucleated by small ice particles from the air atomizing nozzle. (Bachler (2017))

# 4 Modelling of Snow Movement

## 4.1 Introduction

High snowmaking efficiency is desirable for all resorts. Increasing the amount of produced snow that can be utilized in the skiing tracks from a given mass of water remains a major problem in snowmaking facilities (Spandre et al. (2017)). The width of the ski slopes and wind may affect the percentage of produced snow falling within the tracks. As the cross-country skiing tracks are narrower than alpine ski slopes, this leads to even greater losses in cross-country facilities.

The goal of creating the model is to get a better understanding of how to adjust the snowmaking unit according to meteorological conditions. The goal is to optimize the *hit rate*, the percentage of produced droplets that fall into the track. The model should answer questions about:

- How the wind affects the hit rate,
- How nozzle angles influence flight time, throw length and hit rate,
- How droplet size affect air time, throw length and hit rate,
- Required wet-bulb temperature for certain nozzle configurations.

## 4.2 Theoretical Background

The main forces acting on the droplets in the air are aerodynamic forces and the weight of the droplet,  $\vec{G}_{drop}$ . These forces depend on the shape and speed of the droplet, which is determined by the pressure and the nozzle type of the snow gun.

### 4.2.1 Aerodynamic Forces

The aerodynamic forces on a body are caused by

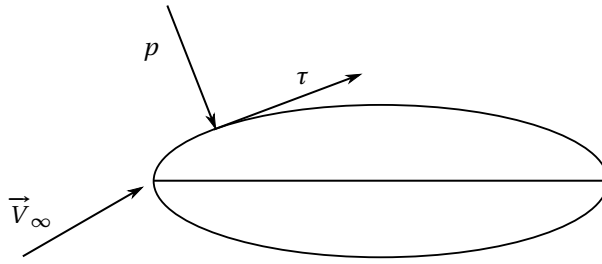


Figure 4.1: Aerodynamic pressure and shear stress on a body

1. Pressure distribution over the body surface,  $p = p(s)$
2. Shear stress distribution over the body surface,  $\tau = \tau(s)$

as shown in Figure 4.1. The net effect of the pressure and shear stress distributions integrated over the complete body surface is the resultant aerodynamic force,  $\vec{R}$ , (and moment) on the body.  $V_\infty$ , in Figures 4.1 and 4.2 is defined as the relative wind far ahead of the body, often called the *freestream* velocity.  $\vec{R}$  can be split into components, as shown in Figure 4.2. These are:

$\vec{L} \equiv$  lift  $\equiv$  the component of  $R$  that is perpendicular to  $V_\infty$ ,

$\vec{D} \equiv$  drag  $\equiv$  the component of  $R$  that is parallel to  $V_\infty$ ,

$\vec{N} \equiv$  normal force  $\equiv$  the component of  $R$  that is perpendicular to the line from the leading edge to the trailing edge of the body (the *chord*,  $c$ ),

$\vec{A} \equiv$  axial force  $\equiv$  the component of  $R$  that is parallel to the chord.

As per today, it is not possible to calculate the theoretical aerodynamic forces based on  $p(s)$  and  $\tau(s)$ , given the shape of the body and the freestream conditions. Therefore, the aerodynamic forces are determined experimentally, e.g., in wind tunnels. For this purpose, dimensionless force coefficients are defined as:

Drag coefficient:

$$C_D \equiv \frac{D}{q_\infty S} \quad (4.1)$$

Lift coefficient:

$$C_L \equiv \frac{L}{q_\infty S} \quad (4.2)$$

Where  $S$  is a reference area and  $q_\infty$  is defined as the *freestream dynamic pressure*:



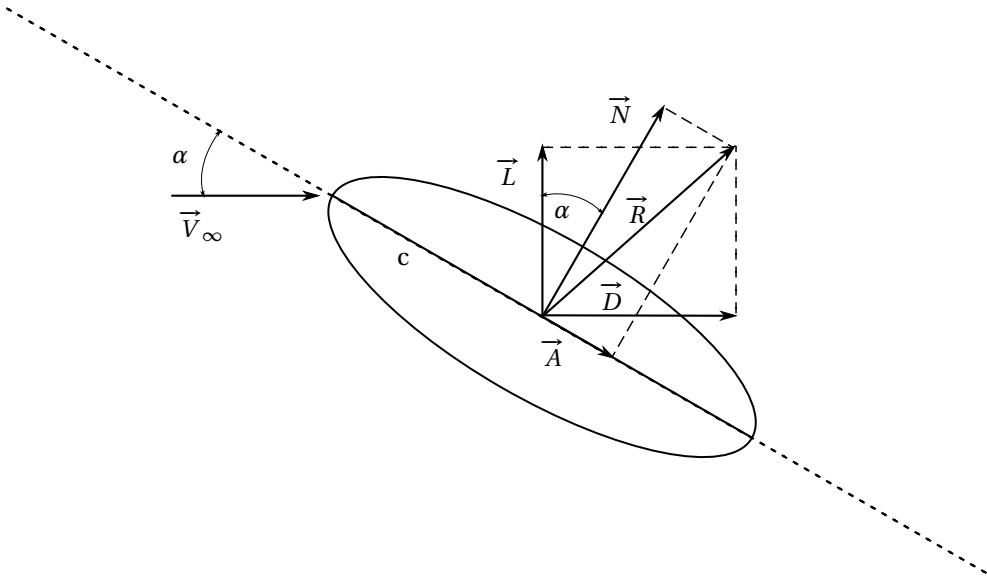


Figure 4.2: Aerodynamic resultant force on a body, decomposed

$$q_{\infty} \equiv \frac{1}{2} \rho_{\infty} V_{\infty}^2 \quad (4.3)$$

where  $\rho_{\infty}$  is the freestream density (the density of the stream far ahead of the body). Substituting Equation 4.3 into Equations 4.1 and 4.2 yields scalar expressions for the drag and lift forces:

$$C_D \equiv \frac{D}{q_{\infty} S} = \frac{D}{\frac{1}{2} \rho_{\infty} V_{\infty}^2 S} \Leftrightarrow D = \frac{1}{2} \rho_{\infty} S C_D V_{\infty}^2 \quad (4.4)$$

$$C_L \equiv \frac{L}{q_{\infty} S} = \frac{L}{\frac{1}{2} \rho_{\infty} V_{\infty}^2 S} \Leftrightarrow L = \frac{1}{2} \rho_{\infty} S C_L V_{\infty}^2 \quad (4.5)$$

Having obtained experimental values of  $C_D$  and  $C_L$  for given freestream conditions, one can estimate the behavior of the body when exposed to these conditions.

### 4.3 Problem Analysis

The nozzle affects the start speed, the size and the projection of the droplets. Assuming that the flow is steady and incompressible, we can use the mass conservation principle to estimate

the initial speed of the droplets exiting the nozzle:

$$\begin{aligned} \sum_{in} \dot{m} &= \sum_{out} \dot{m}, & m &= \rho Q, \\ \sum_{in} Q\rho &= \sum_{out} Q\rho \Rightarrow & \sum_{in} Q &= \sum_{out} Q \end{aligned}$$

Volume flow rates at given pressures are usually provided in the technical manual for a snow gun. Knowing this, as well as the cross-sectional area of the nozzle opening, one can calculate the average speed of the flow through the nozzle,  $\bar{v}_{out}$ .

$$Q_{in} = Q_{out} = A_{out} v_{out} \Leftrightarrow \bar{v}_{out} = \frac{Q_{in}}{A_{out}} \quad (4.6)$$

### 4.3.1 Wind

In reality, wind can change rapidly with time and position. These changes are difficult to represent and recreate. Therefore, the no-slip condition is ignored. This way, the wind can be represented as a constant vector. This simplification is illustrated in Figure 4.3.

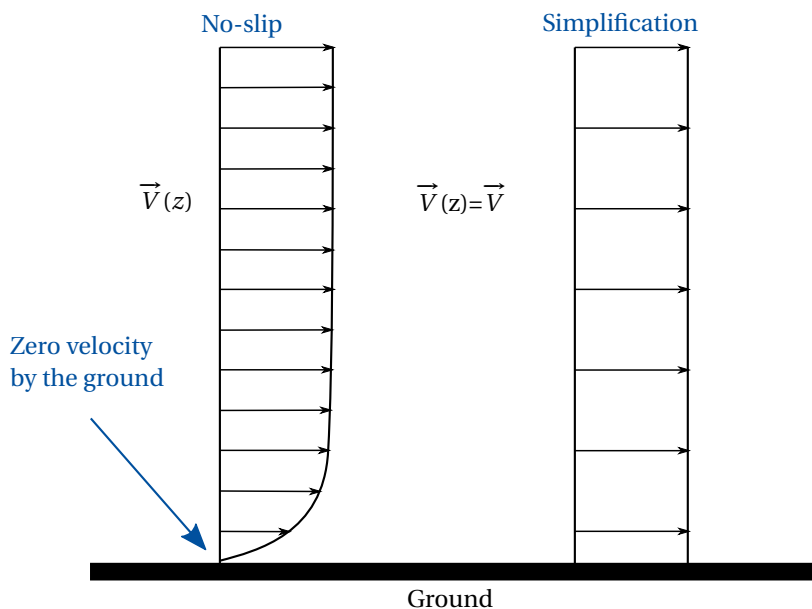


Figure 4.3: Simplification of the wind by ignoring the no-slip condition

### 4.3.2 Droplet Movement

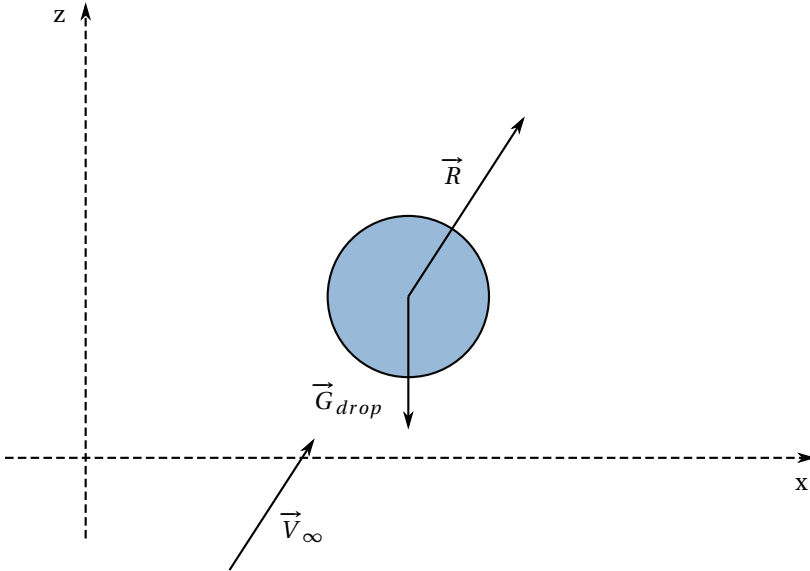


Figure 4.4: Droplet free body diagram

The movement of the droplets can be simulated by using a numerical method to solve the initial value problem. Assuming that the droplets are spheres and do not change their shape, we can also assume that the resultant acts parallel with the freestream velocity, as the sphere is symmetrical about all possible lines through the center. Looking at the free body diagram in Figure 4.4, a movement equation for the droplet can be established. Applying Newton's second law of motion yields:

$$\sum \vec{F} = m \frac{d\vec{v}}{dt} = \vec{F}_g + \vec{D} \quad (4.7)$$

The vector expression of the drag force  $\vec{D}$  can be obtained by multiplying Equation 4.4 with the unit vector that has the same direction as the relative wind:

$$\vec{D} = \frac{1}{2} \rho_{\infty} S C_D |\vec{V}_{\infty}|^2 \frac{\vec{V}_{\infty}}{|\vec{V}_{\infty}|} = \frac{1}{2} \rho_{\infty} S C_D |\vec{V}_{\infty}| \vec{V}_{\infty}$$

The reference area  $S$  is the cross sectional area. In terms of the velocity of the droplet relative to the wind,  $\vec{v}_{d|w}$  (for simplicity,  $\vec{v}_{d|w} = \vec{v}$  in the formulas), the expression becomes

$$\vec{D} = -\frac{1}{2}\rho_{\infty}SC_D|\vec{v}|\vec{v} \quad (4.8)$$

Inserting Equation 4.8 into Equation 4.7, and solving for the acceleration, yields:

$$\frac{d\vec{v}}{dt} = -\frac{m\vec{g}}{m} - \frac{1}{2}\frac{\rho_{\infty}SC_D|\vec{v}|}{m}\vec{v} = -\vec{g} - \frac{1}{2}\frac{\rho_{\infty}SC_D|\vec{v}|}{m}\vec{v} \quad (4.9)$$

## 4.4 Euler's Method

Euler's method can be derived from the Taylor expansion, as shown in Equation 4.10, assuming that the solution will be completely dominated by the first two terms if the step size  $h$  is small:

$$y(t_0 + h) = y(t_0) + hy'(t_0) + \frac{1}{2}h^2y''(t_0) + \dots + \frac{1}{p!}h^p y^{(p)}(t_0) + \frac{1}{(p+1)!}h^{p+1}y^{(p+1)}(\xi), \quad (4.10)$$

where  $\xi$  is a number within  $[t_0, t_{end}]$  and  $p$  is a chosen number such that  $y^{(p+1)}$  exists. Euler's method is defined as:

$$y_{n+1} = y_n + hf(t_n, y_n), \quad \text{where } n = 0, 1, \dots, N_{step} - 1, \quad (4.11)$$

For a scalar ordinary differential equation  $y' = f(t, y)$ . Using Euler's method results in the approximation  $y_n \approx y(t_n)$ . The step size  $h = (t_{end} - t_0)/N_{step}$  divides the interval  $[t_0, t_{end}]$  into  $N_{step}$  equal fragments. Euler's method is chosen over other numerical methods due to performance considerations. Euler's method is explicit, which makes it cheaper computationally than implicit methods. Moreover, many other explicit numerical methods require more calculations per step, which requires more time. Euler's method is also very easily implemented.

Applying Euler's method to the problem described in Section 4.3.2 gives:

$$\vec{f}(t_n, \vec{v}_n) = -\vec{g} - \frac{1}{2} \frac{\rho_\infty S C_D |\vec{v}_n|}{m} \vec{v}_n, \quad (4.12)$$

so that

$$\vec{v}_{n+1} = \vec{v}_n + h(-\vec{g} - \frac{1}{2} \frac{\rho_\infty S C_D |\vec{v}_n|}{m} \vec{v}_n) = \vec{v}_n - h(\frac{1}{2} \frac{\rho_\infty S C_D |\vec{v}_n|}{m} \vec{v}_n) - h\vec{g} \quad (4.13)$$

Here,  $t_{end}$  is unknown. The iterations will stop when the droplet hits the ground, that is, when  $z = 0$ .  $t_{end}$  is then the fall time of the droplet, which is an important parameter in snowmaking.

The position of the droplet can be calculated similarly to the velocity:

$$\frac{d\vec{u}}{dt} = \vec{v}, \quad \text{so that} \quad \vec{u}_{n+1} = \vec{u}_n + h\vec{v}_n$$

#### 4.4.1 Error Using Euler's Method

When solving an ordinary differential equation numerically using some computer program, the solution will not be exact. Two types of error may occur: Round-off error, as the computer can only store a finite number of digits; and *truncation error*. The dominating part of the error is usually the truncation error. The local truncation error  $d_{n+1}$  is the error done in one step when starting at the exact solution  $y(t_n)$ . For each step, an error is made. These errors are propagated to the next steps and accumulated at the end. The global error is the difference between the exact solution and the numerical solution at point  $t_n$ , that is  $e_n = y(t_n) - y_n$ .

When all the terms in the Taylor-expansion are kept, the Taylor-expansion is exact. When assumed that  $h \ll 1$ , Euler's method states that the solution is dominated by the first two terms. It follows that the error is dominated by the third term:

$$d_{n+1} = y(t_n + h) - y(t_n) - hf(t_n, y(t_n)) = \frac{1}{2} h^2 y''(\xi)$$

where  $\xi \in [t_n, t_{n+1}]$ . This means that the error done in one step can be written  $d_{n+1} = O(h^2)$ . As the number of steps for a given  $t_{end}$  is proportional to  $1/h$ , the global error can be written  $e_{N,step} = O(h)$ . Decreasing the step size will therefore tend to decrease the numerical error by the same factor.

## 4.5 The Drag Coefficient

The aerodynamic forces and moments on a body is expected to be a function of many parameters: The freestream velocity  $V_\infty$ ; freestream density  $\rho_\infty$ ; viscosity of the fluid  $\mu_\infty$ ; compressibility of the fluid (related to the freestream speed of sound,  $a_\infty$ ); and the size and shape of the body, represented by the chord  $c$ . Thus, the resultant aerodynamic force could be written as

$$R = f(V_\infty, \rho_\infty, \mu_\infty, a_\infty, c)$$

Through dimensional analysis,  $R$  can be reduced to depend on two independent variables: The freestream Reynolds' Number,  $Re = \rho_\infty V_\infty c / \mu_\infty$ ; and the freestream Mach number  $M_\infty = V_\infty / a_\infty$  (Anderson (2001)). It follows that  $C_D$  can be expressed as a formula of  $Re$  and  $M_\infty$ .

Morrison (2013) presents a correlation of  $C_D$  versus  $Re$  for values of  $Re$  up to  $10^6$  for a smooth sphere:

$$D_D = \frac{24}{Re} + \frac{2,6 \left(\frac{Re}{5,0}\right)}{1 + \left(\frac{Re}{5,0}\right)^{1,52}} + \frac{0,411 \left(\frac{Re}{2,63 \times 10^5}\right)^{-7,94}}{1 + \left(\frac{Re}{2,63 \times 10^5}\right)^{-8,00}} + \frac{0,25 \left(\frac{Re}{10^6}\right)}{1 + \left(\frac{Re}{10^6}\right)}. \quad (4.14)$$

Equation 4.14 is used in the model to estimate the drag coefficient.  $Re$  and the belonging  $C_D$  is updated with every iteration. This has shown to give more realistic results compared to calculating a constant  $C_D$  before starting the Euler iterations.

## 4.6 Implementation

MATLAB has been used to generate droplets with initial velocity and position. Euler's Method has been implemented and executed for each droplet. The model consists of several MATLAB functions. The most important of these are:

`main.m` contains most of the parameters that can be changed, such as nozzle position and angle, wind, droplet size and initial speed. Each droplet is given a radius from a normal distribution with expected value  $\mu$  and standard deviation  $\sigma$ , which can be varied depending on the nozzle type that is imitated. The flat fan shape of the spray is imitated

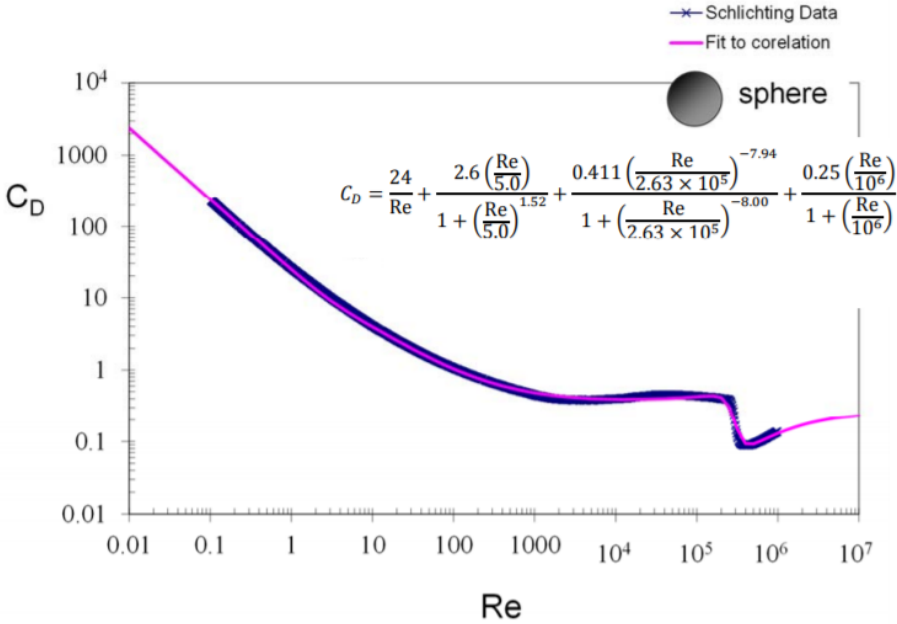


Figure 4.5:  $C_D$  plotted versus  $Re$ . Equation (4.14) captures  $C_D$  as a function of  $Re$  (Morrison (2013)). The function is plotted along with experimental data for uniform flow around a sphere (Schlichting (2006)).

by giving the droplets an initial velocity with a random angle between  $\pm 25^\circ$  (assuming a  $50^\circ$  flat fan) of the direction in which the nozzle points.

`onestep_euler.m` takes in the current position  $\vec{u}_n$  and velocity  $\vec{v}_n$ , performs one iteration of Euler's method, and returns the next position  $\vec{u}_{n+1}$  and velocity  $\vec{v}_{n+1}$ .

`euler_solver.m` takes in a droplet that was generated in `main`, and calls `onestep_euler.m` until the z-value of the droplet is equal to or less than zero. The function then returns final and intermediate positions of the droplet.

`controller.m` makes it possible to run the model many times for different set-ups or conditions, to compare the outcome of the different scenarios without manually having to run `main.m` one time for each scenario.

The entire MATLAB code can be found in Appendix C.

## 4.7 Important Parameters

### 4.7.1 Droplet Speed

The initial speed of the droplets is estimated using Equation 4.6, for standard values of pressure and nozzle size. The initial speed was estimated to ca.  $60m/s$ . Small changes to the initial speed have shown to have little effect on the final result, as the droplet speed is slowed down very fast after leaving the nozzle.

### 4.7.2 Droplet Size

The droplet size is normally distributed around some expected value  $\mu$  with some standard deviation  $\sigma$ . These values depend on the type of nozzle which the model intends to imitate. Manufacturers usually specify the expected droplet diameter for each nozzle. Therefore, different droplet sizes have been used in different tests. This is a simplification of the real droplet size distribution, as the real distribution is unknown.

### 4.7.3 Fan Angle

The fan angle produced by most lance nozzles is  $50^\circ$ . However, a real-life nozzle will not produce a perfect fan shape. Therefore, the direction of the start velocity of each droplet is normally distributed around  $0^\circ$  from the pointing direction, with a chosen standard deviation of  $12,5^\circ$ . Figures 4.6 and 4.7 illustrates why this choice was made.



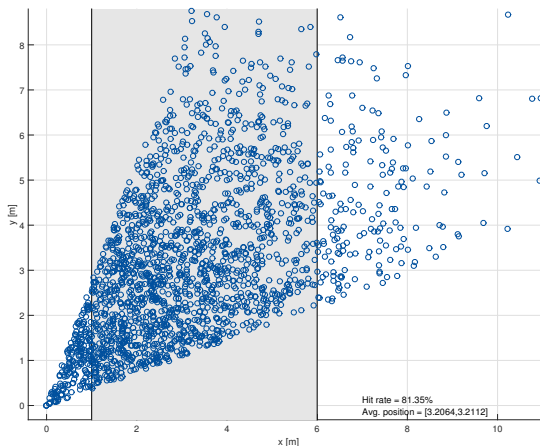


Figure 4.6: Landing projection. Uniform distribution of the initial velocity angle. Droplet size  $\mu = 200\mu\text{m}$ ,  $\sigma = 70\mu\text{m}$ . Zero wind. Nozzle rotation of  $45^\circ$ .

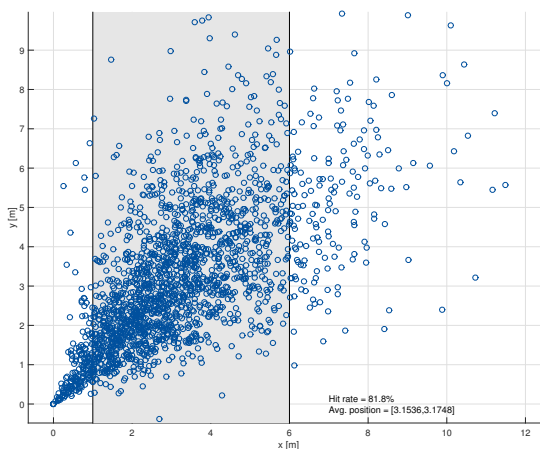


Figure 4.7: Landing projection. Normal distribution of the initial velocity angle. Droplet size  $\mu = 200\mu\text{m}$ ,  $\sigma = 70\mu\text{m}$ . Zero wind. Nozzle rotation of  $45^\circ$ .

Comparing Figures 4.6, 4.7 and real piles made from flat fan nozzles, it is clear that a normal distribution of the droplets is more realistic.

### 4.7.4 Constants

The following constants are used in the model:

Table 4.1: Physical constants used in the analytic model

Constant	Value
Earths gravity, $g$	$9,81 m/s^2$
Air density, $\rho_{air}$	$1,226 kg/m^3$
Dynamic viscosity of air, $\mu_{air}$	$1,738 \times 10^{-5} kg/(m \times s)$

## 4.8 Discussion

How well the model performs, as well as its strengths and weaknesses are discussed in this section.

### 4.8.1 Comparison to Physical Experiments

The model has been compared to the results from the Master Thesis of Shea (1999) with title "Calibration of Snowmaking Equipment". In this thesis, the deposition of snow from different snow lance setups in different weather conditions were measured. The comparisons have been performed by copying as much as possible from the lance setup in the physical experiments onto the parameters in the model. As it is not possible to reproduce the exact conditions from the physical tests exactly, these comparisons can only serve as an indication of the correctness of the model. More detailed results from these comparisons can be found in Appendix D.

The primary outcome of the comparison with the physical experiments from Shea (1999) is that the centers of the "piles" produced by the model match the physical experiment in most cases. The exceptions are when the wind blows in the opposite direction of the spray. In this case, the model tends to overestimate the impact of the wind. In the test cases with strong wind, the model seems to underestimate the impact of the wind (for all wind directions). Also, the physical results generally show more spread in the droplet distribution than the model produces.

### 4.8.2 Weaknesses

The model is a simplification of snowmaking by lances, which means that some physical effects have been neglected or simplified. Euler's method produces some error at each step.

With a step size of 0,002s, the analytic error is irrelevant compared to the error from the simplifications.

How water temperature, air temperature and evaporation of water from the droplets' surfaces before freezing can affect the movement of the droplets have been neglected in the model. These are complex thermodynamic effects, and implementing these would require more simplifications and assumptions. It is therefore not sure whether implementing this would produce better results or not.

The model does not consider the flow past the droplets or collision of droplets. In reality, the flow will be separated when it hits the droplet, and the flow behind will change depending on  $Re$ . Moreover, the droplets are in reality sprayed simultaneously, and will thus affect each other. The droplets are assumed to be spherical. In reality, the aerodynamic forces will change the shape of the water droplets, as they are liquid before freezing.

### 4.8.3 Strengths

The model includes many snowmaking parameters that are possible to change. It is, therefore, possible to get an idea of how the snow from nozzles will behave under different conditions, depending on the lance setup, without testing it in real-life. It is also easier to reproduce the results from this model than it could be to reproduce real-life testing.

The model is modularized and is therefore easily adapted and changed. For example, if it were needed to implement another numerical method, this could be done by changing the `onestep.m` file.

The model is, for these reasons, well suited as an early prototype.



# 5 Concept generation

The concept generation process builds on the customer needs and target specifications found in the pre-study (Auganæs & Opheim (2017)). These requirements are reflected in Tables 5.1 and 5.2. The primary focus of the concept generation has been on the design of the snow production functionality. The most critical sub-problem is how to enable adjustment of the snow production, to meet the requirements of minimizing snow outside the tracks. The unit must at the same time be able to produce snow of sufficient quality at marginal temperatures. The light armature should be placed higher and not in too close range to the snow production unit, as reflected in the product requirements.

## 5.1 Exploration

The first step of concept generation was to explore the solution space. The information gathering process done in the pre-study can be seen as an external search for solutions. Interviews with operators and literature search has given a better understanding of the challenges of snow production. The process of gathering information is iterative through the development process. The gathered information and knowledge was then used to generate solution concepts. A brainstorming session was conducted early in the concept generation process, with the goal of collecting possible solutions to the sub-problem of adjusting the snow production. Some of the ideas can be seen in Table 5.3.

Table 5.3: Result from brainstorming

<b>Subproblem</b>	<b>Function</b>
Regulating water pressure	Can enable adjustment of droplet size and output speed
Automatic valves	Can enable switching between nozzles in different directions and sizes
Electric motor	Can enable movement of the nozzles vertically and horizontally
Foldable wind shield	Can shelter the unit from wind
Flexible joint	Can enable nozzle head movement
Swivel joint nozzles	Can enable movement of the nozzle

Table 5.1: User requirements from the pre-study

<b>Requirement description</b>	<b>Required</b>	<b>Should</b>	<b>(Value)</b>
<b>1 Operational Requirements</b>			
1.1 Easy to maintain	x		
1.2 Evenly distributed snow production	x		
1.3 Require less start-up time	x		Maximum 30 minutes
1.4 Require less people to start the production	x		
1.5 Enable snow production at marginal temperatures	x		
1.5 Minimize the amount of snow entering the ground outside the tracks (when this is expedient)		x	
1.6 The units should be automated	x		
1.7 Remote starting of the production	x		
1.8 The light from the units should satisfy requirements for international competitions	x		
<b>2 Design requirements</b>			
2.1 Nice design (approved by TV producers)	x		
2.2 Discreet (blend in with the nature)		x	
2.3 Look modern		x	
Designed to minimize stray light		x	
<b>3 Usability Requirements</b>			
3.1 Should be easy to operate	x		
3.2 Employees should be able to operate the units after one day of training		x	
3.3 Include advising system based on weather data		x	
3.4 Degree of manual control can be changed	x		

Table 5.2: Product requirements from the pre-study

Requirement description	Required	Should	Value
<b>1 Snow Production Requirements</b>			
1.1 Minimum height	x		3-6 m
1.2 Adjustment for wind	x		
1.3 Throw length		x	5-20 m
1.4 Energy consumption	x		< 1 kWh/m <sup>3</sup>
1.5 Start up time		x	
1.6 Maximum production temperature	x		-2° C
1.7 Production rate	x		10-20 m <sup>3</sup> /h
<b>2 Environmental requirements</b>			
2.1 Temperature range			-30° C to 30° C
2.2 Corrosion resistance	x		Life-time of 25 years
2.3 Withstand Wind load	x		35 $\frac{m}{s}$
2.4 Withstand fatigue			Life-time of 25 years
2.5 Withstand impact	x		
<b>3 Luminaire and lighting requirements</b>			
3.1 Heat can not affect the snow production	x		
3.2 Lighting should be able to satisfy the requirements from Lighting Class I according to European Standards	x		Avg. of min. 20lx
3.3 Light levels should be automatically adjusted according to ambient light, clock, etc.	x		
3.4 Luminaire design prevents accumulation of dirt	x		
3.4 Minimize stray light		x	
3.5 Minimum height		x	>6m is recommended for lighting
3.6 Power consumption		x	< 200 W

## 5.2 Concepts

In this section, initial concepts are presented. Some of the ideas from the initial brainstorming session was included into the concept generation. The concept generation resulted in rough sketches and 3D-models with short descriptions.

### 5.2.1 Concept 1

This concept uses a joint between the inlet pipe and lance head. Two actuators that are mounted within the mast will be able to move the head in both horizontal and vertical direction. This is illustrated in Figure 5.1. With input data from a weather station, the lance head can be moved to compensate for wind and temperature. The horizontal movement will lead to better distribution of snow along the track. Vertical tilting will control the airtime of the droplets, which could eliminate the need for nozzles at different sizes.

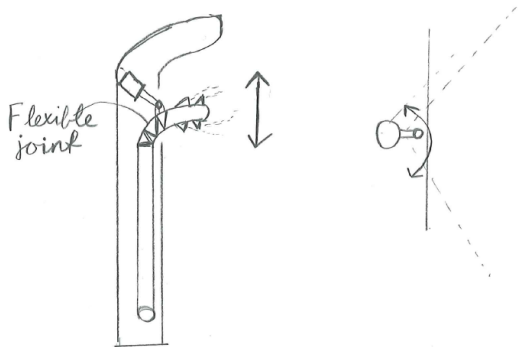


Figure 5.1: Sketch of Concept 1



Figure 5.2: CAD model of Concept 1



### 5.2.2 Concept 2

Concept 2 consists of an internal lance with nozzles in several steps, where each step has a different vertical tilt. The nozzle tilting upwards should be the largest, since bigger droplets need more time to freeze. For horizontal adjustment, an actuator or a motor should enable the lance to rotate 180° (independently of the rest of the mast) as illustrated in Figure 5.3.

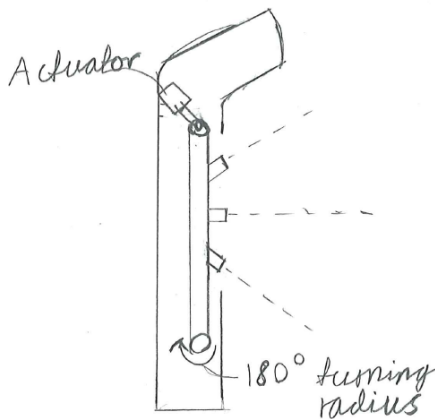


Figure 5.3: Sketch of Concept 2



Figure 5.4: CAD model of Concept 2

### 5.2.3 Concept 3

Concept 3 resembles an ordinary lance that is integrated within a light mast. For horizontal adjustment, a motor should be mounted at the foundation. The lance should also be allowed to turn ca.  $180^\circ$  in the horizontal plane. For vertical adjustment, an actuator should raise the arm from  $0^\circ$  to  $90^\circ$  as shown in Figure 5.5. When the lance is not producing snow, the lance should be raised in line with the mast, and thereby be "hidden" inside the mast.

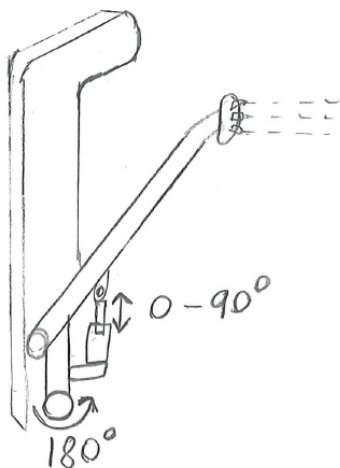


Figure 5.5: Sketch of Concept 3



Figure 5.6: CAD drawing of Concept 3

### 5.2.4 Concept 4

This concept uses a rack and a gear to adjust the lance arm up and down. This should make it possible to adjust the air time and hit rate, according to the weather conditions. The nozzles on the arm should be placed over the middle of the track, which should eliminate the need for horizontal adjustment. The nozzles should be pointed in opposite directions along the track, while one nozzle should enable production straight down in the track as illustrated in Figure 5.7.

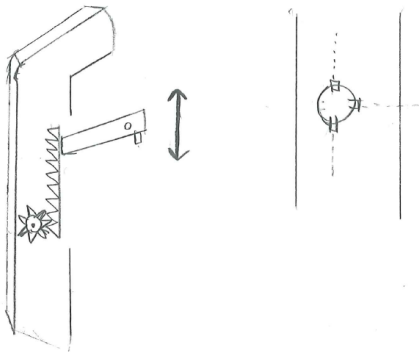


Figure 5.7: Sketch of Concept 4



Figure 5.8: CAD drawing of Concept 4

### 5.2.5 Concept 5

Concept 5 was created in conversation with the operators at Granåsen Ski Arena. The concept utilizes several nozzles, which are positioned at different horizontal angles. Valves are used to switch between different nozzles in stages. This nozzle configuration makes it possible to adjust the snow production in different horizontal directions, as illustrated in Figure 5.9. Two different sizes of nozzles should be utilized to have efficient production at different temperatures.

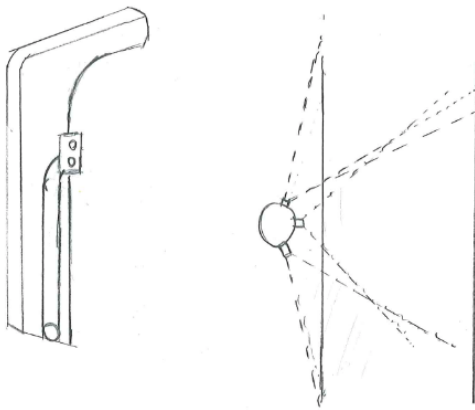


Figure 5.9: Sketch of Concept 5



Figure 5.10: CAD Drawing of Concept 5

## 6 Concept Testing and Evaluation

Concept testing is closely related to product prototyping. Ulrich & Eppinger (2012) defines prototype as “an approximation of the product along one or more dimensions of interest.” In this thesis, the most important dimension of interest is to find the best way to adjust the snow production for cross-country tracks. The primary purpose of testing is to learn if the designs work as intended or not. Testing also provides a basis for comparing the different concepts. Evaluation of the concept is based on feedback from operators at Granåsen Ski Arena and Åre Ski Resort.

### 6.1 Analytic Prototyping of the Concepts

An analytic prototype is a mathematical or visual approximation of the product. They are often more flexible than a physical prototype, meaning that it requires little effort to change different parameters to test different designs. For concept testing, the analytic model explained in Chapter 4 has been used as a prototype.

Each concept has undergone the same test procedure. Each concept has been tested with zero wind to find the best height, angle, and size of the nozzle for conditions where there is virtually no wind. After that,  $1\text{ m/s}$  wind has been introduced at  $0^\circ$ ,  $45^\circ$ ,  $90^\circ$ ,  $135^\circ$  and  $180^\circ$  degrees.  $0^\circ$  rotation corresponds to the x-axis, while  $90^\circ$  rotation corresponds to the y-axis, as described in Figure 6.1. At each wind angle, the different horizontal and vertical adjustment possibilities for the nozzles has been tested, to reach the best possible hit rates.

After each test run, the variable input parameters have been registered along with the corresponding air-time and hit rate. These test data can be found in Appendix E.

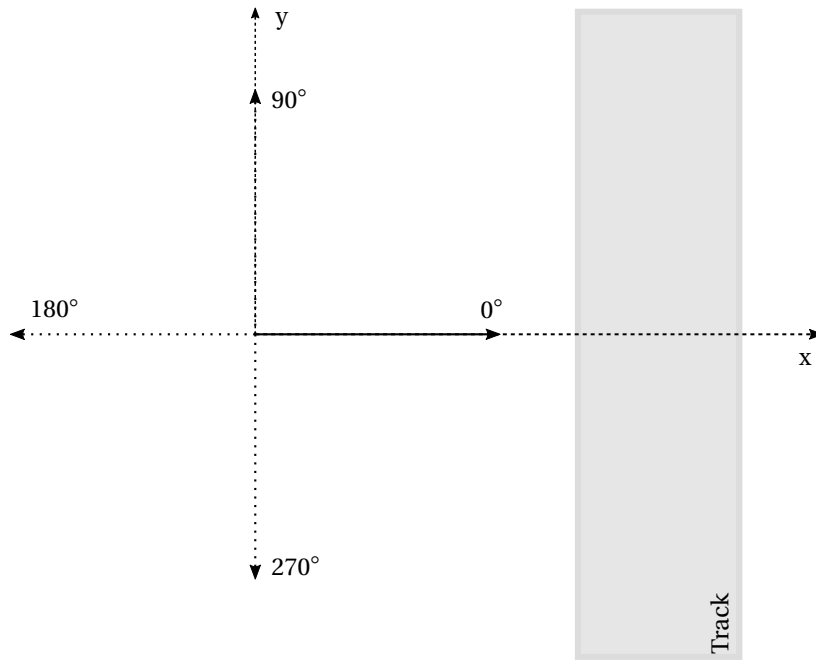


Figure 6.1: Reference coordinate system for nozzle and wind orientation

Table 6.1: Fixed test parameters for concept testing

Parameter	Value
Outlet speed	60m/s at 30 bar
Fan angle	$\approx 50^\circ$ (normal distribution)
Number of droplets	$\geq 1000$
Droplet radius	$\mu \in [150, 300], \sigma \in [25, 75]$
Track width	5m
Distance from the track	2m

### 6.1.1 Concept 1

The flexible joint was set to be adjusted from  $0^\circ$  to  $90^\circ$  horizontally and  $0^\circ$  to  $45^\circ$  vertically. It was found that a height of  $7m$  was good in order to ensure sufficient air-time.

Table 6.2: Learning Outcome, Concept 1

Dimension of Interest	Learning Outcome
Droplet size	The droplet diameter should be $300\mu m$ on average to secure fully freezing at a wet bulb temperature of $-4^\circ C$ , given a height of $7m$ . Such small droplets are sensitive to wind. If the nozzle sprays at $0^\circ$ relative to the track, a wind speed of $1m/s$ in the same direction is sufficient to carry the snow beyond the track.
Rotation	It is possible to obtain a good hit rate for wind angles between $0^\circ$ and $90^\circ$ . Wind angles that are closer to $180^\circ$ are critical.
Vertical adjustment	Vertical tilting of the nozzle gives better airtime. The adjustment have little effect on hit rate in windy conditions. A low nozzle position will not give sufficient air time.
Temperature adjustment	This concept offers no way to increase the production when the temperature allows it.

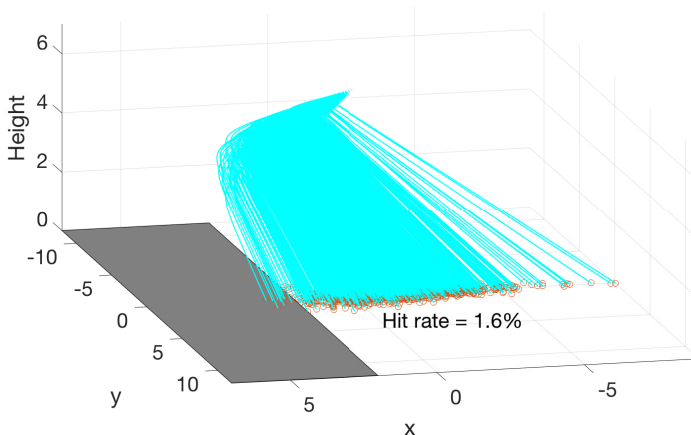


Figure 6.2: Example simulation: Simulation 17. Tilting the nozzle  $25^\circ$  down does not increase the hit rate when the wind is oriented  $180^\circ$ .

### 6.1.2 Concept 2

Three droplet sizes were tested at different vertical angles:  $d = 300\mu\text{m}$  at  $0^\circ$ ;  $d = 400\mu\text{m}$  at  $25^\circ$ ; and  $d = 500\mu\text{m}$  at  $45^\circ$ . The horizontal adjustment was tested from  $0^\circ$  to  $90^\circ$ . Also for Concept 2, a height of  $7\text{m}$  gave sufficient air time.

Table 6.3: Learning Outcome, Concept 2

Dimension of Interest	Learning Outcome
Droplet size	A droplet diameter between $d = 400\mu\text{m}$ and $d = 500\mu\text{m}$ need more air time to freeze entirely at minimal temperatures. These droplet sizes would be better for colder conditions.
Rotation	With $1\text{m/s}$ wind at $0^\circ$ it is important to have horizontal adjustment up to $90^\circ$ . Larger droplets can give a better hit rate at $135^\circ$ and $180^\circ$ wind direction. However, in line with expert recommendations, it is still to low for production.
Vertical adjustment	The vertical tilting of the bigger nozzles is not enough to ensure sufficient airtime.
Temperature adjustment	The smallest nozzles can produce snow at a wet-bulb of $-4^\circ\text{C}$ . At colder temperatures, the other nozzles can be used as well. Such a solution enables the production of snow with good quality at marginal temperatures, as well as opportunity to produce a large volume at better temperatures. To secure enough air time for the biggest droplets

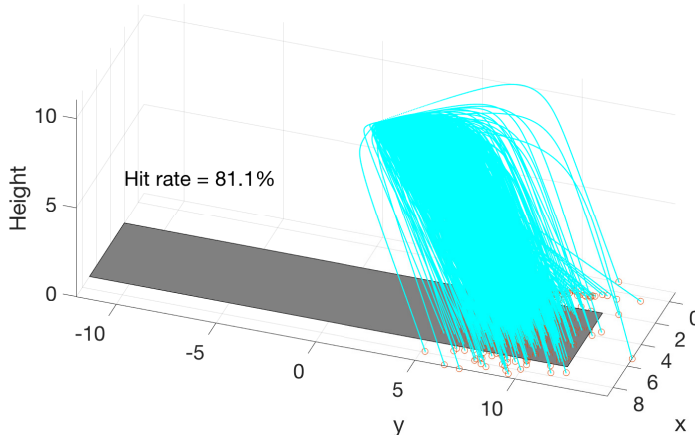


Figure 6.3: Example simulation: Simulation 22. When the wind is oriented  $90^\circ$ , a horizontal adjustment of  $45^\circ$  of the nozzle gives the best hit rate.



### 6.1.3 Concept 3

A lance with a height of  $10m$  is tested with three different steps. Because Concept 3 has an arm, the nozzles will not be  $2m$  from the track, but somewhere above. With a vertical angle of  $80^\circ$ , the nozzles will be  $9,8m$  above the ground, and they will spray  $35^\circ$  upwards compared to the ground. When the arm is lowered to  $45^\circ$ , the nozzles will be  $7m$  above the ground, and spray parallel to the ground.

Table 6.4: Learning Outcome, Concept 3

Dimension of Interest	Learning Outcome
Droplet size	At zero wind, one can note that the hit rate goes down as the droplet size increases. This decrease is due to the increased trajectory of larger droplets, making them deposit beyond the track.
Rotation	This solution can to some extent handle wind between $135^\circ$ and $180^\circ$ , because the lance arm have a long range. A hit rate of about 60% can be achieved.
Vertical adjustment	Vertical adjustment have little effect on hit rate in windy conditions. When the arm is lowered to $45^\circ$ , with a horizontal angle of $73^\circ$ , the hit rate is 49%, but the airtime for the large droplets is too short.
Temperature adjustment	Three different steps enable temperature adjustment. The smallest droplets have sufficient air time.

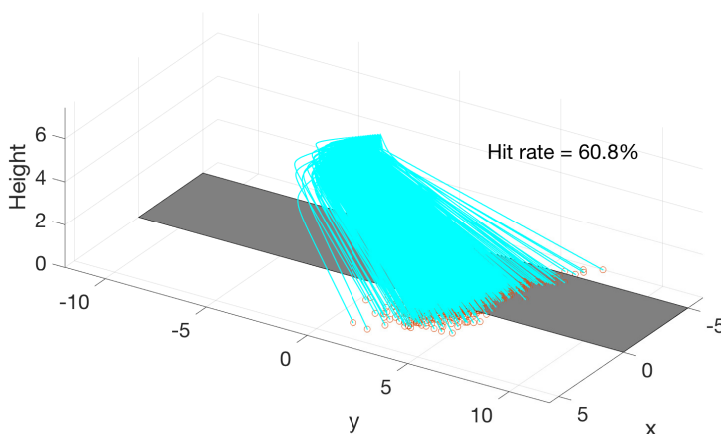


Figure 6.4: Example simulation: Simulation 23. The only simulation that gives moderate hit rates when the wind is oriented  $135^\circ$ .

### 6.1.4 Concept 4

The nozzle was tested in the middle of the track, with one nozzle pointing straight down, and one pointing along the track. The height adjustment of the arm was set from 5m to 9m.

Table 6.5: Learning Outcome, Concept 4

Dimension of Interest	Learning Outcome
Droplet size	The nozzle pointing down needs a droplet diameter of $200\mu\text{m}$ or smaller to be able to freeze in time. The nozzle pointing along the track with a droplet size of $300\mu\text{m}$ have good air time at 9m.
Rotation	At wind speeds of $1\text{m/s}$ the smaller nozzle pointing down had a slightly better hit rate in all wind directions, than the large nozzles pointing to the side. This solutions only produce good hit rates at wind at $90^\circ$ . For the other directions, the hit rates are somewhat to low.
Vertical adjustment	The height adjustments are only useful at 0 wind or at $90^\circ$ to increase air time. In other wind directions, height adjustment affects the hit rate negatively.
Temperature adjustment	When temperature is $-4^\circ\text{C}$ the arm must be at 7m or higher. But at colder conditions it can be placed at 5m.

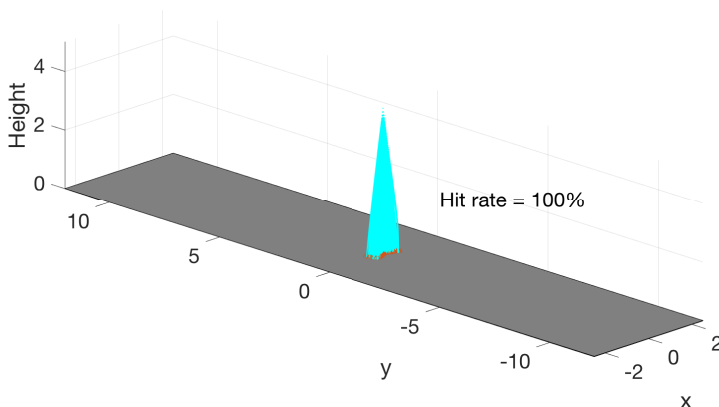


Figure 6.5: Example simulation: Simulation 1. Nozzle producing straight down in no wind.

### 6.1.5 Concept 5

It was chosen to test three nozzles at different horizontal angles. It was also tested two different sizes of nozzles.

Table 6.6: Learning Outcome, Concept 5

Dimension of Interest	Learning Outcome
Droplet size	A droplet size of $d = 300\mu\text{m}$ is required to have sufficient airtime at $-4^\circ\text{C}$ and a height of 7m.
Rotation	Possible to obtain good hit rates for many wind directions. At zero wind the preferred vertical angle is low for smaller droplets and around $45^\circ$ s for bigger droplets. At $1\text{ m/s}$ wind at $0^\circ$ , it would be best to have a horizontal angle close to $90^\circ$ . At wind oriented between $135^\circ$ and $180^\circ$ , hit rates are bad, so production would not be recommended.
Vertical adjustment	A vertical tilt of $35^\circ$ gives the same hit rate as $0^\circ$ tilt, but better air time.
Temperature adjustment	The smallest nozzle can produce snow at a wet-bulb of $-4^\circ\text{C}$ . At colder temperatures, the bigger nozzle can be used as well.

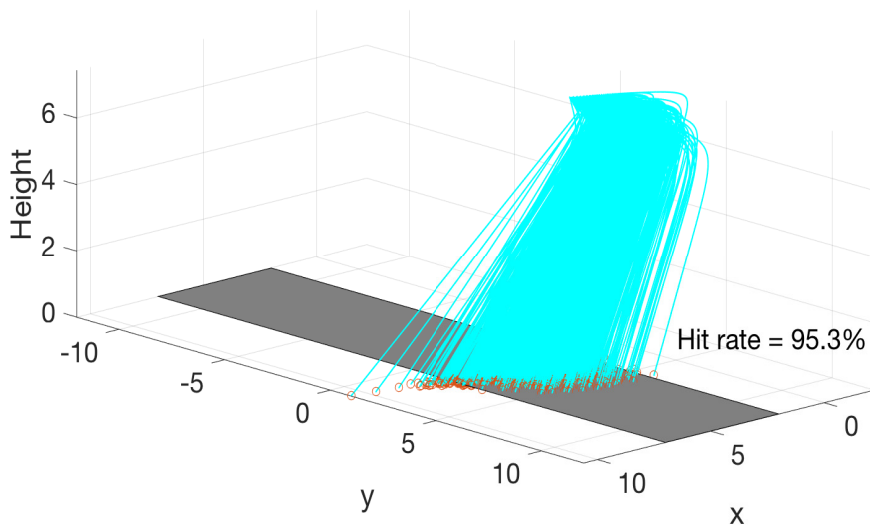


Figure 6.6: Example simulation: Simulation 11. This simulation shows how a horizontal nozzle adjustment of  $90^\circ$  is great when the wind is oriented  $0^\circ$ .

## 6.2 Feedback from Operators at Granåsen and Åre

Feedback from meetings with experienced snow operators has been necessary to get an understanding of what their thoughts on the concepts were. Notes from the interview in Åre is found in Appendix B. Both general insights on snowmaking and specific learning about the concepts were obtained from the discussions. A summary from the conversations can be found in Appendix A. Specific feedback on the concepts is presented in Tables 6.7 to 6.11.

### 6.2.1 Concept 1

Table 6.7: Feedback on Concept 1

Aspect	Feedback
Nozzles	Making the nozzles point downwards is often not relevant, as the droplets will not get sufficient air time, causing poor snow quality.
Maintenance	It should be easy to lower and dismount the lance head for maintenance. Operators should not need to use a ladder to dismount the lance head at a fixed height.
Design/Aesthetics	It would be aesthetically pleasing to hide the lance head within the mast.

### 6.2.2 Concept 2

Table 6.8: Feedback on Concept 2

Aspect	Feedback
Nozzles	The operators expressed the same concern about nozzles tilted downwards. They do not think it is possible to point the nozzle downwards, even if the nozzles produce small droplets. They meant that a turn radius of 180° was very much, and proposed that 90° would be sufficient to cover the tracks.
Maintenance	It should be easy to lower and dismount the lance head for maintenance. Operators should not need to use a ladder to dismount the lance head at a fixed height.
Design/Aesthetics	The lance looks more discreet. This is positive considering TV-production, etc. The operators mentioned some concern about the significant cut in the mast.

### 6.2.3 Concept 3

Table 6.9: Feedback on Concept 3

Aspect	Feedback
Nozzles	Similar to the existing lances.
Maintenance	Similar to the existing lances.
Design/Aesthetics	Not as discreet. Easier solution. The first concern was that the lance would come too close to the light and then snow could drift onto the armature and block the light.

### 6.2.4 Concept 4

Table 6.10: Feedback on Concept 4

Aspect	Feedback
Nozzles	Similar to the existing lances. One concern was that the lance would come too close to the light armature.
Maintenance	It should be easy to lower and dismount the lance head for maintenance. Operators should not need to use a ladder to dismount the lance head at a fixed height.
Design/Aesthetics	This solution looks simpler. It is more similar to the existing lances. The mast appears massive and is not as discreet.

### 6.2.5 Concept 5

Concept 5 was developed on the basis on the experience from the trip to Åre and discussion with supervisor.

Table 6.11: Feedback on Concept 5

Aspect	Feedback
Nozzles	Concern that this solution could end up with too many nozzles was expressed.
Maintenance	Fixed nozzles at 7m can make maintenance harder.
Design/Aesthetics	No moving parts will simplify the design. Switching between many stages will require several valves and pipes. This concept has a minimalist look.



# 7 Concept selection

To choose a concept is an important part of the product development process. The goal of concept selection is to compare relative strengths and weaknesses of the concepts and to select one or more ideas for further investigation and development. The selection is made based on customer needs and other relevant criteria.

## 7.1 Concept scoring

To better differentiate between competing concepts, scoring is used. The relative importance of the selection criteria is used to focus the selection. The weighted sum of the ratings serves as the score of the concept (Ulrich & Eppinger (2012)). The first task is to select the criteria which the concepts are scored after. These should be based on measurable parameters to be able to distinguish between the concepts. However, criteria like discreet design are hard to measure and are based on feedback from the visual part of the design. Table 7.1 explains the chosen selection criteria for the scoring.

Table 7.1: Selection Criteria

<b>Selection criteria</b>	<b>Explanation</b>
Simplicity of Design	Complex design includes complex parts and shapes. A complex design can complicate the manufacturing and make the unit expensive.
Discreet design	Discreet design is essential to make the unit blend in with the environment. The television production demands to capture the natural environment.
Hit rate	Hit rate is the percentage of the produced snow that reach the slope. How good hit rate a concept can produce is a result of the adjustment possibilities.
Air-time	The droplets require a certain air-time to be able to freeze. The needed air-time varies with the wet-bulb temperature and droplet size.
Ease of maintenance	If any parts get broken, the operators should not experience much difficulty or use too much time while fixing it.

### 7.1.1 Rating the Concepts

When rating the concepts, a reference concept is used for comparison. In this thesis, Concept 3 will be the reference. This concept was chosen because Concept 3 consists of an existing solution where some of the selection criteria are known. Table 7.2 shows how the rating is compared to the reference concept.

Table 7.2: Description of the Rating Scores

Relative performance	Rating
Much worse than reference	1
Worse than reference	2
Same as reference	3
Better than reference	4
Much better than reference	5

In the ranking of the concepts, weighted scores are used because some functions are more critical than others. The percentage of the weighted score in table 7.3 are identified through customer needs and product requirements. The total score of the concept  $S_j$  is then the sum of the weighted score:

$$S_j = \sum_{i=1}^n k_{ij} w_i$$

Where  $k_{ij}$  is the raw rating of concept  $j$  for the  $i$ 'th criterion,  $w_i$  is the weight of the  $i$ 'th criterion, and  $n$  is the total number of criteria.

Table 7.3: Concept Scoring

Selection Criteria	Weight	C1	C2	C3	C4	C5
Simplicity	20%	1	2	3	1	4
Discreet Design	10%	4	5	3	3	5
Hit Rate	35%	5	5	3	2	5
Airtime	20%	2	2	3	1	2
Ease of Maintenance	15%	2	2	3	2	2
<b>Weighted Sum</b>	<b>100%</b>	<b>3,05</b>	<b>3,35</b>	<b>3,00</b>	<b>1,70</b>	<b>3,75</b>



### 7.1.2 Ranking the Concepts

As seen in Table 7.3, Concept 5 scores the best. It stands out from the others by having a simple design, while it still provides good hit rates in the testing. The air time score is lower than for Concept 3 because the nozzle height is fixed. Still, Concept 5 secures sufficient airtime at minimal conditions with a nozzle height of  $7m$  and droplet size of  $d = 300\mu m$ . The ease of maintenance is lower for Concept 5 because it is assumed that maintenance on a fixed unit of  $7m$  is harder than a lance that can be lowered. However, a less complicated design, with no moving parts, would most likely need less maintenance overall.



# 8 Concept Refinement

After some considerations and discussions, a refinement of concept five was performed. This refinement involved specifying the pointing angle of the nozzles, and how many nozzles that are needed. The distance from the track was reduced from  $2m$  to  $1m$ . This was done to avoid having to clear the forest, and to ensure proximity to the track for the light armature. By using the analytic prototype, the best possible nozzle configuration has been found. The model has been run setting the angle from  $0^\circ$  to  $90^\circ$  (according to Figure 6.1), with an interval of  $5^\circ$  or  $10^\circ$ . The same procedure was repeated for different wind angles and speeds. When evaluating the results, hit rates are classified as good, medium and bad according to Table 8.1.

Table 8.1: Hit rate classification

Classification	Hit rate
Good	70% to 100%
Medium	45% to 69%
Bad	0% to 44%

## 8.1 Rotation of Nozzles (Horizontal Angle)

In all simulations, the height of the nozzles was set to  $7m$ . The vertical angle is set to  $0^\circ$  while changing the horizontal angle. The track width is set to  $6m$ .

Figure 8.1 shows that the best possible horizontal nozzle angle is at ca.  $45^\circ$ . This result insinuates that one of the horizontal nozzle angles should be ca.  $45^\circ$ , as there is often good wind conditions (ca.  $0,5m/s$ ) in Granåsen Ski Arena. The track will, in many places, be naturally shielded from wind, as there is forest or rocks on each side.

Figure 8.2 shows that the best possible hit rate in wind oriented  $0^\circ$  (from behind the mast) is obtained with a nozzle rotation of  $90^\circ$ . Nozzles rotated  $45^\circ$  will, in this case, obtain a bad hit rate, as the wind makes the snow fly to the other side at the track. Figure 8.3 shows that the best hit rate when the wind is oriented  $45^\circ$  is obtained at a nozzle rotation of  $80^\circ$ .

Figures 8.4 and 8.5 show that the best possible hit rates at wind oriented  $90^\circ$  are obtained with a nozzle rotation of ca.  $50^\circ$ . At  $1m/s$ , good hit rates are obtained with rotations from  $35^\circ$  to

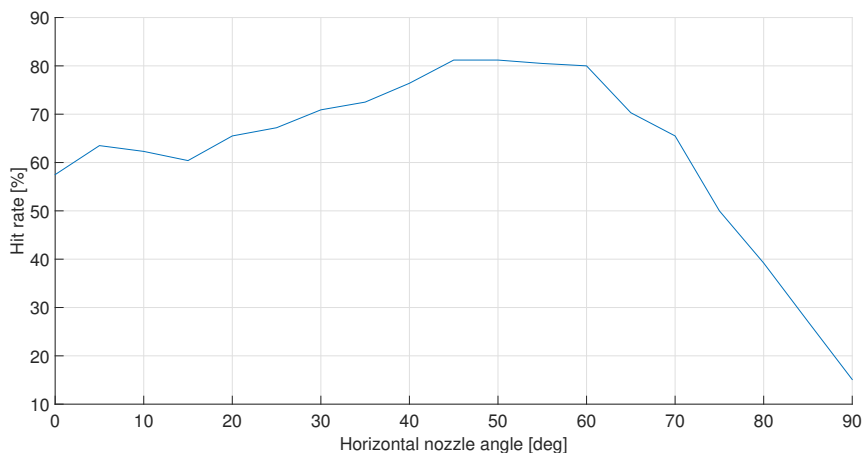


Figure 8.1: Hit rates in  $0m/s$  wind at horizontal angles from  $0^\circ$  to  $90^\circ$  ( $0^\circ$  vertical angle)

$65^\circ$ . As the wind strength increases, the domain of rotation angles which can produce good hit rates decreases.

The analyses show that when there is no wind or  $90^\circ$  wind angle, the best hit rates are obtained with  $45^\circ$  to  $50^\circ$  angle of horizontal rotation. A nozzle rotation of  $45^\circ$  was therefore chosen, as this rotation performed best in windless conditions. In conditions where the wind is oriented  $0^\circ$ , a nozzle rotation close to  $90^\circ$  is preferred. However, spraying the snow directly to the side would in many cases require open space next to the unit. This would require nearby trees to be cut down, and, moreover, digging or cracking of rocks. Therefore, a second nozzle rotation of  $80^\circ$  was chosen, even though an angle of  $90^\circ$  theoretically gives the best hit rates. The chosen nozzle configuration is illustrated in Figure 8.6. The nozzles are oriented  $45^\circ$  and  $80^\circ$  and mirrored about the x-axis. At each orientation, there are two nozzle steps. The first step (marginal step) can be used in marginal conditions ( $T_{wb} \leq -3^\circ$ ), whereas the second step can be turned on when the conditions are good ( $T_{wb} \leq -7^\circ$ ).

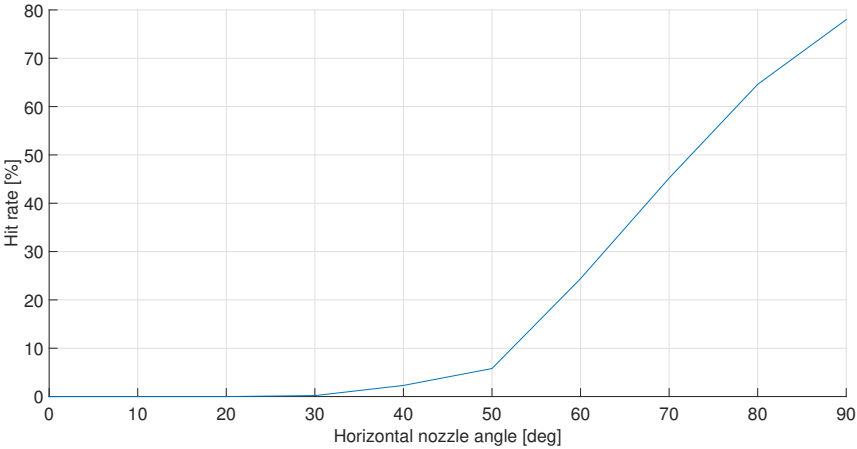


Figure 8.2: Graph showing hit rates in 1 m/s wind oriented 0° (0° vertical angle)

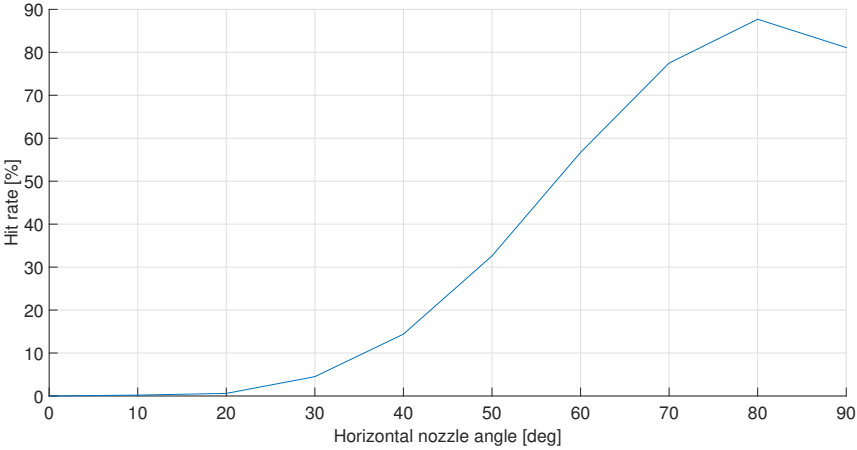


Figure 8.3: Graph showing hit rates in 1 m/s wind oriented 45° (0° vertical angle)

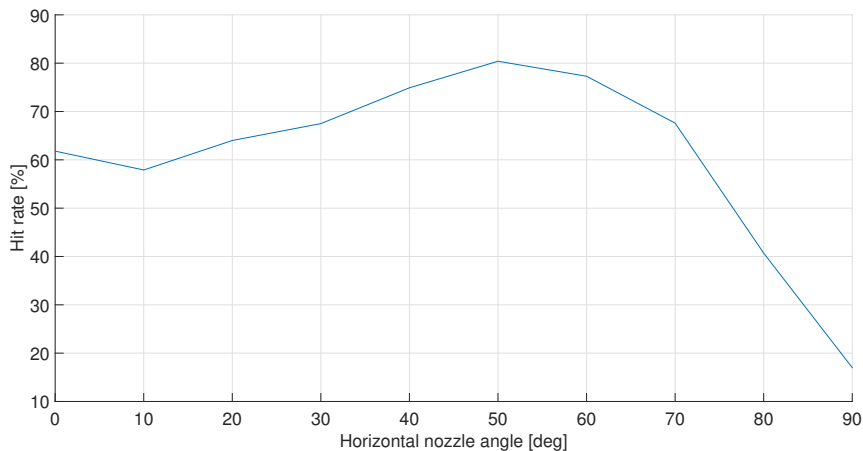


Figure 8.4: Graph showing hit rates in 1 m/s wind oriented 90° (0° vertical angle)

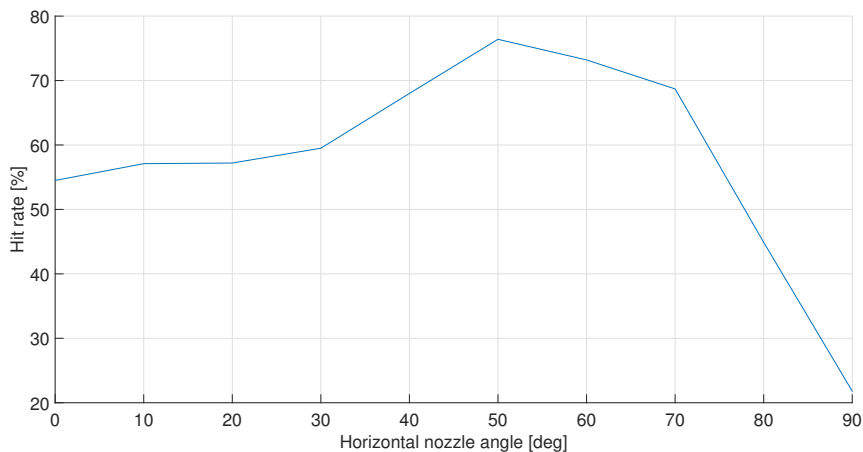


Figure 8.5: Graph showing hit rates in 5 m/s wind oriented 90° (0° vertical angle)

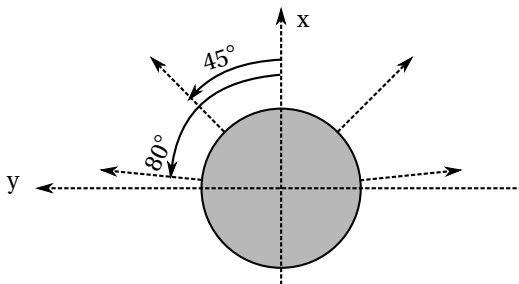


Figure 8.6: Nozzle configuration

## 8.2 Tilting of Nozzles (Vertical Angle)

Tilting the nozzle upwards will contribute to the droplets' airtime and hit rate to some extent. However, tilting of the nozzles has much less impact on the hit rates than the horizontal angle. Figure 8.7 shows that the hit rates can be increased by ca. 5% with a vertical tilt of  $50^\circ$ . However, tilting the nozzles  $50^\circ$  could make the droplets very exposed to the wind, as they will achieve a height much higher than  $7m$  and increased air time.

Figure 3.4 shows that a droplet with diameter of  $300\mu m$  will require about  $6s$  to freeze at a wet bulb temperature of  $-4^\circ C$ . The height of  $7m$  was chosen with this requirement in mind. Therefore, it is not necessary to tilt the nozzles upwards, even if increased airtime could be beneficial in some cases. The vertical angle of the nozzles is therefore chosen to be  $0^\circ$ .

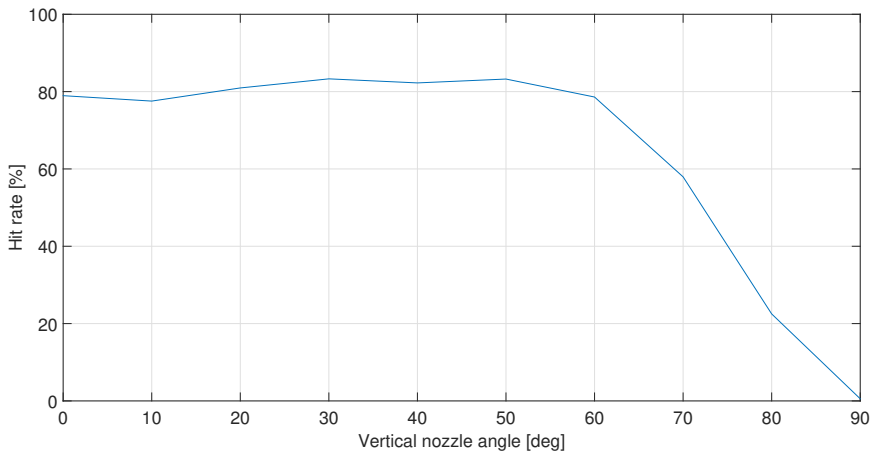


Figure 8.7: Hit rates with vertical nozzle tilting, zero wind, nozzles rotated  $45^\circ$





## 9 Structure and Design

The goal of the structure and design phase is to determine the design with regard to structural and functional requirements. A design proposal has been carried out to be able to give an estimate of the product cost and proportions. Strength calculations should verify the structure according to standards for wind load.

### 9.1 Pipe Dimensions

Appendix F provides information about flow rates and drop size distribution of BETE flat fan nozzles. For the marginal step, a droplet diameter smaller than  $300\mu m$  is desirable. For this droplet diameter, an NF 15 flat fan nozzle can be used. At 30 bar, these have a water flow of  $18,7l/min$ . For the second stage, a droplet diameter of  $400\mu m$  or larger is wanted. Therefore will the NF 30 nozzle be used. These nozzles have a flow of  $37,4l/min$ . The air atomizer nozzles can produce droplets with diameter between  $20\mu m$  and  $200\mu m$ , and will consume  $8m^3/h$  air (at normal atmospheric pressure) and  $9l/h$  water. Table 9.1 provides an overview of the different stages. Each stage will have four nozzles (one per nozzle orientation). However, it is assumed that only two of them will be in use at the same time (two at 45 degrees and two at 80 degrees). To estimate the required diameter of the water and air pipes the following equation is used:

$$d = \sqrt{\frac{Q}{3600v} \frac{4}{\pi}},$$

where  $Q$  is the flow rate,  $v$  is the velocity and  $d$  is the inner pipe diameter. Allowable water velocity is set to  $1,5m/s$  and air velocity to  $20m/s$ . These values are set to avoid high-pressure losses due to friction (Saskatchewan Environment (2004)).

Table 9.1: Snow production stages

Stage	Description	Nozzles	Flow
Marginal stage	Configured for marginal conditions. Can produce high quality snow at a wet-bulb temperature of $-4^{\circ}C$ .	2 (water nozzles)	$37,4l/min$
Second stage	For use in colder weather. This stage will supplement the marginal stage at wet-bulb temperatures lower than $-8^{\circ}C$	2 (water nozzles)	$74,8l/min$
Nucleator	The nucleator stage produces very small droplets. These help the bigger droplets from the water nozzles to freeze	2 (air atomizing nozzles)	$16m^3/h$ (at normal atmospheric pressure)

Table 9.2: Pipe selection

Flow	Inner diameter	Pressure class	Suitable pipe diameter	Wall thickness
$37,4l/min$ (water)	$23,0mm$	ANSI sch.40	$26,67mm$ (3/4")	$2,87mm$
$74,8l/min$ (water)	$32,5mm$	ANSI sch.40	$42,16mm$ (1 1/4")	$3,56mm$
$2,62m^3/h$ (Actual air flow)	$6,83mm$	ANSI sch.40	$10,29mm$ (1/8")	$1,73mm$

## 9.2 Standard for Wind Load

The characteristic wind pressure  $q(z)$  is calculated according to Standard Norge (2013a) and Standard Norge (2009):

$$q(z) = \delta \beta f c_e(z) q(10) = 0,91 \times 1,3 \times 1 \times 1,63 \times 388,7 \frac{N}{m^2} = 749,5 \frac{N}{m^2}, \quad (9.1)$$

, where  $\delta$  is a factor related to column size,  $\beta$  is a factor dependent on the dynamic behavior,  $f$  is a factor related to topography,  $c_e(z)$  is a factor dependent on the terrain of the site and height above the ground  $z$ .  $q(10)$  is the reference wind pressure according to Equation 9.2:

$$q(10) = \frac{1}{2} \rho C_s^2 V_{ref}^2 = \frac{1}{2} \times 1,25 \frac{kg}{m^3} \times (\sqrt{0,92})^2 \times \left(26 \frac{m}{s}\right)^2 = 388,7 \frac{N}{m^2}, \quad (9.2)$$

where  $V_{ref}$  is the mean wind velocity at 10m above ground level. This value is found in NS-EN 1991-1-4:2005 to be 26m/s for Trondheim Municipality.  $C_s$  is a factor that converts  $V_{ref}$  from an annual probability of exceedence of 0,02 to other probabilities. For lighting columns with a mean return period of 25 years,  $C_s$  can be set to  $\sqrt{0,92}$ .  $\rho$  is the air density.

Deflection is also an important design factor according to Standard Norge (2013b). Max horizontal deflection of each luminary connection should not exceed  $0,04 \times (h + w)$ , where  $h$  is the nominal height of the mast, and  $w$  is the bracket projection.

### 9.3 Jet Discharge Propulsion

As there should be no snow production in such strong wind, the pressure forces which occur when the production is ongoing is not relevant when designing for wind loads. The force induced by the water sprayed from the nozzle can be expressed using B:

$$F = 2A(p_1 - p_2) = 2 \times \pi \times (0,0017m)^2 \times (30 \times 10^5 Pa - 10^5 Pa) = 52,7N, \quad (9.3)$$

where  $A$  is the orifice area of the nozzles and  $p_1$  is the pressure before the nozzle and  $p_2$  is the pressure after the nozzle (Engineering ToolBox (2013)). Multiplied with the total number of nozzles, the force will still not extend the maximum wind force which the unit must withstand. It is therefore not interesting to consider this force when designing the unit

### 9.4 Global Design by Hand Calculations

This section presents hand calculations for design against material failure. Yield and elastic deformations have been considered. For these hand calculations, the mast is simplified to a hollow cylinder with inner radius  $r_i$  and outer radius  $r_o$  as shown in Figure 9.1. The lighting armature is simplified to a rectangular prism. The dimensions of this prism are shown in Figure 9.2 and the weight of it is assumed to be 7kg.

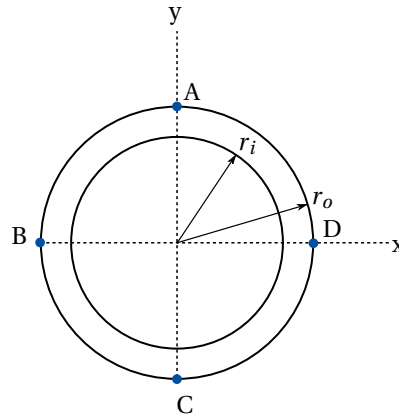


Figure 9.1: Cross-sectional area of the unit . The points A, B, C, and D are critical points where maximal stresses may occur.

### 9.4.1 Governing Equations

The following equations are the area  $A$ , second area moment of inertia  $I$ , and the polar area moment of inertia  $J$ :

$$A = \pi (r_o^2 - r_i^2), \quad (9.4)$$

$$I = \frac{\pi}{4} (r_o^4 - r_i^4), \quad I_x = I_y = I, \quad (9.5)$$

$$J = \frac{\pi}{2} (r_o^4 - r_i^4) \quad (9.6)$$

For an evenly distributed force along a beam (cantilever beam), the following formulas apply for shear  $V$ , moment  $M$  and deflection  $\delta$ :

$$V(L) = qL, \quad M(L) = -\frac{qL^2}{2}, \quad (9.7)$$

$$\delta_{max} = \frac{qL^4}{8EI}, \quad (9.8)$$

where  $E$  is the Elastic Modulus and  $G$  is the shear modulus of the material. For a concentrated load  $P$ , the corresponding formulas are:

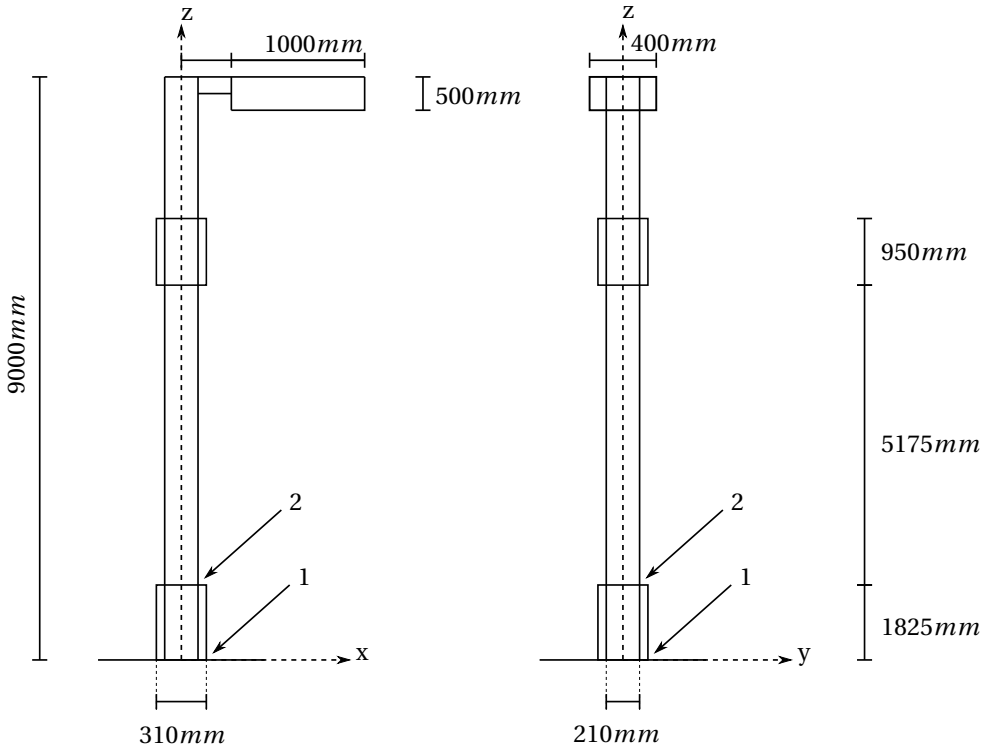


Figure 9.2: Simplified geometry of the mast

$$V(L) = P, \quad M(L) = PL, \quad (9.9)$$

$$\delta_{max} = \frac{PL^3}{3EI}. \quad (9.10)$$

Shear force and moment cause normal stress  $\sigma$  and transverse shear stress  $\tau$ :

$$\sigma = \frac{Mc}{I}, \quad \sigma_{max} = \frac{My}{r_o}, \quad (9.11)$$

$$\tau = \frac{VQ'}{It}, \quad \tau_{max} = \frac{VQ'}{Ir_o}, \quad Q' = \bar{y}' A', \quad (9.12)$$

where  $c$  is the distance perpendicular from the neutral axis to the point where  $\sigma$  is to be determined, and  $t$  is the width of the cross-sectional area at the point where  $\tau$  is to be determined.  $A'$  is the portion of the cross-sectional area above (or below) the line where  $t$  is measured and

$\bar{y}'$  is the distance from the neutral axis to the centroid of  $A'$ . If there is a force causing torque  $T$ , this will cause shear stress  $\tau$  according to:

$$\tau = \frac{Tr_i}{J}. \quad (9.13)$$

Von Mises criterion suggests that yield occurs when  $\sigma_e = \sigma_y$ , where  $\sigma_y$  is the yield strength of the material, and the von Mises equivalent  $\sigma_e$  is:

$$\sigma_e = \sqrt{\frac{1}{2} \left[ (\sigma_x - \sigma_y)^2 + (\sigma_y - \sigma_z)^2 + (\sigma_z - \sigma_x)^2 \right] + 3\tau_{xy}^2 + 3\tau_{yz}^2 + 3\tau_{zx}^2} \quad (9.14)$$

for stresses in three dimensions. For the calculations, the material constants  $E$ ,  $G$  and  $\sigma_y$  for aluminium are used.

### 9.4.2 Load Cases

Two load cases considered in this design: one where the wind is parallel to the y-axis and thus hits the light armature sideways, causing torsion in the mast; and one where the wind is parallel to the x-axis. Points 1 and 2 marked in Figure 9.2 are the two critical points on the mast that need to be considered in each case. There are two critical points of the cross-section that have to be checked for each point on the mast: at  $y_{max}$  and  $x_{max}$  where  $\sigma_{max}$  and  $\tau_{max}$  may occur. It can be shown that the point where the stress from the wind bending is biggest always will be the critical point.

The weight of the light armature  $W_L$  causes a bending moment about the y-axis that is the same for both cases. The moment diagram for this load is shown in Figure 9.3.  $l$  is the distance from the center of the mast to the lighting armature's center of mass. The bending moment from the light armature causes tension in point B and D in the cross-section.

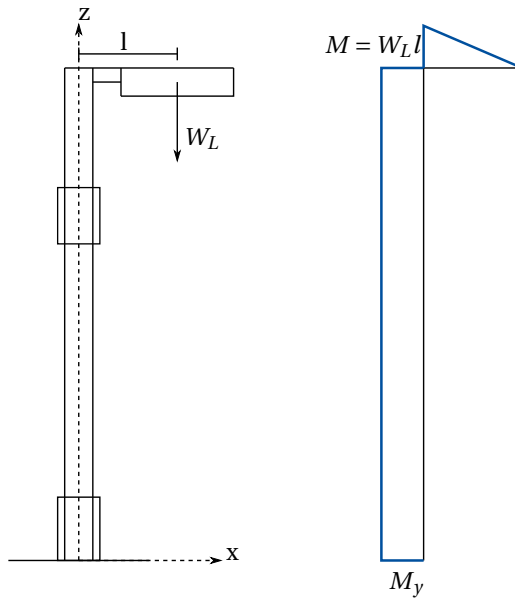


Figure 9.3: Bending moment caused by the weight of the light armature

The dimensions of the cross-section is set to be  $r_{i,1} = 150\text{mm}$  and  $r_{o,1} = 155\text{mm}$  at Point 1, and  $r_{i,2} = 100\text{mm}$  and  $r_{o,2} = 105\text{mm}$  at Point 2. Inserting these radii into Equations 9.5 and 9.6 gives  $I_1 = 5,572 \times 10^7 \text{mm}^4$  and  $I_2 = 1,963 \times 10^7 \text{mm}^4$ , and  $J_1 = 1,115 \times 10^8 \text{mm}^4$  and  $J_2 = 3,385 \times 10^7 \text{mm}^4$ . This is shown in Figure 9.4.

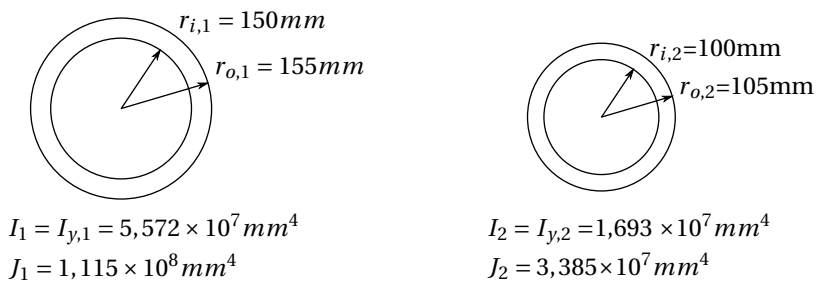


Figure 9.4: Dimensions and moments of inertia at point 1 and 2

### 9.4.3 Case 1

Case 1 is described in Figure 9.5, with corresponding moment and torque diagrams in Figure 9.6. The wind causes inner torque  $T$  in the mast as it hits the light armature sideways. It is

required that:

$$\begin{aligned}\sum M_z = 0; qA_L l - T = 0 &\Leftrightarrow T = qA_L l \\ &= 749,5 \times 10^{-6} \frac{N}{mm^2} \times 500000 mm^2 \times 1000 mm = 374750 Nmm\end{aligned}$$

where  $a$  is the distance from the center of the mast to the middle of the light armature, which is set to be  $1 m$  as shown in Figure 9.3 (in reality, the middle of the light armature may not be the same as the centre of mass, depending on the geometry and the internal design. For these calculations, however, they are assumed to be the same).

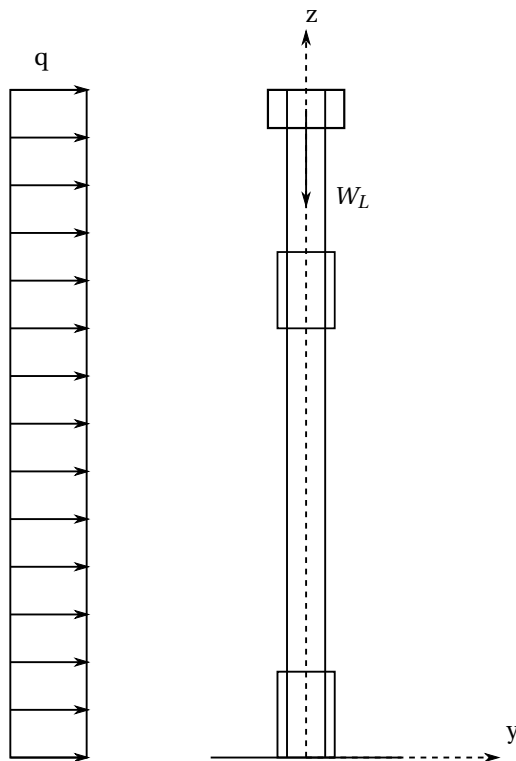


Figure 9.5: Load Case 1



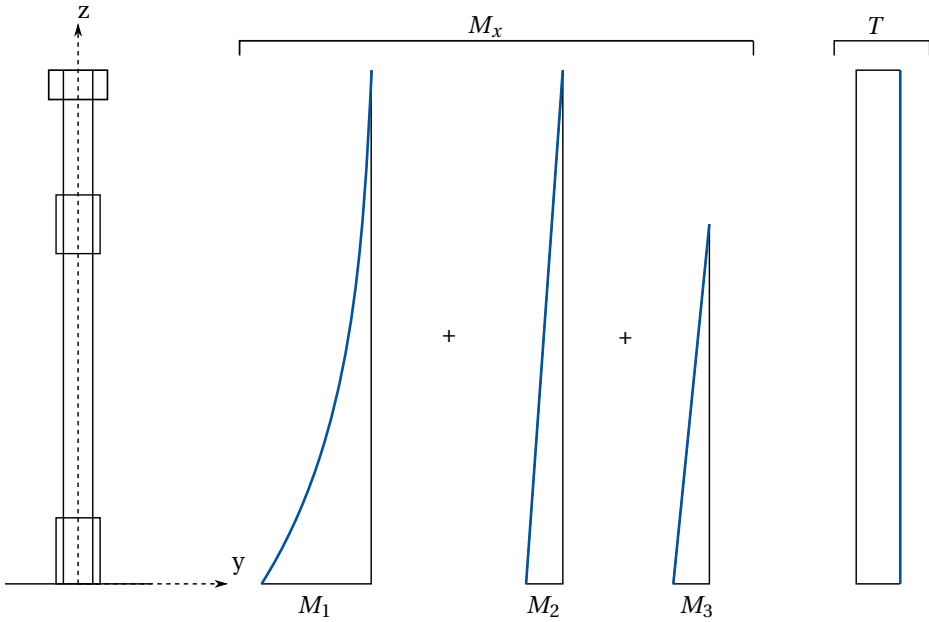


Figure 9.6: Moment and torque diagrams for Load Case 1

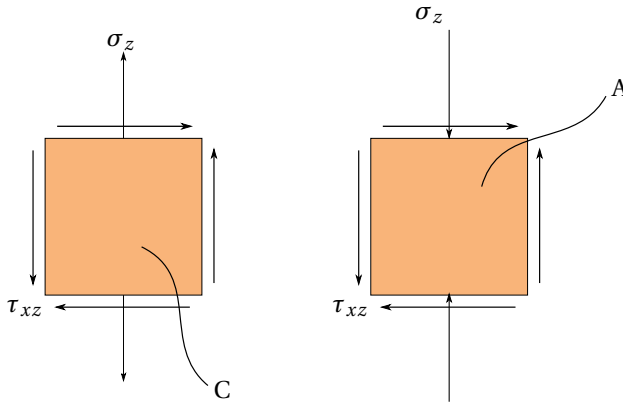


Figure 9.7: Material element for Case 1, point A and C

By the nozzles and the light armature, the mast is wider, which increases the wind load. This increase is represented by a concentrated load, which is the wind load multiplied with the additional cross-sectional area. These forces cause  $M_2$  and  $M_3$  from Figure 9.6.

The bending moment caused by the wind causes normal stress which is biggest in point C (tension) and point A (compression) and smallest in points B and C. Point A is therefore considered below. The Normal stress (compression) from the weight of the light armature  $W_L$  occurs over the entire cross-section. Material elements with belonging stresses is illustrated in

Figure 9.7.

### Point 1-A

The wind load causes a total moment of  $11,679kNm$  at Point 1 about the x-axis. According to Equations 9.11 and 9.13, this gives:

$$\sigma_{z,1-A} = \frac{11,679kNm \times 155mm}{5,572 \times 10^7 mm^4} + \frac{7kg \times 9,81 \frac{m}{s^2}}{4,791 \times 10^3 mm^2} = 32,486MPa$$

$$\tau_{zx,1-A} = \frac{Tr_o}{J} = \frac{374750Nmm \times 155mm}{1,115 \times 10^8 mm^4} = 0,521MPa$$

Applying Equation 9.14 yields:

$$\sigma_{e,1-A} = \sqrt{\sigma_z^2 + 3\tau_{zx}^2} = \sqrt{(32,486MPa)^2 + 3(0,521MPa)^2} = 32,513MPa$$

This gives a security factor  $f_s$  of

$$f_s = \frac{\sigma_y}{\sigma_e} = \frac{276MPa}{32,513MPa} = 8,489$$

Looking at these numbers, it is evident that the torque is negligible as  $\sigma_e \approx \sigma_z$ . Therefore, it is not of interest to evaluate Point B for this load case.

### Point 2-A

In Point 2-A, the same type of stress components as in Point 1-A are present. The cross-section, however, is smaller. The wind load causes a total moment of  $7,953kNm$  at Point 2 about the x-axis. This gives:

$$\sigma_{z,1-B} = \frac{7,953kNm \times 105mm}{1,693 \times 10^7 mm^4} + \frac{7kg \times 9,81 \frac{m}{s^2}}{3,220 \times 10^3 mm^2} = 49,357MPa$$

Neglecting shear causes  $\sigma_e = \sigma_z = 49,357MPa$ . This gives a safety factor  $f_s$  of

$$f_s = \frac{276MPa}{49,357MPa} = 5,592$$

**9.4.4 Case 2**

Load Case 2 is described in Figure 9.8. The wind causes a bending moment about the y-axis in this load case. This bending moment causes normal stress which is most significant in point B (tension) and point D (compression) and zero in point A and B. Point D is therefore considered below. Normal stress (compression) from the weight of the light armature  $W_L$  occurs over the entire cross-section.

The moment diagram will look similar for Case 2 as for Case 1. However, there will be no inner torque in Case 2. The moment corresponding to  $M2$  will be smaller, but the moment diagram will have the same shape.

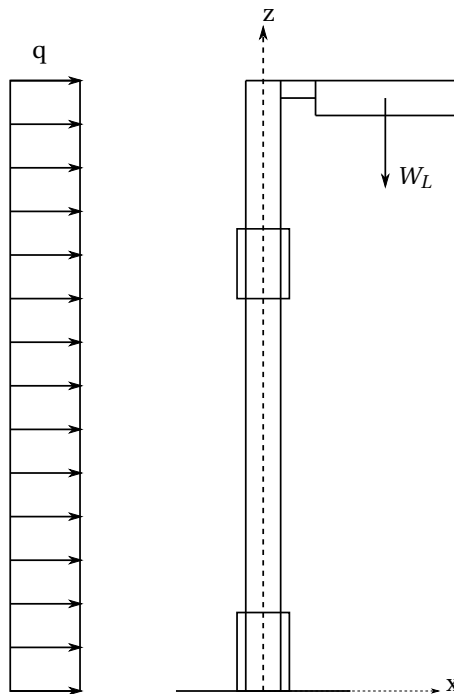


Figure 9.8: Load Case 2

**Point 1-D**

The wind load causes a total moment of  $9,656kNm$  at Point 1 about the y-axis and the weight of the lamp causes a moment of  $7kg \times 9,81 \frac{m}{s^2} \times 1000mm = 0,0687Nmm$  about the y-axis. This gives:

$$\begin{aligned}\sigma_{z,1-D} &= \frac{9,656kNm \times 155mm}{5,572 \times 10^7 mm^4} + \frac{0,0687kNm \times 155mm}{5,572 \times 10^7 mm^4} + \frac{7kg \times 9,81 \frac{m}{s^2}}{4,791 \times 10^3 mm^2} \\ &= 26,872MPa\end{aligned}$$

$\sigma_e = \sigma_z = 26,872MPa$  gives:

$$f_s = \frac{276MPa}{26,872MPa} = 10,271$$

**Point 2-D**

The wind load causes a total moment of  $6,340kNm$  at Point 2 about the y-axis, and the weight of the lamp still causes a moment of  $0,0687Nmm$  about the y-axis. This gives:

$$\begin{aligned}\sigma_{z,2-D} &= \frac{6,340kNm \times 105mm}{1,693 \times 10^7 mm^4} + \frac{0,0687kNm \times 155mm}{1,693 \times 10^7 mm^4} + \frac{7kg \times 9,81 \frac{m}{s^2}}{3,220 \times 10^3 mm^2} \\ &= 39,349MPa\end{aligned}$$

$\sigma_e = \sigma_z = 39,349MPa$  gives

$$f_s = \frac{276MPa}{39,349MPa} = 7,014$$

**9.4.5 Deflection**

As the moment is bigger for Case 1, it is interesting to check the deflection at the top of this load case. The geometry of the mast is simplified so that the width of the mast is  $210mm$  over

the entire height. Equation 9.8 gives:

$$\delta_{max} = \frac{qL^4}{8EI_x} = \frac{0,158 \frac{N}{mm} \times 9000 mm^4}{8 \times 69 GPa \times 1,69 \times 10^7 mm^4} = 111,12 mm$$

### 9.4.6 Stresses in the Mast Openings

The mast has two openings with lids that can be removed for maintenance. In these openings, it is likely that the stresses will be greater because there is less material to absorb the external forces. Using the definition of the area moment of inertia, this can be calculated, and the stresses in this section of the mast can be determined. Equation 9.15 is the definition of the second moment of area with respect to the x-axis.

$$I_x = \int \int_R y^2 dA \quad (9.15)$$

As the cross-sectional area of the mast is circular, it is expedient to transform Equation 9.15 into polar coordinates:

$$I_x = \int \int_R y^2 dA = \int \int_R (r \sin \theta)^2 dA = \int_{\theta_1}^{\theta_2} \int_{r_i}^{r_o} (r \sin \theta)^2 (r dr d\theta)$$

Evaluating this integral yields:

$$\begin{aligned} I_x &= \int_{\theta_1}^{\theta_2} \int_{r_i}^{r_o} (r \sin \theta)^2 (r dr d\theta) = \int_{\theta_1}^{\theta_2} \frac{r_o^4 - r_i^4}{4} \sin^2 \theta d\theta = \frac{r_o^4 - r_i^4}{4} \left[ \frac{1}{2} (\theta - \sin \theta \cos \theta) \right]_{\theta_1}^{\theta_2} \\ &= \frac{1}{2} \frac{r_o^4 - r_i^4}{4} [\theta - \sin \theta \cos \theta]_{\theta_1}^{\theta_2} \end{aligned}$$

The angle of the cut is chosen to be ca.  $72^\circ = 2\pi/5$  radians, which gives  $\theta_1 = \frac{7\pi}{10}$  and  $\theta_2 = \frac{3\pi}{10}$ .

Inserting these angles, as well as the inner and outer radius, yields  $I_x = 1,958 \times 10^7 mm^4$ .

As the cross-section is not symmetric about the x-axis, the neutral axis, which goes through the centroid with y-value  $y_c$ , has to be determined according to:

$$y_c = \frac{S_z}{A} = \frac{\int \int y dA}{A} \quad (9.16)$$

Transforming Equation 9.16 to polar coordinates and evaluating it yields:

$$\begin{aligned} y_c &= \frac{\int_{\theta_1}^{\theta_2} \int_{r_i}^{r_o} (r \sin\theta)(r dr d\theta)}{A} = \frac{\int_{\theta_1}^{\theta_2} \frac{r_o^3 - r_i^3}{3} \sin\theta d\theta}{A} = \frac{\frac{r_o^3 - r_i^3}{3} \sin\theta [-\cos\theta]_{\theta_1}^{\theta_2}}{A} \\ &= \frac{\frac{r_o^3 - r_i^3}{3} \sin\theta (\cos\theta_1 - \cos\theta_2)}{A} \end{aligned} \quad (9.17)$$

The area of a circle sector has the area  $\pi r^2(\Theta/2\pi)$ , where  $\Theta$  is the angle of the sector. Which means that the area of the mast's cross-section by the cut is:

$$A = \pi (r_o^2 - r_i^2) \frac{\Theta}{2\pi} = (r_o^2 - r_i^2) \frac{\Theta}{2} = \frac{1}{2} ((155\text{mm})^2 - (150\text{mm})^2) \frac{8}{5} \pi = 3,833 \times 10^3 \text{mm}^2$$

Inserting values for  $A$ ,  $r_o$  and  $r_i$  into Equation 9.17 gives  $y_c = -35,669\text{mm}$ . The distance from the cut to the neutral axis is  $y = 155\text{mm} \times \cos(2\pi/10) + 35,669\text{mm} = 161,067\text{mm}$ . Assuming the same moment as in Case 1 at point 1,  $M_x = 11,679\text{kNm}$ , yields:

$$\sigma_{cut,max} = \frac{M_x y}{I_x} = \frac{11,679\text{kNm} \times 161,067\text{mm}}{1,958 \times 10^7 \text{mm}^4} = 96,073\text{MPa},$$

which gives:

$$f_s = \frac{276\text{MPa}}{96,073\text{MPa}} = 2,873.$$

### 9.4.7 Stresses in Weld

The cylindrical mast is welded onto a square plate with bolt holes at the bottom with a fillet weld. Residual stresses may occur in the weld, as it contracts during cooling. This contraction is held back by the surrounding, colder, material, causing tension in the weld and moderate compression in the rest of the construction. The following calculations are done to determine the required thickness.

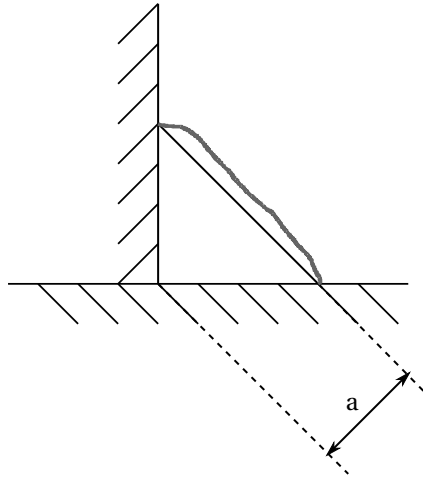


Figure 9.9: Weld thickness. For a fillet weld, the thickness is determined with a basis in the biggest isosceles triangle that can be fitted into the welds cross-section (Härkegård (2014)). The height of this triangle is the thickness of the weld.

The design strength of the weld is given by

$$\sigma_{max} = \frac{R_{p0.2}}{\gamma_m} \quad (9.18)$$

where  $R_{p0.2}$  is the materials yield strength and  $\gamma_m$  is a material dependent safety factor, which is determined by the consequences of failure. Assuming  $a \ll R$ , the second area of moment of the weld can be determined as for a thin walled cylinder,  $I_x = \pi R^3 t$  (Härkegård (2014)). Assuming the same moment as in Case 1 at point 1,  $M_x = 11,679 kNm$ , we have:

$$I_x = \pi R^3 t = \pi r_o^3 a$$

$$t_{max} = \frac{M_x y_{max}}{I_x} = \{y_{max} = r_o\} = \frac{M_z}{\pi a r_o^2}$$

$$\sigma_{\perp} = \tau_{\perp} = \frac{t_{max}}{\sqrt{2}}$$

Von Mises yield criterion follows:

$$\sqrt{\sigma_{\perp}^2 + 3\tau_{\perp}^2} \leq \frac{R_{p0.2}}{\gamma_m}$$

Manipulating the equations above, an expression for the minimum thickness can be obtained:

$$\sqrt{2} \frac{M_z}{\pi a r_o^2} \leq \frac{R_{p0.2}}{\gamma_m} \Leftrightarrow a \geq \frac{\sqrt{2}}{R_{p0.2}} \frac{M_z \gamma_m}{\pi r_o^2}$$

Requiring a safety factor  $\gamma_m = 3$  we get:

$$a \geq \frac{\sqrt{2}}{R_{p0.2}} \frac{M_z \gamma_m}{\pi r_o^2} = \frac{\sqrt{2}}{276 \text{MPa}} \frac{11,679 \text{kNm} \times 3}{\pi \times 155 \text{mm}} = 2,379 \text{mm}$$

### 9.4.8 Summary of Stress Calculations

The results from the stress calculations by hand is summarized in Table 9.3.

Table 9.3: Summary of stress calculations

Load case	Point	von Mises Equivalent, $\sigma_e$	Safety factor, $f_s$
1	1-A	32,513MPa	8,489
1	2-A	49,357MPa	5,592
2	1-D	26,872MPa	10,271
2	2-D	39,349MPa	7,014
1	Cut	96,073MPa	2,873



## 9.5 Finite element analysis

The design has been verified by Finite Element Analysis (FEA) in Autodesk Fusion360 and compared to the hand calculations. The CAD model represents the final design of the unit, and differs slightly from Figure 9.2. The difference is the thickness of the unit above the nozzles, as well as chamfers and rounded edges that are introduced in the CAD model. The material is set to aluminium for the FEA. Material properties are as given in Table 9.7.

### 9.5.1 Boundary Conditions

The light mast will be fastened to the fundamental by four M20 bolts. It is therefore chosen to constrain the mast in each bolt hole, with no degrees of freedom. Figure 9.10 shows where the structural constraints are placed.

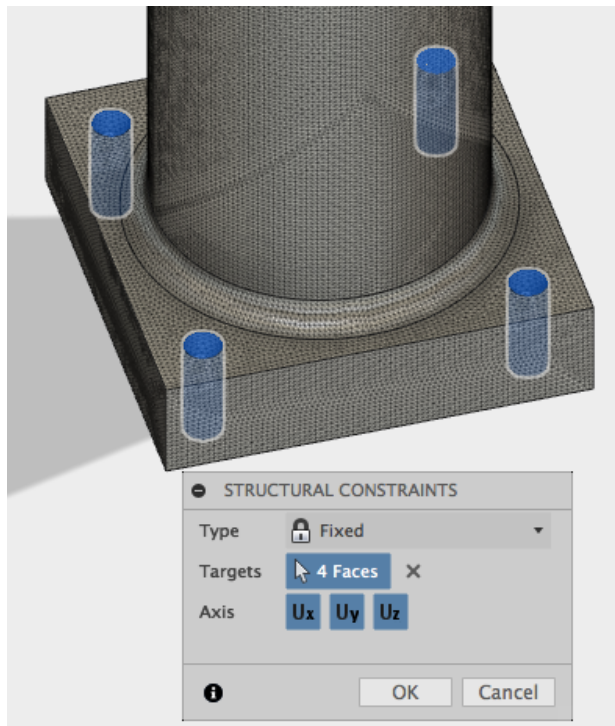


Figure 9.10: Structural constraints

### 9.5.2 Loads

The loads are as shown in Figure 9.5. The wind load  $q(z)$  is simplified to a resulting force on each section. The magnitude of this force on each section is shown on figure 9.11.



Figure 9.11: Simulation model with corresponding loads



Figure 9.12: Simulation model with cut in bottom section

### 9.5.3 Mesh

Tetrahedral mesh elements were used in the FEA. These elements are triangular shaped and fit better for complex geometry such as circular objects.

In strength calculations by FEA, the mesh size is important for the results. Usually, a smaller mesh size gives more accurate results, since there are more nodes over the same area. However, it is computationally expensive to solve for many nodes. Moreover, the probability that the model contains a singularity increases with reduced mesh size. Therefore, it was chosen to decrease the mesh size in the area of interest gradually. This area is shown as local mesh in Figures 9.11 and 9.12. The global mesh was set to a constant size of  $50\text{mm}$ . Table 9.4 and 9.5 shows how the Von Mises stress varies with the mesh size.

Table 9.4: Resulting Von Mises stress for each element size

Mesh size	100mm	50mm	25mm	10mm	5mm
Elements	31483	28436	53066	223864	1150774
Von Mises stress	48,38MPa	38,29MPa	39,76MPa	38,34MPa	38,18MPa

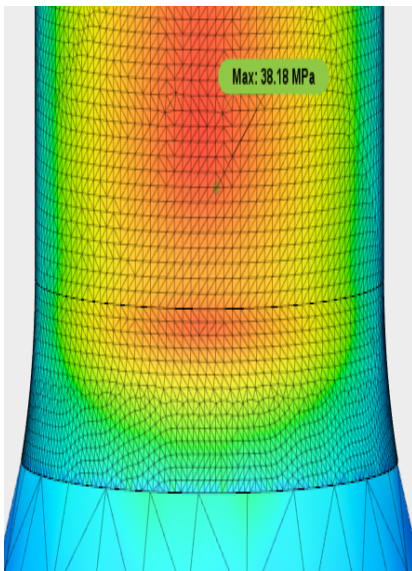


Figure 9.13: FEA model with  $5\text{mm}$  local mesh size

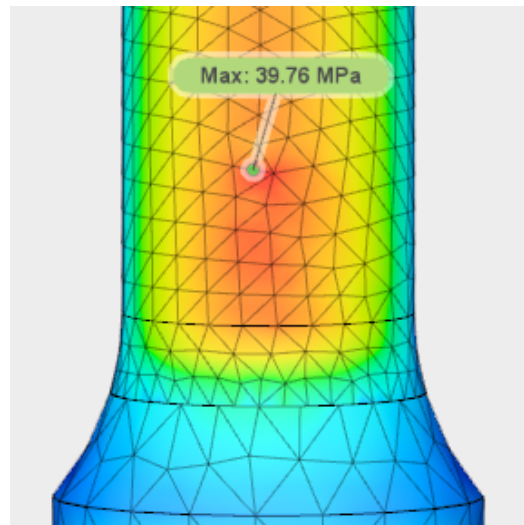


Figure 9.14: FEA model with  $25\text{mm}$  local mesh size

Table 9.5: Resulting Von Mises stress for each element size

Mesh size	100mm	50mm	25mm	10mm	5mm
Elements	31384	30970	34428	522235	117454
Von Mises stress	81,67MPa	80,04MPa	81,21MPa	78,79MPa	81,98MPa

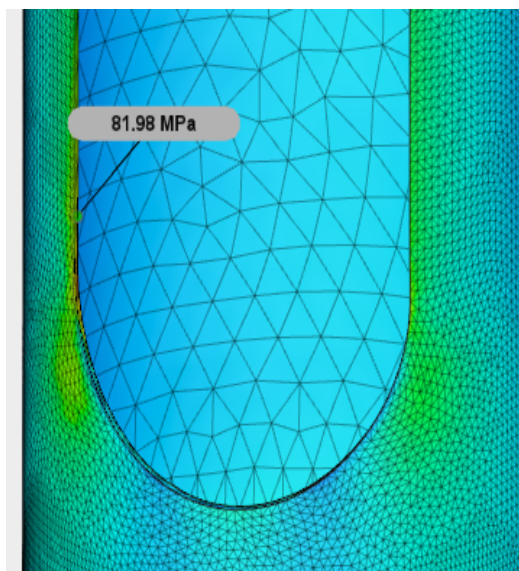


Figure 9.15: FEA model with cut and 5mm local mesh size

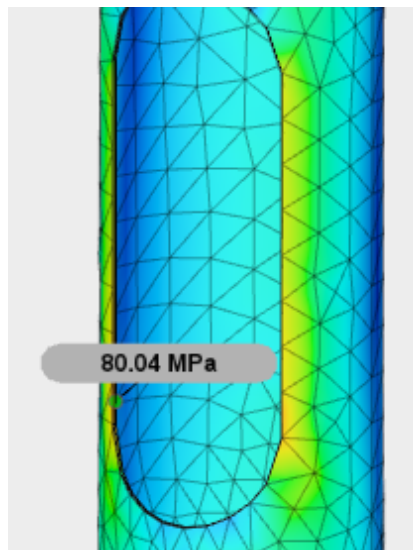


Figure 9.16: FEA model with cut and 50mm local mesh size

## 9.6 Comparison of FEA and Hand Calculations

As seen in Table 9.6, the stress and deflection found by hand calculations match the result from FEA quite good. The stress and deflection found by hand calculations are slightly higher than the stress and deflection found by FEA. This is most likely due to the conservative simplifications made in the hand calculations. When calculating the deflection, only the smallest cross-section was considered to make the calculation easier.

Table 9.6: Comparison of results

Results	FEA	Hand calculations	Design requirements
Von Mises stress $\sigma_e$	81,98MPa	96,07MPa	$\sigma_y = 276MPa$
Safety factor	3,31	2,87	>2
Deflection	107,1mm	111,12mm	< 380mm

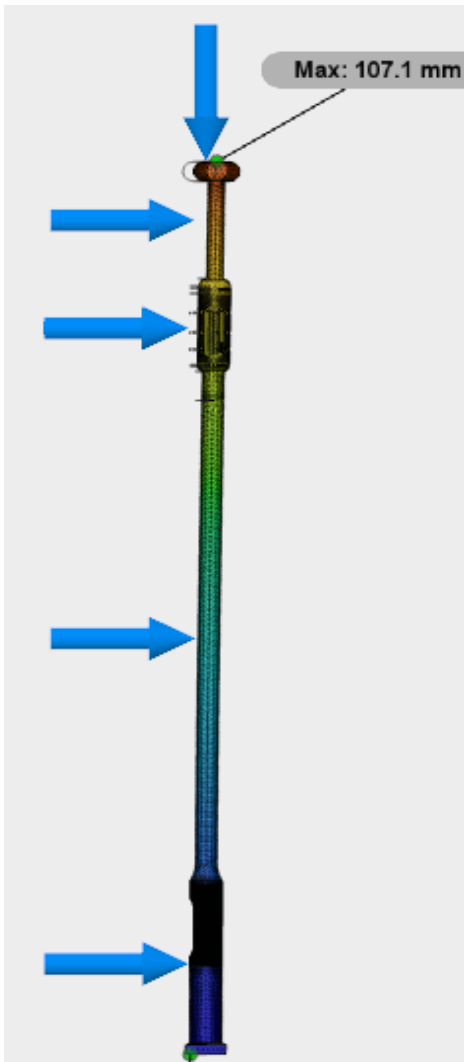


Figure 9.17: Maximum deflection occurs at the top.

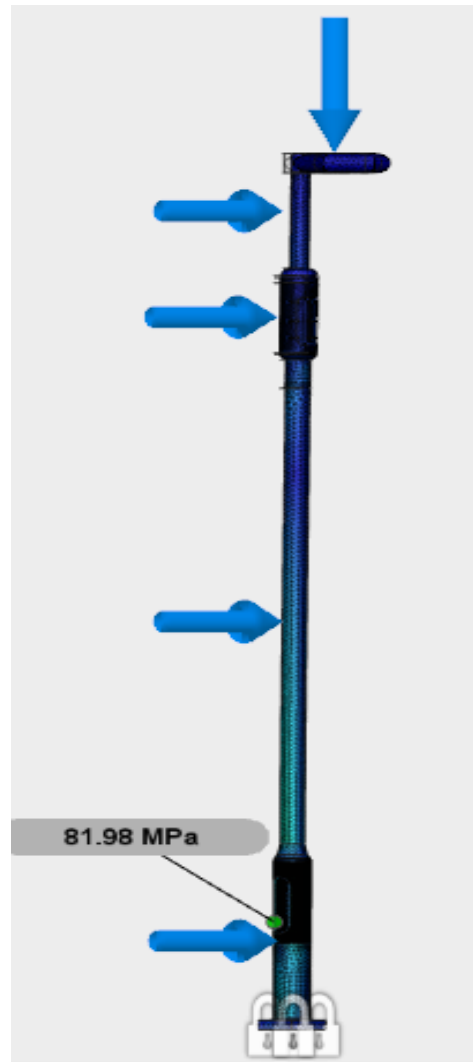


Figure 9.18: Maximum stress occurs in the cut at the bottom section.

## 9.7 Materials Selection

With regards to material selection, the unit needs to be made of a durable material. It needs to be strong enough to handle the required wind loads and stiff to prevent large deflections. The material should be able to resist corrosion for at least 25 years. Ideally, the material should also ensure low installation and maintenance cost.

Aluminium and steel has been considered to be the best suited materials. As aluminium is the

weakest of these material, strength calculations has been carried out using aluminium material properties. If the design holds for aluminium, it will therefore also hold for steel.

Table 9.7: Material properties

Material	Yield strength	Poisson's ration	Elastic Modulus
Aluminum 6061-T6	276 MPa	0.33	68,9 GPa
Steel S355	355 MPa	0.3	210 GPa

### 9.7.1 Aluminium

Aluminium has the advantage of easy fabrication, making it better for producing complex shapes at a fair price. The lower stiffness compared to steel will result in larger deflections when exposed to big wind loads. The most widely used aluminum alloys in the lighting industry are the 6061-T6 and 6063-T6 (Philipps (2012)). These alloys have a high strength-to-weight ratio, which makes transportation and assembly easier compared to steel. Aluminium is also easy to recycle, which can make projects more sustainable. The surface of aluminium can be polished, buffed or electrobrightened to give an attractive appearance. Another advantage is the excellent corrosion resistance, which increases the lifetime of the material. Because of the advantages mentioned above, aluminium has been accepted as an ideal material for street lighting poles (The Aluminum Association (2017)).

### 9.7.2 Steel

Steel masts are often chosen in areas with strong winds or when the mast is very tall, since the requirements for stiffness is higher. The high strength and stiffness makes steel the most common structural material. Another advantage is that steel is easy to weld. The main disadvantage for steel is the poor corrosion resistance. Steel usually needs surface treatment to avoid corrosion, like hot-dip galvanizing. The most commonly used alloy for lighting poles are S355 (VikØrsta (2018)).

## 9.8 Part List and CAD drawings

Proposed manufacturing parts are summarized in Table 9.8, and can be found in more detailed at <https://www.mcmaster.com>. The part numbers in Table 9.8 are highlighted in Figures

9.19, 9.20 and 9.22, to show the composition of the parts. The hydraulic hoses are not shown in any of the figures. These will, however, be connected from the bushings to the weld nuts where the nozzles are placed. The nozzles that are used in the drawings are provided by BETE. Part 20 is the air atomizing nozzle with inlets to water and compressed air, while Part 21 and 22 are high-pressure water nozzles. The air atomizing nozzles come with a 45° adapter to make the spray interact with the water nozzles. Nozzle data can be found in Appendix F, while machine drawings of the unit can be found in Appendix G.

Table 9.8: Part list

Item	Quantity	Part Number	Description	Price /pcs (\$)
1	4	4813K69	Stainless steel pipe 1-1/4" Threaded ends	159,40
2	4	4813K79	Stainless steel pipe 1" Threaded ends	199,74
3	4	4813K39	Stainless steel pipe 1/4" Threaded ends	67,75
4	4	4640K34	Solenoid valve	569,34
5	2	1194N22	Solenoid valve	155,90
6	2	5943K291	Inline Tee Adapter	54,82
7	2	45525K556	Inline cross adapter	108,43
8	2	4428T23	Pressure regulating valve	352
9	4	4464K415	Pipe bushing	23,96
10	4	52245K533	Tube to pipe adapter	12,13
11	4	4464K412	Pipe bushing	14,47
12	2	7818K217	Inline tee adapter	110,42
13	4	91247A498	M20 Stainless Steel Hex Head Screws	10,29
14	1	3680450	Light fuse box by Larel	N/A
15	8	90596A031	Steel Round-Base Weld Nuts	7,69/50 pcs
16	3	51205K164	Right-angle T-adapter	188,25
17	8	9459K121	1/4" Hydraulic hose with Threaded fittings	19,85
18	4	5201K71	1/8" Hydraulic Hose with Threaded Fittings	26,27
19	4	1593N45	1/8" Air Hose with Threaded Fit- tings	5,98
20	4		BETE Air atomizing XAAD Nozzles	N/A
21	4		N/A BETE Standard flat fan NF15 Nozzles	N/A
22	4		BETE Standard flat fan NF30 Noz- zles	N/A
23	4	91287A394	M12 Stainless Steel Hex Head Screws	7,5/5 pcs
				= 6087 \$
			With 1 USD = 8 NOK	= <b>48696 NOK</b>

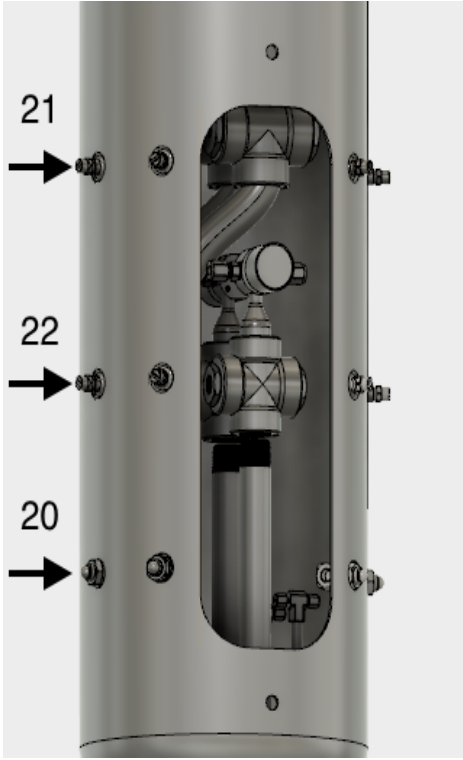


Figure 9.19: Nozzle arrangement

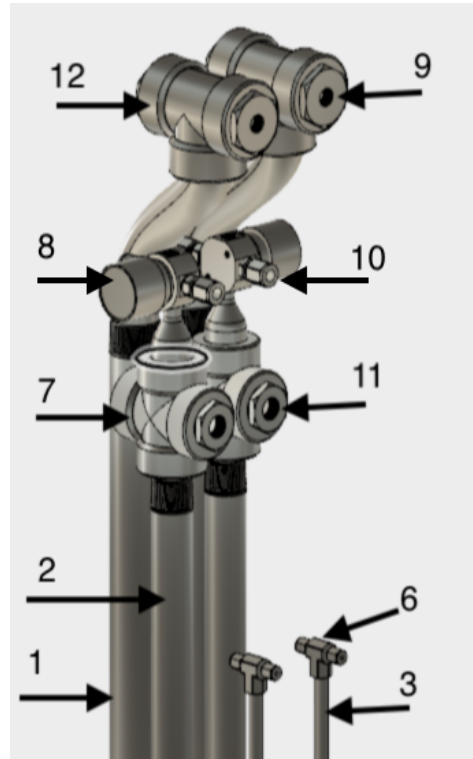


Figure 9.20: Pipe arrangement inside the mast



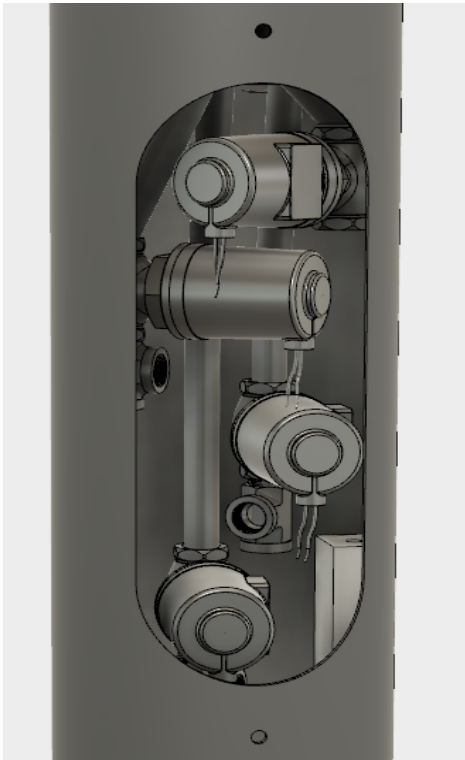


Figure 9.21: Valve placement within the mast in bottom section

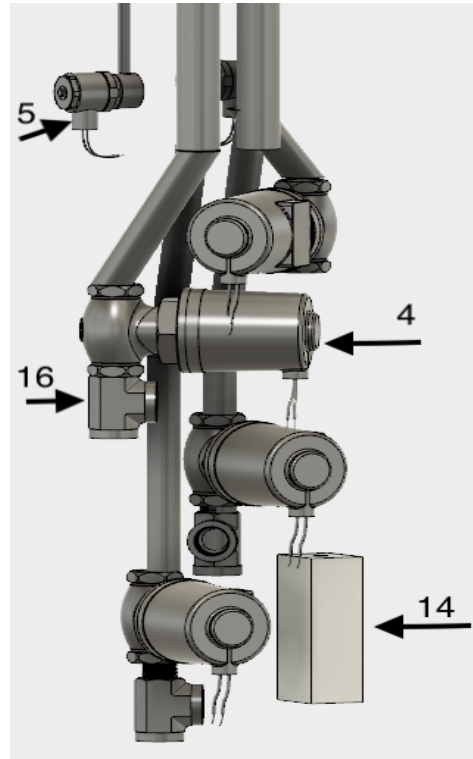


Figure 9.22: Solenoid valve arrangement with corresponding pipes



# 10 Remote Control System

A remote control system is needed to make the unit automatic. The control system should facilitate fast start-up time, efficient production control and less manpower. The control system should be able to take input from weather stations to control the valves in each unit. It should also be able to control the system manually, or with guidance from the control system.

## 10.1 Control System

A bachelor thesis (Jaworski, Johansen, Tjore & Torvund 2018) was performed parallel to this master thesis at NTNU, also in cooperation with SIAT. The result from this bachelor thesis is a prototype system for controlling the snow production in Granåsen remotely. The control system is designed with a Viking V2 lance (Figure 10.1) in mind. This lance is one of the lances used in the ski jumping hill in Granåsen. The Viking V2 has four operating steps and two manual valves that control which steps that are activated. The lance head of the Viking V2 lance resembles the lance from this master thesis to some extent.

The prototype they have created consists of three parts:

1. A web application that shows information about the snow production system and controls the system,
2. A server that stores data and handles communication,
3. A lance control unit which regulates the lance and actuators.

The web application is based on HTML5, CSS3, and JavaScript in front end, and python in back end. The prototype uses a Raspberry Pi (RP) in the lance control unit. The RP is installed within a cabinet that should be placed either by/within the lance or by the well. The cabinet also involves the other components that are necessary for controlling the lance, such as terminal blocks for external cables and grounding, fuse, etc. The dimensions of the prototypes cabinet are  $400 \times 300 \times 150 \text{mm}^3$  which is too big to fit within the lance. There should, however, not be a problem making this cabinet a bit smaller, as the RP is rather small.

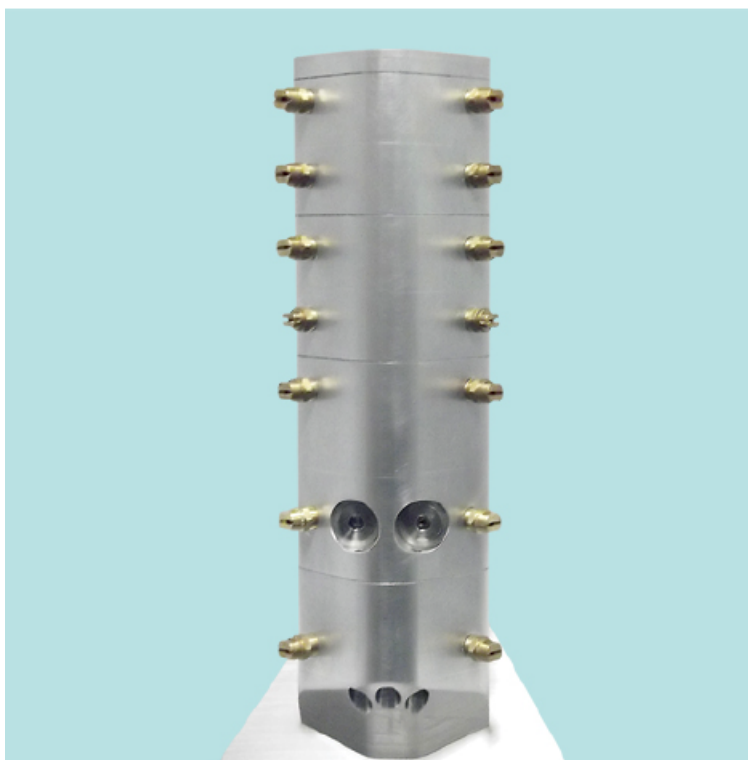


Figure 10.1: The lance head of the Viking V2 lance

The cabinet could be placed either within the mast, on the mast, or by the wells. There are pros and cons of every solution. Centralizing the control units could decrease the number of needed control units if there are several lances per well. However, it would make the control system more vulnerable in case of failure, as many lances would be out of operation if only one of the units fail. It should therefore preferably be one control unit per snow production unit. Placing the control unit within the mast will shield it, but also make it harder to access. The different possibilities should be explored in cooperation with the operators at Granåsen Ski Arena to find the optimal solution.

## 10.2 Recommendations for Controlling Algorithms

The following section presents some rules for snow production with the multifunctional unit. These rules are preliminary, which means that they could be changed after physical testing. Moreover, it should be easy for the operators of the system to change the production settings

at any time, and they should always be able to override the rules.

### 10.2.1 Temperature

The unit has been designed to be able to start production at marginal temperatures ( $T_{wb} = -3^{\circ}\text{C}$ ). At such temperatures, only the smallest nozzles should be utilized. At lower temperatures, the bigger nozzle should be used in addition to the small. A rule of thumb can be to start using the bigger nozzles at a wet-bulb of  $-7^{\circ}\text{C}$ , as this is the limit wet bulb temperature for good snow quality according to the chart in Figure 3.3.

### 10.2.2 Wind Strength and Direction

The analytic model has been useful when deciding nozzle position. Directing nozzles  $45^{\circ}$  and  $80^{\circ}$  was done to enable snowmaking in a wide range of wind directions. Normal practice for snowmaking in downhill tracks is to turn off production if the wind speed exceeds ca.  $10\text{ m/s}$ . In cross-country tracks, one would have to turn the production off somewhere between  $3\text{ m/s}$  and  $10\text{ m/s}$ . Figures 10.2 and 10.3 show hit rates for the nozzles pointing  $45^{\circ}$  in wind directed  $10^{\circ}$  to  $360^{\circ}$ . At  $0,5\text{ m/s}$  wind, the hit rate never drops below 45%. At  $5\text{ m/s}$  wind, on the other hand, small changes in wind direction cause hit rates to drop to 0%.

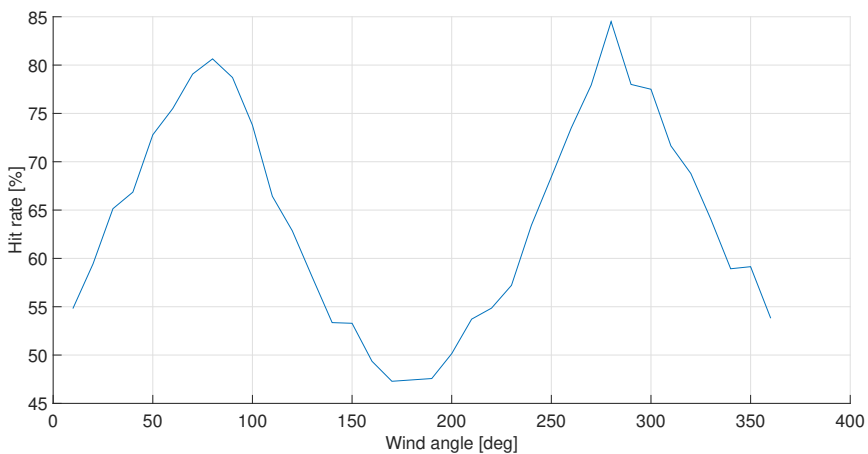


Figure 10.2: Hit rates for the  $45^{\circ}$  nozzles  $0,5\text{ m/s}$  varying wind

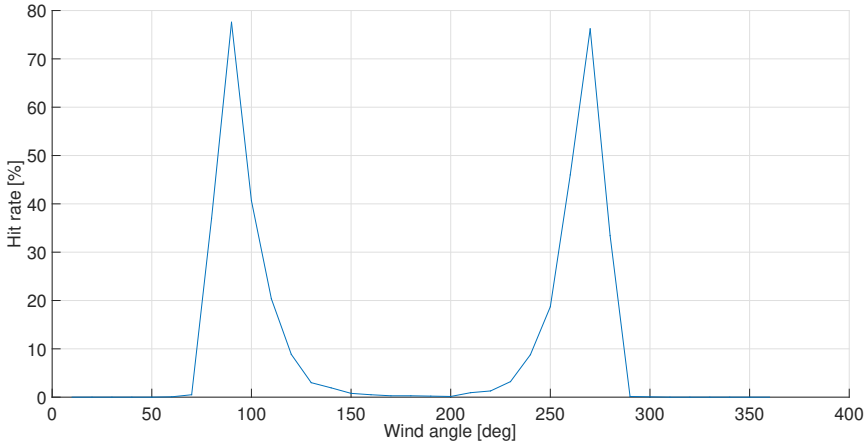


Figure 10.3: Hit rates for the 45° nozzles at 5m/s varying wind

Figure 10.4 shows that the hit rate for the nozzles pointing 80° is good for wind directions between 0° and 75° and between 285° and 360°.

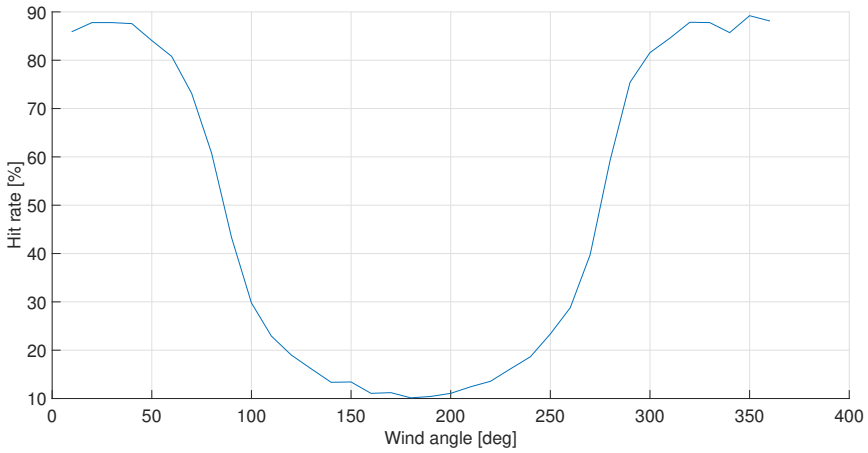


Figure 10.4: Hit rates for the 80° nozzles at 0,5m/s varying wind

Figure 10.5 shows how the hit rate varies with wind direction when all nozzles are in use. As shown, the hit rate is medium for all angles between 0° and 120° and between 250° and 360°, and good for angles between 0° and 80° and between 280° and 360°.

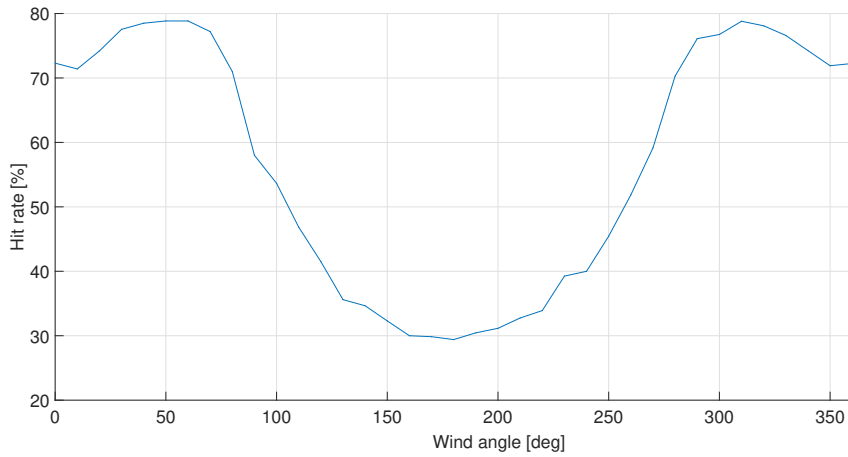


Figure 10.5: Hit rates for all nozzles at 0,5 m/s varying wind

Based on the results in this chapter, a mapping of which nozzles that should be used at which wind angles has been made. This map is showed in Figure 10.6. This map applies for low wind speeds, that is, lower than ca. 3 m/s. At wind speeds between 3 m/s and 5 m/s, the circle sectors will be narrowed.

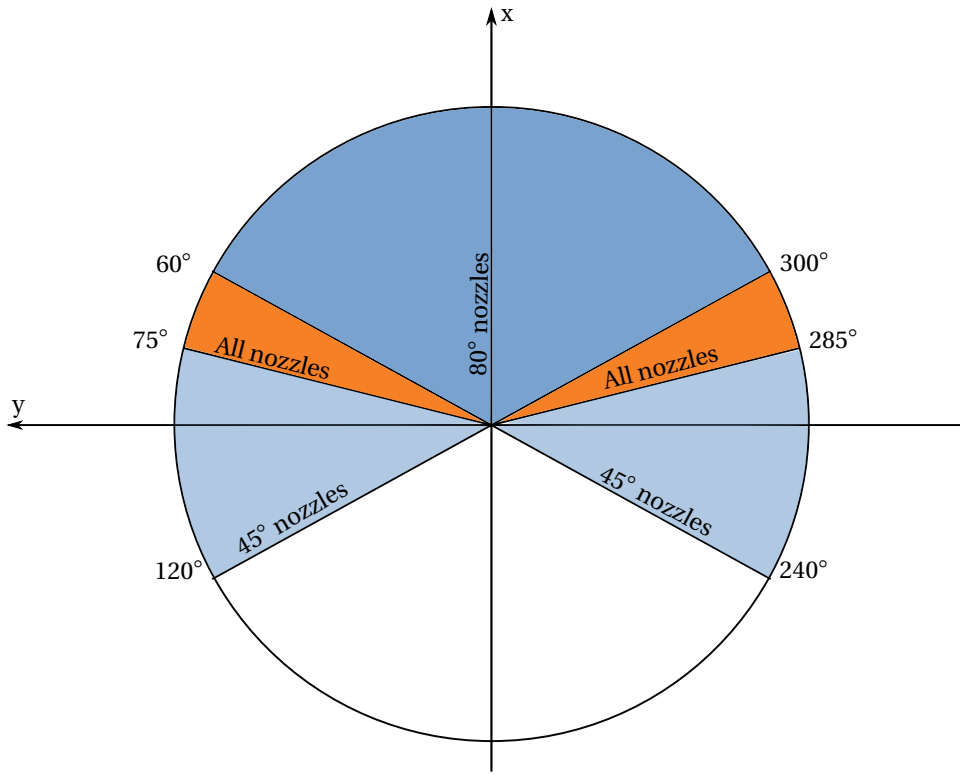


Figure 10.6: Map showing at which wind angles the different nozzles should be used



# 11 Result

Rendered images of the final design are shown in Figures 11.1 and 11.2. The multifunctional snow production unit has eight water nozzles and four nucleator nozzles. The nozzles are divided into four horizontal orientations and two vertical steps, plus the nucleator step. The nozzle arrangement enables production at lower temperatures and horizontal adjustment from 45° to 80°, depending on wind direction. The light armature in the drawings is currently just a placeholder (for illustration). Table 11.1 shows the product specification. Some of the product requirements from Table 5.2 need physical testing to be verified, and some has not been considered yet. These requirements are therefore not listed as specifications. The lighting specifications are example specifications from the Sirius 200W LED-streetlight armature from LADELYS. Technical specifications for this armature can be found in Appendix H.

## 11.1 Integration of the Unit in Granåsen

The unit is designed with a flat, straight track in mind. In reality, however, only segments of the track is flat and straight. How the units are distributed along the track is therefore as important as the performance and precision of the unit itself. It is therefore suggested that not all of the lighting units along the tracks also are snowmaking units - some should be standard light masts (with a similar design as the multifunctional units). This way, producing snow in areas of the track where the quality will be poor, where the track is particularly exposed to strong wind, etc., can be avoided and resources will be saved. Examples of points where the units should not be placed are:

**Close to sharp turns** In sharp turns, it is likely that the snow will hit the ground outside the track.

**In steep hills** In steep hills, the snow produced towards the top of the hill may have shortened airtime, which could cause poor quality. The snow produced towards the bottom will receive drained water from the snow further up in the hill and will become very wet and heavy.



Figure 11.1: Final design of unit

**Windy tops** In windy areas, the production may be subject to big losses.

With the results from the analytic prototype in mind, a rule of thumb could be not to place the unit within a radius of ten meters from these points. In other words, each snowmaking unit requires  $20m$  of relatively flat and straight tracks.

As each unit can only make snow in specific wind directions, placing the units on each side of the track could enable snowmaking independent of the wind direction. However, not all of the units in the same area could produce at the same time with such a solution. Moreover, placing the units on different sides of the tracks would be unfortunate, as the underground pipes and hoses would have to go zigzag under the tracks. This way, maintenance or reparation of the pipes would require the track to be dug up, which is just out of the question. An advantage



Figure 11.2: Final design showing nozzle arrangement and proposed light fixture

of having all the units on the same side is that this allows production of big volumes once the right conditions are present.

Table 11.1: Product Specification

<b>Description</b>	<b>Value</b>
<b>1 Snow production specifications</b>	
1.1 Height	7m
1.2 Horizontal adjustment	45° or 80°
1.3 Throw length	5m to 10m
1.4 Air consumption	0,33m <sup>3</sup> /min
1.5 Air pressure	5 bar
1.6 Water consumption	37,4l/min to 112,2l/min
1.7 Water pressure	30 bar
1.8 Maximum production temperature	$T_{wb} = -3^{\circ}C$
1.9 Production rate (snow)	5m <sup>3</sup> /h to 25m <sup>3</sup> /h
1.10 Price estimate (internal components)	48696 NOK
<b>2 Structural specifications</b>	
2.1 Corrosion resistance	25 years
2.2 Withstand wind load	26m/s
2.3 Weight	137 kg
2.4 Material	Aluminium 6061-T6
2.5 Price estimate (external components)	15000 NOK
<b>3 Luminaire specifications (example from Ladelys)</b>	
3.1 Lifetime	100.000 Hours
3.2 Lighting Class I according to European Standards	Avg. of min. 20lx
3.3 Weight	5-10kg
3.4 Height	9m
3.5 Power consumption	200 W
3.6 Price estimate (light armature)	9000 NOK

### 11.1.1 Distance Between the Units

As the light armature has not been the priority of this thesis, it is not possible to determine the optimal distance between the masts at this point. However, it is likely that the lighting requirements will demand smaller distance between the masts than snowmaking considerations. The snow from the masts has a range of about ten meters (depending on wind). The snow will fall in piles, which will be dosed along the track. It is therefore not necessary that the snow cover the entire track before dosing. A distance between the masts can, therefore, be chosen to some distance bigger than 16 meters, depending on how production time Granåsen can allow before the snow has to be distributed and prepared (longer time allows for greater distance and thus fewer units). Therefore, if lighting considerations suggest very little distance between the units, then every other or every third unit should be a multifunctional unit, and the rest should be light masts with a similar design.



# 12 Conclusion, Discussion and Suggestions for Further Work

## 12.1 Conclusion

In order to maintain good skiing facilities in the winter to come, Granåsen Skiing Arena will benefit from an automated snow production system. The operators are not satisfied with the present system and look forward to an upgrade of the facilities.

The main scope of this thesis was to continue the development process of a multifunctional snow production unit that was started in the pre-study. The main result is a design proposal for a comprehensive, physical prototype. It is estimated that a prototype would cost about 75.000 NOK, excluded the remote control system and related components. The most critical decisions that have been made when designing the unit has been regarding the nozzle configuration and adjustment possibilities. The design of the light armature is left out of this thesis, as this can be delivered by a lighting company when building the prototype. However, lighting is facilitated in the design by reserving space for the necessary electrical components within the mast.

Through analytic prototyping, it was learned that the simplest design was achieved with stationary nozzles. The simulation showed that small water droplets are highly sensitive to wind and hard to control. Because of this, a more advanced nozzle setup, with mobile nozzles did not necessarily produce better hit rates than the chosen concept. The best hit rates were obtained for nozzle angles of  $45^\circ$  and  $80^\circ$ , on both sides of the mast.

FEA of the design has been conducted, along with affirmative hand calculations. These calculations show that the unit is designed with a safety factor of  $f_s = 3$ , with respect to wind loads according to Norwegian Standard. The critical point is by the cut where the cross-section is reduced.

## 12.2 Discussion

The primary sources of learning in the product development process so far have been interviews and conversations with snowmaking experts and operators, as well as several inspections of the snowmaking facilities in Granåsen and Åre. The analytic prototype has also played an important part in the decision making. The feedback from the experts has been weighted more in some decisions where uncertainty or opposing views have been present, as there remain some uncertainties in the analytic prototype. The results from analyses and other information obtained while working with the unit should not be considered to be an established truth. When making decisions during the development, interpretations, and assumptions have been made. Therefore, physical testing is needed to verify the results.

We believe this unit has the potential to streamline the snow production in Granåsen. A system of evenly distributed stationary lances that automatically change the settings according to local conditions, like wet-bulb temperature and wind, would save time, energy and cost in operation. Feedback from the operators reinforces this viewpoint.



## 12.3 Suggestions for Further Work

The unit that is described in this thesis should be considered a prototype. The next step of the development process should be to build and test the prototype, preferably in cooperation with a snow production company. We suggest that the prototype is built in aluminium. However, steel can also be used if this is more convenient. The main outcome of the testing should be to test the nozzle setup and the proposed algorithms.

After testing, a product designer should be involved to refine the design of the unit. A good looking, complete design is important to satisfy future TV-productions of sports events, as well as the experience of the skiers. It is also desirable to make the unit cheaper, if possible. The price of each unit will, by now, approach 100.000 NOK. Replacing the nozzles and the components inside the unit with similar, cheaper components could make the unit in total cheaper.

It should be mentioned that there has not been done any calculations regarding the economic and environmental benefits from the solution with multifunctional lances compared to a solution with mobile fan guns or snow storages. Assumptions from earlier states that the investment cost of the multifunctional lances will be high, but that reduced operating costs will even this out during an unknown number of years. When the unit has been refined, and the price of the unit is known, these calculations should be carried out.



# Bibliography

- Aas, B. & Vagle, B. H. (2017), *Granåsen skisenter - Forprosjekt snøproduksjon*, Technical Report 3, Senter for idrettsanlegg og teknologi (SIAT), Høgskoleringen 7A.
- Anderson, J. D. (2001), *Fundamentals of Aerodynamics*, Series in Aeronautical and Aerospace Engineering, 3 edn, McGraw-Hill, 1221 Avenue of the Americas, New York, NY 10020.
- Auganæs, S. & Opheim, S. (2017), '*Development of a Multifunctional Snow Production Unit for Granåsen Arena*'. [Project thesis, Department of Mechanical and Industrial Engineering, Norwegian University of Science and Technology].
- Bachler (2017), '*New Energy-efficient snowgun system*', URL: <https://www.bachler.ch/media/archive1/produkte/NESSy-Brochure-en.pdf>, note = "[Online; accessed 3-June-2018]",.
- Bete (2017), '*Snow Making (Nucleation) Nozzles*', URL: <http://www.bete.com/applications/snowmaking.html>. [Online; accessed 1-June-2018].
- Callister, W. D. & Rethwisch, D. G. (2007), *Materials science and engineering: an introduction*, 7th edn, Wiley, New York.
- Curry, J. A. & Webster, P. J. (1998), *Thermodynamics of Atmospheres and Oceans*, International Geophysics, Elsevier Science, Burlington.
- Dunlop, S. (2008), *A dictionary of weather*, Oxford Paperback Reference, 2nd edn, Oxford University Press, Oxford.
- Engineering ToolBox (2013), '*Jet Discharge Propulsion*', URL: [https://www.engineeringtoolbox.com/jet-discharge-propulsion-force-d\\_1868.html](https://www.engineeringtoolbox.com/jet-discharge-propulsion-force-d_1868.html). [Online; accessed 15-March-2018].
- Fauve, M. & Rhyner, H, U. (2004), 'Physical description of the snowmaking process using jet technique and properties of the produced snow', *Snow Engineering V* pp. 215–218.
- Gjerland, M and Olsen, G.Ø (2014), '*Snøproduksjon og snøpreparering*', URL: <https://www.regjeringen.no/globalassets/upload/kud/idrett/publikasjoner/>

- v-0965\_kud\_veileder\_snoproduksjon\_og\_snopreparering\_2014.pdf. [Online; accessed 4-June-2018].
- Hildre, H. P. (2004), '*Produktutvikling*'. NTNU, Institutt for produktutvikling og materialer.
- Hoffman, V. & Solseng, E. (2014), '*Spray Equipment and Calibration*', North Dakota State University. URL <https://www.ag.ndsu.edu/pubs/plantsci/crops/ae73.pdf> [Online; accessed 24-October-2017].
- Härkegård, G. (2014), *Dimensjonering av maskindeler*, 3rd edn, Bokforlaget Vigmonstad og Bjørke AS, Kanalveien 53, 5068 Bergen.
- Jaworski, M., Johansen, H. F., Tjore, M. & Torvund, P. G. (2018), '*Design av styresystem for effektivisering av snøproduksjon*'. [B.Sc., Norwegian University of Science and Technology].
- Langedal, M. (2017), '*Støtte til klimasatsing i kommunene 2017*'. URL: <http://www.miljokommune.no/Temaoversikt/Klima/Klimasats---stotte-til-klimasatsing-i-kommunene/Klimasats---tildeling-av-tilskudd-2017/> [Online; accessed 15-May-2018].
- Linzén, N. (2016), Properties of Snow with Applications Related to Climate Change and Skiing, PhD thesis, Luleå University of Technology. URL: <http://ltu.diva-portal.org/smash/get/diva2:1038717/FULLTEXT02.pdf> [Online; accessed 20-October-2017].
- Morrison, F. A. (2013), *An Introduction to Fluid Mechanics*, 1st edn, Cambridge University Press, 32 Avenue of the Americas, New York, NY 10013-2473, USA.
- Philips (2012), '*Steel vs Aluminum*', URL: <http://applications.nam.lighting.philips.com/blog/index.php/2012/04/18/steel-vs-aluminum/>. [Online; accessed 5-June-2018].
- Saskatchewan Environment (2004), '*Water Pipeline Design Guidelines*'. URL: <http://www.sask2o.ca/dwbinder/epb276waterpipelinedesignguidelines.pdf> [Online; accessed 15-May-2018].
- Schlichting, H. (2006), *Boundary Layer Theory*, Series in Mechanical Engineering, 6th edn, McGraw-Hill, 1221 Avenue of the Americas, New York, NY 10020.
- Shea, E. J. (1999), '*Calibration of Snowmaking Equipment for Efficient Use on Virginia's Smart Road*'. M.Sc., Virginia Polytechnic Institute and State University, <https://>

- [//theses.lib.vt.edu/theses/available/etd-090799-160020/unrestricted/Main\\_Document.pdf](http://theses.lib.vt.edu/theses/available/etd-090799-160020/unrestricted/Main_Document.pdf) [Online; accessed 24-October-2017].
- Snowathome (2017), 'Wet-bulb temperature chart', URL: [https://www.snowathome.com/pdf/wet\\_bulb\\_chart\\_celsius.pdf](https://www.snowathome.com/pdf/wet_bulb_chart_celsius.pdf). [Online; accessed 5-June-2018].
- Sommer, A. F., Hedegaard, C., Dukovska-Popovska, I. & Stege-Jensen, K. (2015), 'Improved product development performance through agile/stage-gate hybrids', *Industrial Research Institute*. URL: [https://www.projectmanagement.com/content/attachments/jwoolcott\\_260515093635.pdf](https://www.projectmanagement.com/content/attachments/jwoolcott_260515093635.pdf) [Online; accessed 15-May-2018].
- Spandre, P., François<sup>1</sup>, Hugues Thibert<sup>1</sup>, E., Morin, S. & George-Marcelpoil<sup>1</sup>, E. (2017), 'Determination of snowmaking efficiency on a ski slope from observations and modelling of snowmaking events and seasonal snow accumulation', *The Cryosphere*. URL: <https://www.the-cryosphere.net/11/891/2017/tc-11-891-2017.pdf> [Online; accessed 5-June-2018].
- Standard Norge (2009), *NS-EN1991-1-4 - Eurokode 1: laster på konstruksjoner-Del 1-4*.
- Standard Norge (2013a), *NS-EN40-3-1 - Lightning columns - Part 3-1: Design and verification*.
- Standard Norge (2013b), *NS-EN40-3-3 - Lightning columns - Part 3-3: Design and verification*.
- The Aluminum Association (2017), 'Related structural applications of Aluminum', URL: <http://www.aluminum.org/sites/default/files/aecd18.pdf>. [Online; accessed 20-May-2018].
- Trondheim Municipality (2017), 'Granåsen 2023', URL <https://www.trondheim.kommune.no/granasen-2023/>. [Online; accessed 5-June-2018].
- Ulrich, K. T. & Eppinger, S. D. (2012), *Product Design and Development*, McGraw-Hill, 1221 Avenue of the Americas, New York.
- VikØrsta (2018), 'Teknisk informasjon lysmaster', URL: <http://www.vikorsta.no/lysmast/teknisk-informasjon/teknisk-informasjon-lysmaster/>. [Online; accessed 15-March-2018].
- Wolfsperger, F., Hansueli, R. & Schneebeli, M. (2018), *Pistenpräparation und Pistenpflege*, 1st edn, WSL - Institute for Snow and Avalanche Research, Davos.



# A Report from Interviews at Granåsen

## A.1 Adjustment Possibilities

- When switching to large nozzles, the lances were pushed back by the enormous pressure of the water leaving the nozzle. Then the operators had to place weights to hold them down.
- Making the nozzles point down is often not relevant, as the droplets will not get sufficient air time, causing reduced snow quality.
- Many skiing resorts have cross-country tracks going back and forth in the same area to make it more audience-friendly, or to create longer tracks in a smaller space. Such parallel tracks make it possible to cover both sides with snow if the lance can turn 360 degrees.
- Automatic horizontal adjustment can enable the production of an even layer of snow instead of big, pointed piles. An even layer will probably require less time to drain, allow faster preparation for the snowmobiles. Moreover, as a pile grows in size, the distance from the lance to the top of the heap decreases, reducing air time of the droplets.
- Having a motor for adjustment will complicate the design. There is also a risk of freezing for moving parts at the cold and humid environment.
- A turn radius of 90 degrees would in most cases be sufficient.

## A.2 Operation and Maintenance

- Maintenance is a central issue. If the lance head is placed at 5m to 7m, it will be impossible to reach without a ladder. Ways to lower the mast, or lance head should be considered.
- Operators at Granåsen have experienced that it is better to create a sole of 40cm to 50cm, which is more resistant to mild weather, than for example a sole of 20cm. Creating a thick

sole is time demanding early in the season, but will often save time and resources in a larger time perspective.

- The most important requirement for new snow production units is that they must be able to produce snow of good quality at marginal temperatures. The operators have experienced that ceramic nozzles are better suited than brass nozzles.
- The differences in the terrain makes it harder to produce snow in cross country tracks than in alpine skiing hills. As an example of this is at swoops, where drained water will accumulate.
- They also mentioned that it is favorable to have the light on when producing snow at night time because it is easier for the operator to control the hit area and the snow quality. (But this might not apply to an automated unit.)
- Freezing of nozzles is usually not an issue. A build-up of ice can occur when the wind is heading straight towards the nozzle.

### **A.3 Design**

- A discreet design is positive concerning TV-production, nature experience, etc
- The placement of the nozzle unit can obscure for the light in some of the concepts.
- Complex design/parts can make the unit costly to produce.



## B Report from Interview in Åre

Table B.1: Learnings from the field trip to Åre

Setting	A meeting with snow technical Pär Bengtson was planned. He got a lot of experience with different automated snowmaking equipment in Åre. A tour around the snow construction was performed. On-site investigations of different lance towers, pump stations, and control room provided useful information.
Temperature	$-22^{\circ}C$
Wind	$2.2 \frac{m}{s}$
Humidity	Ca. 91%
Notes made from observations	<p>They had to remove all the lances in the slopes where the TV production to the world cup in alpine skiing will be in two weeks.</p> <p>The automated lance head got six water nozzle and two nucleates. Two water nozzles are set up in one step. One can note the different nozzle orifice size between the different steps. At colder temperatures, the step with larger nozzle opening will be used.</p>

Notes made from conversations with the workers	<p>Technical information on lances:</p> <ol style="list-style-type: none"> <li>1. Air pressure @10bar</li> <li>2. Water pressure @55bar</li> <li>3. Lance height from 6-10m</li> <li>4. Throw length from 10-20m (depends on model)</li> <li>5. Wet bulb temperature production start @<math>-2,5^{\circ}C</math></li> <li>6. Nozzles types: Both water and nucleator nozzles were flat fan nozzles. Water nozzles at <math>50^{\circ}</math> and nucleators at <math>65^{\circ}</math>.</li> </ol> <p>The different steps are controlled by a valve, which controls which of the three pipes that water should flow. The air pipe is placed between the three water pipes. By the data from weather stations, the valve controls witch steps to be used.</p> <p>Even though much of the system is automated, they are seven people working when the production is in progress. They have visual control of their area 2 times in their shift. The most common problem is freezing of water and air hoses. There is also a small problem of freezing of valves.</p> <p>They do not have any automatic adjustment for different wind speeds and directions. They have anemometers that can shut the production if the wind speeds reach a critical value. However, it is hard to get the anemometers to show correct values, because of snow and obstacles. One needs to be careful where to place them. It should also be noted that when there is head-wind water can drift back on the lance and freeze the nozzle. The snow also gets wetter because of less air time. So the advantages of tailwind are multiple.</p>
--	---

When we discussed some of our ideas some interesting ideas were made. Bengtson is unsure if adjustment of lance direction with a motor due to wind direction is the way to go. He claims this will complicate the construction and that the droplets will go the way the wind blows independently of start direction. Another way to solve this could be to switch horizontal direction by steps or have a wider angle of the nozzle and just shut the production if the wind speeds and direction reaches a critical value.



## C MATLAB code

```
1 %Angles that are iterated
2 angles = [];
3
4 for a = 0:9
5     angles = [angles, a*10];
6 end
7
8 [sz1, sz2] = size(angles);
9
10 %Arrays holding the results
11 air_times = []
12 hit_rates = [];
13
14 %Recieve results from main
15 for i = 1:sz2
16     [hit_rate, air_time] = main( angles(i));
17     hit_rates = [ hit_rates, hit_rate];
18     air_times = [ air_times, air_time];
19     strmin = ['Hit rate = ', num2str(hit_rate), '%, for nozzle angle of ', num2str( angles(i)
20     ) ), ' degrees' ];
21     disp(strmin)
22 end
23 %Plot result
24 figure
25 hold on
26 grid on
27
28 xlabel('Vertical angle [deg]', 'FontSize', 20)
29 ylabel('Air time [s]', 'FontSize', 20)
30 plot( angles, air_times )
31
32 hold off
```

Listing C.1: controller.m

```
1 function [hit_rate, t_avg] = main(v1)
```

```
2
3 %Air density
4 rho_air = 1.226;
5
6 %Earth's gravitation [m/s^2]
7 g = [0, 0, -9.81];
8
9 %Wind velocity
10 v_w = wind_configuration(0.5, 0, v1);
11 v = 60;
12
13 %Nozzle position and angles
14 H = 7.0;
15 alpha = (v1/360) * 2 * pi;
16 %beta = (0/360) * 2 * pi;
17
18 %Time
19 h = 0.002;
20 t0 = 0;
21
22 %Distance from track
23 distance = 1;
24
25 %Intermediate positions
26 pos_x = [];
27 pos_y = [];
28 pos_z = [];
29
30 %flat fan angle
31 theta = (50/360) * 2*pi;
32
33 %Landing positions
34 end_x = [];
35 end_y = [];
36
37 %Fall times
38 fall_time = [];
39
40 %Hit rate
41 droplets_total = 0;
42 droplets_hit = 0;
43
```

```

44  n = 4; %number of nozzles
45  for i = 1:n
46
47      H_i = H;
48      beta_i = [80, 45, -45, -80] * (1/360) * 2 * pi;
49      for j = 1:1000
50          alpha_j = random('unif', alpha - pi/24, alpha + pi/24);
51          beta_j = normrnd(beta_i(i), theta/4); %normal
52          %beta_j = random('unif', beta - (theta/2), beta + (theta/2)); %
53          %uniform distribution of droplets
54          [p0, v_i] = nozzle_configuration(H_i, v, alpha_j, beta_j); %[
55          %Height, exitation speed, horizontal angle, rotational angle]
56
57          %Creating a droplet with radius R
58          [R, rho_water] = droplet;
59
60          [ pos_xn, pos_yn, pos_zn, tn ] = euler_solver(g, v_i, p0, h, v_w, R, rho_air,
61          rho_water, 0);
62
63          pos_x = [pos_x, pos_xn ];
64          pos_y = [pos_y, pos_yn ];
65          pos_z = [pos_z, pos_zn ];
66
67          end_x = [ end_x , pos_x(end) ];
68          end_y = [ end_y , pos_y(end) ];
69
70          fall_time = [fall_time, tn];
71
72          %Calculating hit rate
73          droplets_total = droplets_total + 1;
74
75          if pos_x(end) > distance && pos_x(end) < distance + 5
76              droplets_hit = droplets_hit + 1;
77          end
78      end
79  end
80
81  hit_rate = (droplets_hit / droplets_total) *100;
82
83  t_avg = mean(fall_time);

```

```

82
83 avg_X = mean(end_x);
84 avg_Y = mean(end_y);
85
86 strmin = {'Hit rate = ', num2str(hit_rate), '%'}, ['Avg. position = ', num2str(avg_X),
87 ', ', num2str(avg_Y), '']};
88
89 stravgpos = ['Avg. position = ', num2str(avg_X), ', ', num2str(avg_Y), ''];
90
91 %
92 % %PLOTS OF THE PATH AND LANDING PROJECTION
93 %
94 % pbaspect([1 1 1])
95 % f = plot3(pos_x, pos_y, pos_z, '.');
96 % f.Color = 'c';
97 % f.MarkerSize = 1;
98 % xlabel('x')
99 % ylabel('y')
100 % zlabel('Height')
101 % text(2,8, strmin, 'HorizontalAlignment', 'left');
102 % grid on
103 % axis equal
104 % hold on
105 % %plot(end_x, end_y, 'O')
106 % rectangle('Position', [distance -12 5 24], 'FaceColor', [0.5,0.5,0.5])
107 %
108 % hold off
109 %
110 % figure
111 % hold on
112 % xlabel('x [m]')
113 % ylabel('y [m]')
114 % axis equal
115 % grid on
116 % text(7,0, strmin, 'HorizontalAlignment', 'left');
117 % text(7,-0.5, stravgpos, 'HorizontalAlignment', 'left');
118 % rectangle('Position', [distance -12 5 24], 'FaceColor', [0.9,0.9,0.9])
119 % plot(end_x, end_y, 'O', 'MarkerEdgeColor', uint8([0 80 158]))
120 % hold off

```



121 end

## Listing C.2: main.m

```

1 function [pos_x, pos_y, pos_z, tn] = euler_solver( g , v0, r0, h, v_w, R_0, rho_air ,
    rho_water, t0)
2
3 %CALCULATED INITIAL CONSTANTS
4 m_0 = (4/3)*pi* R_0^3 * rho_water;
5 A_n = R_0^2 * pi;
6
7 %UPDATED CONSTANTS
8 tn = t0;
9 vn = v0;
10 rn = r0;
11
12 Re_0 = Re(R_0, vn);
13 Re_n = Re_0;
14 C_d0 = drag_coefficient_of(Re_n);
15 C_d = C_d0;
16
17
18 C_0 = - ((1/2) * C_d * rho_air * A_n) / m_0;
19 C_n = C_0;
20
21 %Lists of intermediate positions
22 pos_x = [ r0(1) ];
23 pos_y = [ r0(2) ];
24 pos_z = [ r0(3) ];
25
26 while rn(3) > 0
27     [tn, vn, rn] = onestep_euler(C_n, g, tn, vn, rn, h, v_w);
28     if norm(rn) > 50
29         rn(1) = 0;
30         rn(2) = 0;
31         rn(3) = -0.01;
32     end
33     %JPTADINT List of intermediate position
34     pos_x = [pos_x, rn(1)];
35     pos_y = [pos_y, rn(2)];
36     pos_z = [pos_z, rn(3)];
37
38     Re_n = Re( R_0, vn);

```

```

39     C_d = drag_coefficient_of(Re_n);
40     C_n = - ((1/2) * C_d * rho_air * A_n) / m_0;
41     end
42 end

```

Listing C.3: euler\_solver.m

```

1 function [tnext, vnext, rnext] = onestep_euler(C, g, tn, vn, rn, h, v_w)
2 tnext = tn + h;
3
4 vnext = vn + (h * (C * norm(vn - v_w) * (vn - v_w))) + (h*g);
5
6 rnext = rn + (h * vn);
7 end

```

Listing C.4: onestep\_euler.m

```

1 function [R, rho_water] = droplet
2 %radius [m]
3 R = normrnd(150, 70) * 10^(-6);
4 if R < 0
5     R = 1 * 10^(-6);
6 end
7 rho_water = 960;
8 end

```

Listing C.5: droplet.m

```

1 function [ v_w ] = wind_configuration( v, alpha, beta)
2
3 alpha_r = (alpha / 360) * 2*pi;
4 beta_r = (beta / 360) * 2*pi;
5
6 v_xy = v * cos( alpha_r );
7 v_x = v_xy * cos( beta_r );
8 v_y = v_xy * sin( beta_r );
9 v_z = v * sin( alpha_r );
10
11 v_w = [v_x, v_y, v_z];
12 end

```

Listing C.6: wind\_configuration.m

```

1 function [ r_0, v_0 ] = nozzle_configuration( h, v, alpha, beta)

```

```

2 r_0 = [0,0,h];
3
4 v_xy = v * cos( alpha );
5
6 v_x = v_xy * cos( beta );
7 v_y = v_xy * sin( beta );
8 v_z = v * sin( alpha );
9
10 v_0 = [v_x, v_y, v_z];
11
12 end

```

Listing C.7: nozzle\_configuration.m

```

1 function[ Re_n ] = Re(R, vn)
2
3 mu = 1.783 * 10^(-5); %[kg/m*s]
4 V_inf = norm(vn); %[ m / s ]
5 rho_air = 1.226; %[kg/m^3]
6 Re_n = ( rho_air * V_inf * 2*R )/ mu;
7
8 end

```

Listing C.8: Re.m

```

1 function[ C_d ] = drag_coefficient_of(Re_n)
2 C_d = ( 24 / Re_n ) + ((2.6 * (Re_n / 5)) / ( 1 + (Re_n / 5)^(1.52))) + ( (0.411 * ( Re_n /
   (2.63 * 10^5) ) ) / ( 1 + ( Re_n / (2.63 * 10^5))^(-8) ) ) + (( 0.25 * ( Re_n / (10^6)
   ) ) / ( 1 + ( Re_n / 10^6 ) ));
3 end

```

Listing C.9: drag\_coefficient\_of.m



## **D Comparison of The Analytic Model to the Master Thesis of Shea (1999)**

	Physical Experiment conditions					
Test nr.	Tower angle [degrees]	Height (m)	Horizontal throw angle	Vertical throw angle	Wind direction	Avg wind speed [m/s]
2a	80	10.81	0	45	-45	2.01
2b	80	10.81	0	45	-45	2.01
2c	80	10.81	0	45	-45	2.01
2d	80	10.81	0	45	-45	2.01
4a	35	6.29	0	0	125	1.56
4b	35	6.29	0	0	125	1.56
4c	35	6.29	0	0	125	1.56
4d	35	6.29	0	0	125	1.56
7a	35	6.29	60	0	-80	2.01
7b	35	6.29	60	0	-80	2.01
7c	35	6.29	60	0	-80	2.01
7d	35	6.29	60	0	-80	2.01
10a	35	6.29	-45	0	-80	1.34
10b	35	6.29	-45	0	-80	1.34
8a	75	10.60	0	40	180	1.34
8b	75	10.60	0	40	180	1.34

Model Parameter values			Comparison of Results
Droplet $\mu$ [ $\mu\text{m}$ ]	Droplet $\sigma$ [ $\mu\text{m}$ ]	Fan distribution	Hit area (The center has been calculated as the average x- and y-values of all the droplets.)
200	50	Normal	Center at about (x = 14.1, y = -10.3), vs (x = 18, y = -9.7) from the experiment.
300	50	Normal	Center at about (x = 15.3, y = -8.7), vs (x = 18, y = -9.7) from the experiment.
300	50	Uniform	Center at about (x = 15.3, y = -8.7), vs (x = 18, y = -9.7) from the experiment.
300	100	Uniform	Center at about (x = 14.3, y = -10.4), vs (x = 18, y = -9.7) from the experiment.
200	50	Uniform	Center at about (X = 1.5, Y = 4.5), vs (x = 9.14, y = 5.49) from the experiment.
300	50	Normal	Center at about (x = 6.9, y = 2.8), vs (x = 9.14, y = 5.49) from the experiment.
300	50	Uniform	Center at about (x = 6.5, y = 3.1), vs (x = 9.14, y = 5.49) from the experiment.
300	70	Normal	Center at about (x = 7.4, y = 3.9), vs (x = 9.14, y = 5.49) from the experiment.
200	50	Normal	Center at about (x = 3.6, y = -2.4). This is short in the x-direction, and too negative in the y-direction. This indicates that the droplets are small compared to those in the experiment
250	50	Uniform	Center at about (x = 4.3, y = 0.5). This is short in the x-direction, but good in the y-direction. This indicates that the droplets are small compared to those in the experiment
300	50	Normal	Center at about (x = 5.5, y = 3.2). This is short in the x-direction, and a little too long in the y-direction. This indicates that the droplets are not as affected by the wind as in the experiment. It could be, however, that the wind direction varied in the experiment.
300	70	Uniform	Center at about (x = 5.5, y = 3.1). This is short in the x-direction, and a little too long in the y-direction. This indicates that the droplets are not as affected by the wind as in the experiment. It could be, however, that the wind direction varied in the experiment.
300	50	Uniform	Center at about (7.59, -10.21). Short in both directions (X = 9.1, Y=-18.3 in the experiment)
300	70	Uniform	Center at about (7.57, -10.25). Short in both directions (X = 9.1, Y=-18.3 in the experiment)
300	50	Uniform	(x = -0.64, y = 0.06). Too much affected by the wind. Could be that the average wind in the experiment was less than the median value.
300	70	Uniform	(x = -0.56, y = 0.04). Too much affected by the wind. Could be that the average wind in the experiment was less than the median value.

Spread	Avg. fall time [s]	Comment
Too little.	7.45	The center of the hit area matches with the experiment. The spread of the droplets is too small. Sufficient air time.
Too little, but more even.	5.97	The center of the hit area matches with the experiment. The spread of the droplets is too small. Sufficient (a bit small) air time.
Too little, especially in the y-direction.	5.99	The center of the hit area matches with the experiment. The spread of the droplets is too small. Sufficient (a bit small) air time.
Too little, especially in the y-direction.	6.39	The center of the hit area matches with the experiment. The spread of the droplets is too small, especially in the y-direction. Sufficient air time.
Too little.	3.66	The center of the hit area does not match very good with the experiment. The spread of the droplets is too small. Short air time. Not so short compared to height.
Too little, but better shaped.	2.51	The center of the hit area does not match very good with the experiment. The spread of the droplets is too small. Short air time.
Too little.	2.50	The center of the hit area does not match very good with the experiment. The spread of the droplets is too small. Short air time.
Better.	2.58	The center of the hit area matches better with the experiment. The spread of the droplets is better, but the air time is short.
Fits well with the 4th contour line.	3.46	The center of the hit area does not match with the experiment. The spread of the droplets is better, but the air time is short. The reason the wind is not represented well in the model for this case can be the varied wind in the experiment, which lasted for about 10 minutes.
Fits well with the 4th contour line.	2.82	The center of the hit area does not match very well with the experiment. The spread of the droplets is better, but the air time is short.
Fits well with the 4th contour line.	2.47	The center of the hit area does not match very well with the experiment. The spread of the droplets is better, but the air time is short.
Fits well with the 4th contour line. Can easily spot the shape of the flat fan.	2.53	The center of the hit area does not match very well with the experiment. The spread of the droplets is better, but the air time is short.
Fits well with the 5th contour line. Can easily spot the shape of the flat fan.	2.44	The center of the hit area does not match very well with the experiment. The spread of the droplets is better, but the air time is short.
Fits well with the 5th contour line. Can easily spot the shape of the flat fan.	2.57	The center of the hit area does not match very well with the experiment. The spread of the droplets is better, but the air time is short.
Fits well with the 1st contour line.	5.82	The center of the hit area does not match very well with the experiment. The spread of the droplets is better. Sufficient air time. There does not seem to be a very big difference between standard deviation of 50 and 70.
Fits well with the 1st contour line.	5.91	The center of the hit area does not match very well with the experiment. The spread of the droplets is better. Sufficient air time.



## **E Concept testing**

Concept 1- Test Nr	Wind speed (m/s)	Wind direction	Nozzle angle h=horizontal, v=vertical	Drop size (um)	Air time (s)	Hit rate (%)	Comment
1	0	0	0	200	4,26	77,3	Airtime is too little.
2	0	0	v=45	200	6,17	88,5	Airtime is better, but still too low for this drop size.
3	0	0	v=45	150	7,45	68,9	Airtime is sufficient, but the hit rate is low.
4	0	0	v=25	150	6,75	90	Airtime is sufficient, the hit rate is good
5	0	0	v=25 h=25	150	6,75	81,1	Larger horizontal angle makes the snow enter outside the track.
6	1	0	v=25	150	6,08	0	
7	1	0	h=45	150	5,09	25,1	
7b	1	0	h=90	150	5,1	93,8	Good hit rate by adjusting the nozzle to 90 degrees.
8	1	45	0	150	5,12	61,7	
9	1	45	h=45	150	5,07	96,2	The hit rate is excellent when the nozzle is moved in the same direction as the wind.
10	1	45	v= 25 h=45	150	6,05	81,6	
11	1	90	v=25	150	6,05	90,5	Best hit rate is achieved when the nozzle is perpendicular to the wind.
12	1	90	v=25 h=45	150	6,05	59,9	
13	1	135	v=25	150	6,05	0,5	
14	1	135	v=25 h=45	150	6,05	0	It did not help to turn the nozzle in the horizontal direction.
15	1	135	v=-25 h=0	150	4,2	6,7	It did not help to angle the nozzle down, and the airtime got worse than before.
16	1	180	0	150	5,1	0,6	
17	1	180	v=-25	150	4,26	1,6	

Concept 2- Test Nr	Wind speed (m/s)	Wind direction	Nozzle angle h=horizontal , v=vertical	Drop size (um)	Air time (s)	Hit rate (%)	Comment
1	0	0	0	150	5,62	93,2	Airtime is sufficient and the hit rate is good.
2	0	0	v=25	200	5,4	79,7	This nozzle size is better for colder temperatures.
3	0	0	v=45	250	5,33	81,6	Some of the droplets deposited on the other side of the track.
4	0	0	h=45	150	6,63	62,2	
5	0	0	h=45 v=25	200	5,51	81,4	
6	0	0	h=45 v=45	250	5,35	86,5	
7	1	0	0	150	5,07	0	Droplets deposited at 8-10m.
8	1	0	h=90	150	5,1	93,8	Good hit rate by adjusting the nozzle 90 degrees horizontally.
9	1	0	v=25	200	5,05	0	
10	1	0	v=25 h=90	200	5,07	89,4	
11	1	0	v=45	250	5,19	0	
12	1	0	v=45 h=90	250	5,13	92	
13	1	45	0	150	5,13	61,7	
14	1	45	h=45	150	5,08	96,8	
15	1	45	v=25	200	5,11	0,8	
16	1	45	v=25 h=45	200	5,07	50,9	
17	1	45	v=25 h=65	200	5,06	89,1	
18	1	45	v=45	250	5,16	1,2	
19	1	45	v=45 h=65	250	5,15	93,6	
20	1	90	0	150	5,09	93,9	
21	1	90	v=25	200	5,02	80,9	
22	1	90	v=25 h=45	200	5,07	81,1	
23	1	90	v=45	250	5,14	81,5	
24	1	135	0	150	5,12	4	For this small droplets, any wind against the nozzle will make droplets deposited behind the unit.
25	1	135	v=25	200	5,07	35,7	
26	1	135	v=45	250	5,12	41,8	Larger droplets give better hit rate in the headwind.
27	1	135	v=45 h=25	250	5,11	33,6	
28	1	180	0	150	5,14	0,3	
29	1	180	v=25	200	5,06	17,8	
30	1	180	v=45	250	5,06	17,6	At headwind, there would not be recommended to produce. The adjustment has little effect.

Concept 3- Test Nr	Wind speed (m/s)	Wind direction	Height (m)	Nozzle angle h=horizontal, v=vertical	Drop size (um)	Air time (s)	Hit rate (%)	Comment
1	0	0	9,8	v=35	150	8,66	99,4	
2	0	0	9,8	v=35	200	7,53	69,1	
3	0	0	9,8	v=35	250	5,78	29,2	Large droplets have a too long trajectory.
4	0	0	9,8	v=35 h=45	150	8,57	100	
5	0	0	9,8	v=35 h=45	200	6,96	90,1	
6	0	0	9,8	v=35 h=45	250	5,75	65,3	For this droplet size, a more extensive horizontal angle would give a better hit rate
7	0	0	7	h=73	150	5,64	91,8	
8	0	0	7	h=73	200	4,29	90,3	
9	0	0	7	h=73	250	3,31	85,4	The air time is too small.
10	1	0	9,8	v=35	150	7,76	0	The hit area is way beyond the track.
11	1	0	9,8	v=35	200	6,59	0	
12	1	0	9,8	v=35	250	5,56	0	
13	1	0	7	h=73	150	5,1	13,5	
14	1	0	7	h=73	200	4,07	33,5	
15	1	0	7	h=73	250	3,15	42,7	
16	1	45	9,8	v=35	150	7,7	0	Hit area is 2m beyond the track.
17	1	45	7	h=73	150	5,09	67,5	
18	1	45	7	h=73	200	3,93	66,8	
19	1	45	7	h=73	250	3,15	67,5	It looks like a larger horizontal angle (like 90) would give a better hit rate.
20	1	90	7	h=73	150	5,09	92,3	
21	1	90	7	h=73	200	3,99	88,8	
22	1	90	7	h=73	250	3,16	83,4	
23	1	135	7	0	150	5,15	60,8	Distance from track =-5m. The lance arm is reaching over the track and is producing on the other sides before the snow blows back into the track.
24	1	135	7	0	200	4,04	16	Distance from track =-5m.
25	1	135	7	h=73	200	4,01	25,8	
26	1	135	7	h=45	200	3,99	49,2	Distance from track =-4m
27	1	180	7	0	200	4,1	30,5	Distance from track =-5m
28	1	180	7	h=45	200	4,03	61,5	Distance from track =-4m. Also here the droplets are going to past the track blows back into it.

Concept 4- Test Nr	Wind speed (m/s)	Wind direction	Height (m)	Nozzle angle h=horizontal, v=vertical	Drop size (um)	Air time (s)	Hit rate (%)	Comment
1	0	0	5	v=-90	150	1,73	100	Way too little airtime, the nozzle angled down must be even smaller.
2	0	0	5	v=-90	100	4,93	100	
3	0	0	5	h=90	150	4,06	99,9	
4	0	0	9	h=90	150	7,13	99,8	
5	1	0	5	v=-90	100	4,02	23,3	
6	1	0	5	h=90	150	3,7	12,5	
7	1	45	5	v=-90	100	3,95	48,7	Wind at 45 gives poor hit rates.
8	1	45	5	h=90	150	3,69	43,4	
8a	1	45	5	h=-90	150	3,7	56,2	
9	1	90	5	v=-90	100	4,01	100	
10	1	90	5	h=90	150	3,67	99,2	Air time too small
11	1	90	9	h=90	150	6,5	99,3	
12	1	135	5	v=-90	100	3,95	49,9	
13	1	135	5	h=90	150	3,68	45,9	
13a	1	135	5	h=-90	150	3,7	34,2	Wind at 135 gives poor hit rates.
14	1	180	5	v=-90	100	3,89	20,9	
15	1	180	5	h=90	150	3,71	11,2	

Concept 5- Test Nr	Wind speed (m/s)	Wind direction	Nozzle angle h=horizontal, v=vertical	Drop size (um)	Air time (s)	Hit rate (%)	Comment
1	0	0	v=35	150	7,06	83,2	The trajectory is a little too short, and the airtime is sufficient.
2	0	0	v=25	150	6,77	89,3	
3	0	0	0	150	5,68	93,9	Hit rate is better, but the airtime is too low for entirely freezing.
4	0	0	h=45	150	5,58	63,5	
5	0	0	h=25	150	5,65	87,9	
6	0	0	v=35	200	6,05	85,8	Some drops are depositing on the other side of the track.
7	0	0	v=35 h=45	200	5,81	77,4	
8	0	0	v=35 h=25	200	5,77	87,7	
9	1	0	0	150	5,05	0	
10	1	0	h=45	150	5,12	21,1	
11	1	0	h=90	150	5,07	95,3	Nozzle angle at 90 gives much higher hit rate.
12	1	0	v=35 h=45	200	5,27	4,3	
12a	1	0	v=35 h=90	200	5,44	87,3	
13	1	45	0	150	5,04	59,6	
14	1	45	h=45	150	5,06	95,8	
15	1	45	h=90	150	5,07	92,9	
15a	1	45	h=-90	150	5,14	95,6	
16	1	45	v=35 h=45	200	5,51	50	
17	1	45	v=35 h=90	200	5,46	90,6	
17a	1	45	v=35 h=-90	200	5,44	91,8	
18	1	90	0	150	5,11	94,9	
19	1	90	h=45	150	5,11	67,3	
20	1	90	v=35	200	5,46	83,3	Droplets deposited on both sides of the track.
21	1	90	v=35 h=45	200	5,44	79,1	
22	1	135	0	150	5,14	3,5	
23	1	135	v=35	200	5,49	21,8	
24	1	180	0	150	5,1	0,6	
25	1	180	v=35	200	5,51	8,1	

# F Nozzle Data

<b>NF Flow Rates</b> Call BETE to verify spray angle performance at operating pressures above 5 bar. <i>Fan and Straight Jet, 0°, 15°, 30°, 50°, 65°, 80°, 90°, 110°, and 120° Spray Angles, 1/8" to 2" Pipe Sizes</i>												
Male Pipe Size	Nozzle Number	K Factor	LITERS PER MINUTE @ BAR								Equivalent Orifice Dia. (mm)	
			0.5 bar	0.7 bar	1 bar	2 bar	3 bar	5 bar	10 bar	30 bar		
1/8 or 1/4	NF01	0.228	0.16	0.19	0.23	0.32	0.39	0.51	0.72	1.25	0.66	
	NF015	0.342	0.24	0.29	0.34	0.48	0.59	0.76	1.08	1.87	0.79	
	NF02	0.455	0.32	0.38	0.46	0.64	0.79	1.02	1.44	2.49	0.91	
	NF025	0.569	0.40	0.48	0.57	0.81	0.99	1.27	1.80	3.12	1.02	
	NF03	0.683	0.48	0.57	0.68	0.97	1.18	1.53	2.16	3.74	1.09	
	NF04	0.911	0.64	0.76	0.91	1.29	1.58	2.04	2.88	4.99	1.32	
	NF05	1.14	0.81	0.95	1.14	1.61	1.97	2.55	3.60	6.24	1.45	
	NF06	1.37	0.97	1.14	1.37	1.93	2.37	3.06	4.33	7.49	1.57	
3/8 or 1/2	NF08	1.82	1.28	1.52	1.82	2.57	3.15	4.06	5.74	9.95	1.83	
	NF10	2.28	1.61	1.91	2.28	3.22	3.95	5.10	7.21	12.5	2.03	
	NF15	3.42	2.42	2.86	3.42	4.83	5.92	7.64	10.8	18.7	2.38	
	NF20	4.56	3.22	3.81	4.56	6.45	7.89	10.2	14.4	25.0	2.78	
	NF30	6.84	4.83	5.72	6.84	9.67	11.8	15.3	21.6	37.4	3.57	
	NF40	9.12	6.45	7.63	9.12	12.9	15.8	20.4	28.8	49.9	3.97	
	NF50	11.4	8.06	9.53	11.4	16.1	19.7	25.5	36.0	62.4	4.37	
	NF60	13.7	9.67	11.4	13.7	19.3	23.7	30.6	43.2	74.9	4.76	
3/8 or 1/2	NF70	16.0	11.3	13.3	16.0	22.6	27.6	35.7	50.4	87.4	5.16	
	NF60	13.7	9.67	11.4	13.7	19.3	23.7	30.6	43.2	74.9	4.76	
	NF70	16.0	11.3	13.3	16.0	22.6	27.6	35.7	50.4	87.4	5.16	
	NF80	18.2	12.9	15.3	18.2	25.8	31.6	40.8	57.7	99.9	5.56	
	NF90	20.5	14.5	17.2	20.5	29.0	35.5	45.9	64.9	112	5.95	
	NF100	22.8	16.1	19.1	22.8	32.2	39.5	51.0	72.1	125	6.35	
	NF120	27.3	19.3	22.9	27.3	38.7	47.4	61.1	86.5	150	6.75	

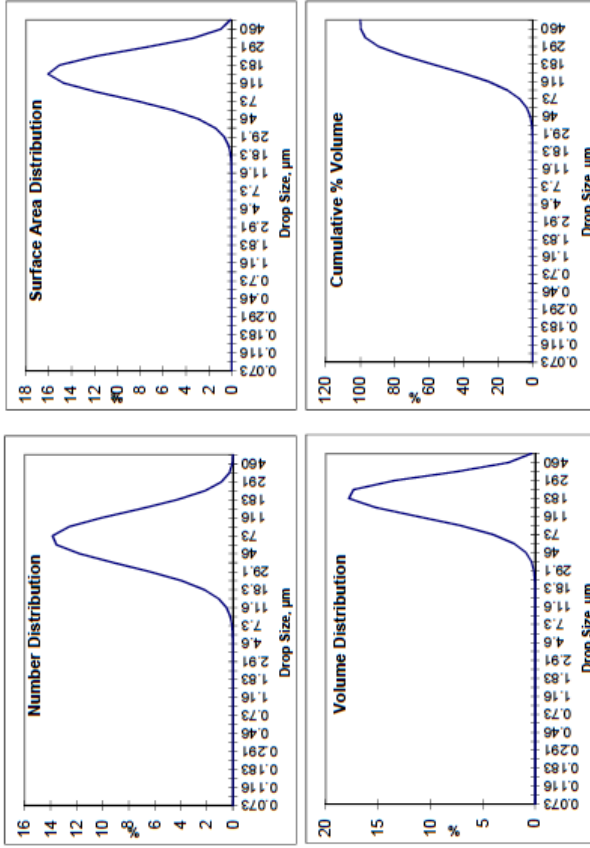
Figure F.1: Overview of NF nozzles

# BETE

Applications Engineering Department  
Estimated Droplet Size Information

Sondre Auganes  
App # 173356  
NF 15.50 at 30 bar

SG= 1  
1 cP  
18.7 l/min  
D32=160  
DV0.5=180  
DV0.1=90  
DV0.9=320



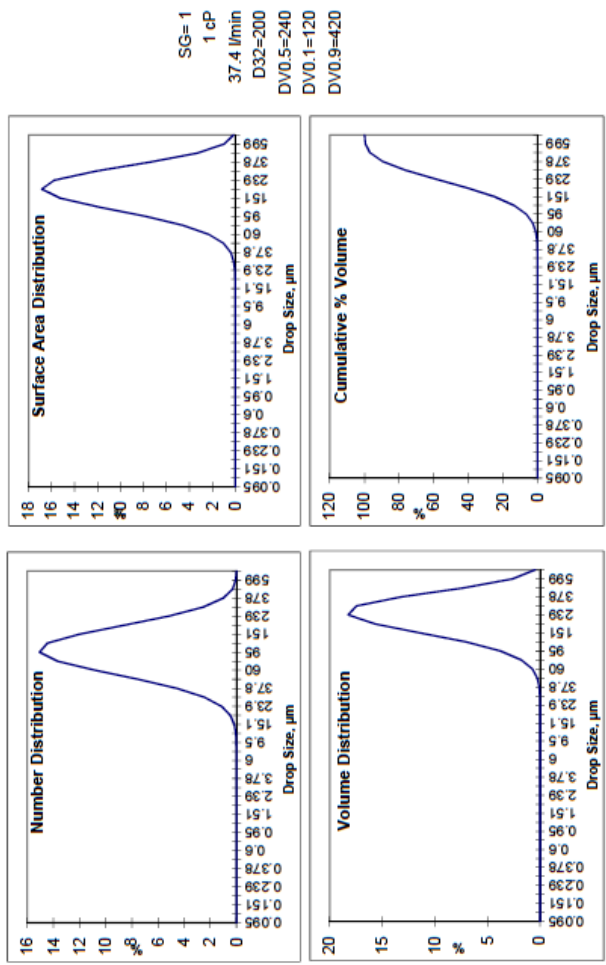
source: automatic

Note: Droplet Sizes are in Microns

Figure E.2: Drop size distribution NF15



Sondre Auganes  
App #173356  
NF 30 50 at 30 bar



Note: Droplet Sizes are in Microns

source: automatic

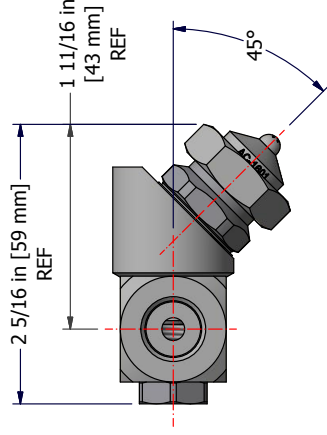
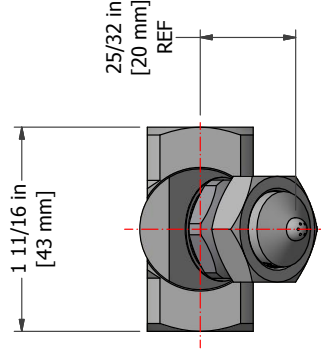
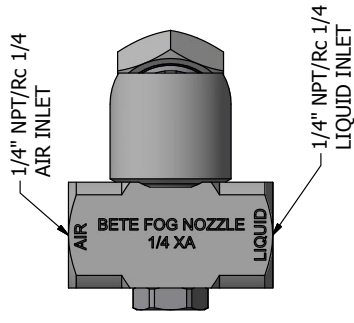
Figure E3: Drop size distribution NF30

**XA AD Set-up Flow Rates and Dimensions**  
*Pressure-fed, Internal Mix, Wide Angle Round Spray Pattern, 1/8" and 1/4" Pipe Sizes, BSP or NP T*

Pipe Size	Spray Set-Up Number	Fluid and Air Cap Numbers	0.7 Bar Liquid			1.5 Bar Liquid			2.0 Bar Liquid			3.0 Bar Liquid			4.0 Bar Liquid			Spray Dimensions						
			l/h	l/h	Mm <sup>3</sup> /h	Air (bar)	l/h	Mm <sup>3</sup> /h	Air (bar)	l/h	Mm <sup>3</sup> /h	Air (bar)	l/h	Mm <sup>3</sup> /h	Air (bar)	l/h	Mm <sup>3</sup> /h	Air	Bar	A	B	C	D	
1/8	AD 050	Fluid Cap FC4 & Air Cap AC1801	0.6	5.3	0.60	1.1	8.1	0.79	1.5	8.1	0.92	2.4	8.9	1.24	3.1	10.5	1.44	0.7	0.7	140	180	230	1.5	
			0.7	4.3	0.72	1.3	7.0	0.88	1.8	6.5	1.09	2.7	8.1	1.40	3.4	9.7	1.68	1.4	1.5	150	190	240	1.8	
			0.9	3.0	0.84	1.4	6.4	0.94	2.1	4.9	1.32	3.0	6.4	1.66	3.9	7.8	2.16	1.8	2.0	160	200	250	2.1	
1/8	AD 100	Fluid Cap FC2 & Air Cap AC1803	1.0	1.7	1.02	1.5	5.5	1.01	2.4	3.2	1.68	3.4	4.2	2.13	4.6	4.4	2.82	3.9	4.0	190	230	300	4.0	
			1.1	1.1	1.1	1.8	3.5	1.30																
			0.9	7.0	3.00	1.7	13.2	4.08	2.0	18.5	4.08	2.8	25.0	5.04	3.7	31.0	5.76							
1/8	AD 150	Fluid Cap FC2 & Air Cap AC1802	1.1	12.3	2.40	2.2	16.3	3.72	2.7	21.0	4.14	4.2	19.3	6.00	5.6	22.0	7.80							
			1.3	9.9	2.70	2.5	12.1	4.26	3.0	16.3	4.68	4.5	14.6	6.78	6.0	17.6	8.52							
			1.4	7.9	3.00	2.8	8.9	4.74	3.2	12.3	5.16	4.9	10.8	7.44	6.3	14.0	9.12	1.5	0.7	150	190	230	2.7	
1/4	AD 200	Fluid Cap FC1 & Air Cap AC1803	1.5	6.1	3.24	3.0	7.6	4.98	3.4	10.7	5.46	5.3	8.1	8.10	6.7	11.4	10.4	3.4	2.0	160	200	240	4.6	
			1.7	4.9	3.48	3.1	6.4	5.22	3.5	9.3	5.64	5.6	6.2	8.76	7.0	9.1	10.4	3.4	2.0	160	200	240	5.5	
			1.8	3.9	3.72	3.2	5.5	5.46	3.9	6.4	6.30	6.0	4.9	9.42	6.3	4.0	10.0	5.3	3.0	180	220	250	7.3	
1/4	AD 250	Fluid Cap FC1 & Air Cap AC1804	2.0	3.1	4.02	3.4	4.7	5.70	4.2	4.7	6.90	6.3	4.0	10.0										
			0.7	23.1	1.70	1.4	37.1	2.38	2.1	26.9	3.91	2.8	48.2	3.91	3.7	57.2	4.59							
			0.9	8.30	2.89	1.5	30.3	2.99	2.2	22.3	4.42	3.0	40.1	4.59	3.8	53.0	5.10	0.9	0.7	190	250	360	2.1	
1/4	AD 250	Fluid Cap FC1 & Air Cap AC1804	1.0	3.40	3.40	1.8	11.7	4.42	2.5	7.20	5.95	3.2	28.8	5.44	4.2	34.4	6.80	1.5	1.5	200	270	370	3.2	
			3.4	20.1	6.63	4.6	18.9	8.83	2.4	20.0	7.90	3.2	20.0	7.90	3.2	3.0	20.0	7.90	3.2	3.0	200	270	370	4.1
			3.5	15.5	7.14	4.9	7.90	10.7	3.9	4.0	10.0	3.7	7.80	8.33	5.6	59.8	14.7	2.0	0.7	200	250	330	5.5	
1/4	AD 250	Fluid Cap FC1 & Air Cap AC1804	2.1	7.60	8.16	3.2	19.3	10.9	3.9	24.5	12.6	6.3	14.8	18.0	7.0	33.9	18.9	3.9	2.0	200	280	370	8.2	
			2.3	4.20	8.63	3.5	12.9	11.9	4.6	11.0	15.0	6.7	7.00	19.2	6.0	3.0	230	290	380	9.1				
			2.4	2.60	9.17	4.2	1.50	14.1	4.9	6.40	16.0	7.0	1.20	20.1	6.3	4.0	240	320	400	10.4				

Figure F4: Overview of air atomizing nozzles

# **G Machine Drawings**



**NOTES:**

1. MATERIAL: NICKEL PLATED BRASS  
GASKETS: BLUE-GARD 3300
2. APPROX WEIGHT: 0.6 lbs [0.27 kg]

**BETE FOG NOZZLE, INC.**  
50 GREENFIELD STREET GREENFIELD, MASSACHUSETTS 01301

1/4" XA AD 050 W/ 45° ADAPTER

APPLICATION #173356

SCALE: 1:1  
DRAWN: JF  
DATE: 5/8/2018

DRAWING NUMBER: XA - 84960

REV -

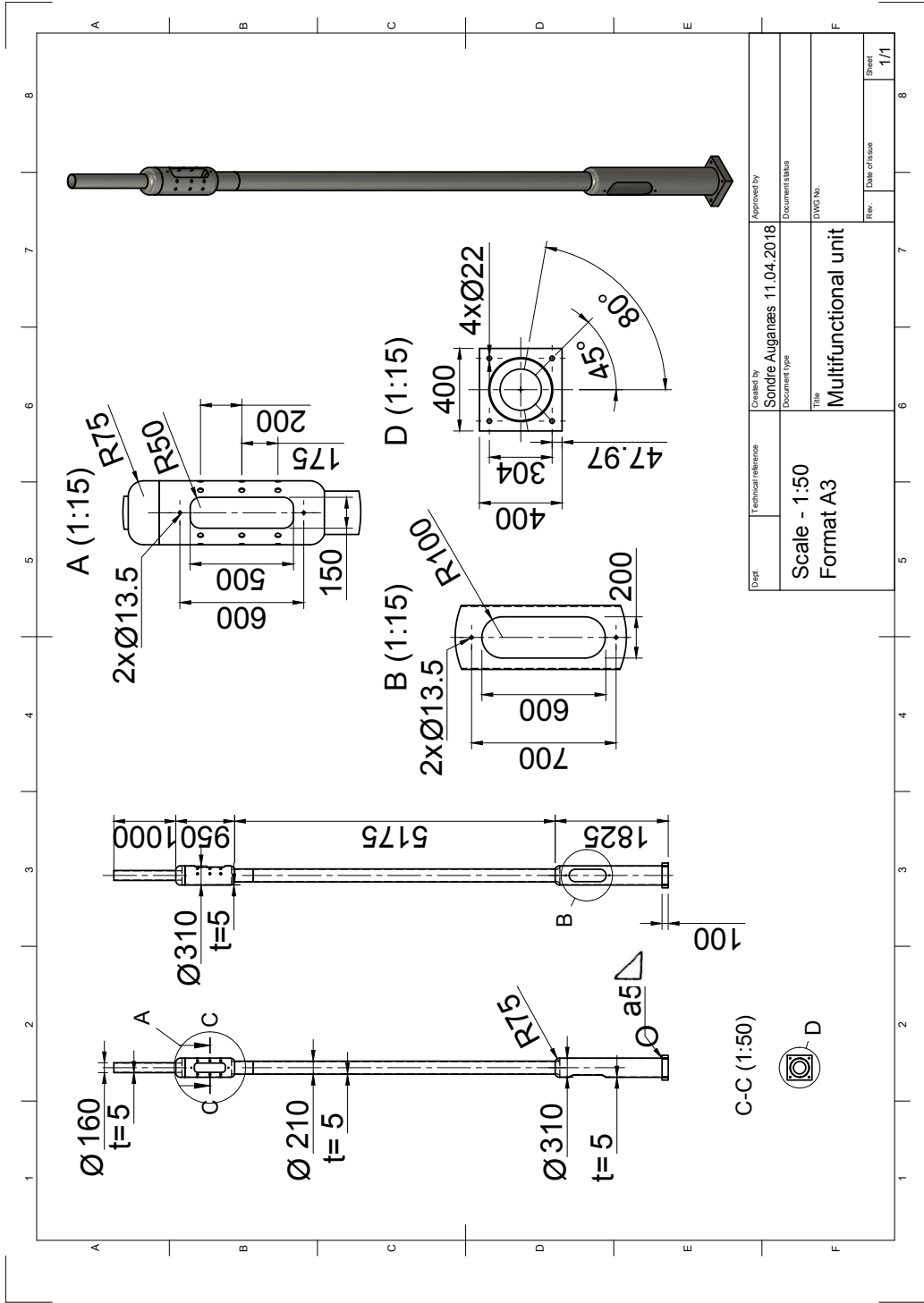
REV	DATE	BY	CHECKED	DCR

UNLESS OTHERWISE NOTED, REMOVE ALL BURRS AND SHARP EDGES

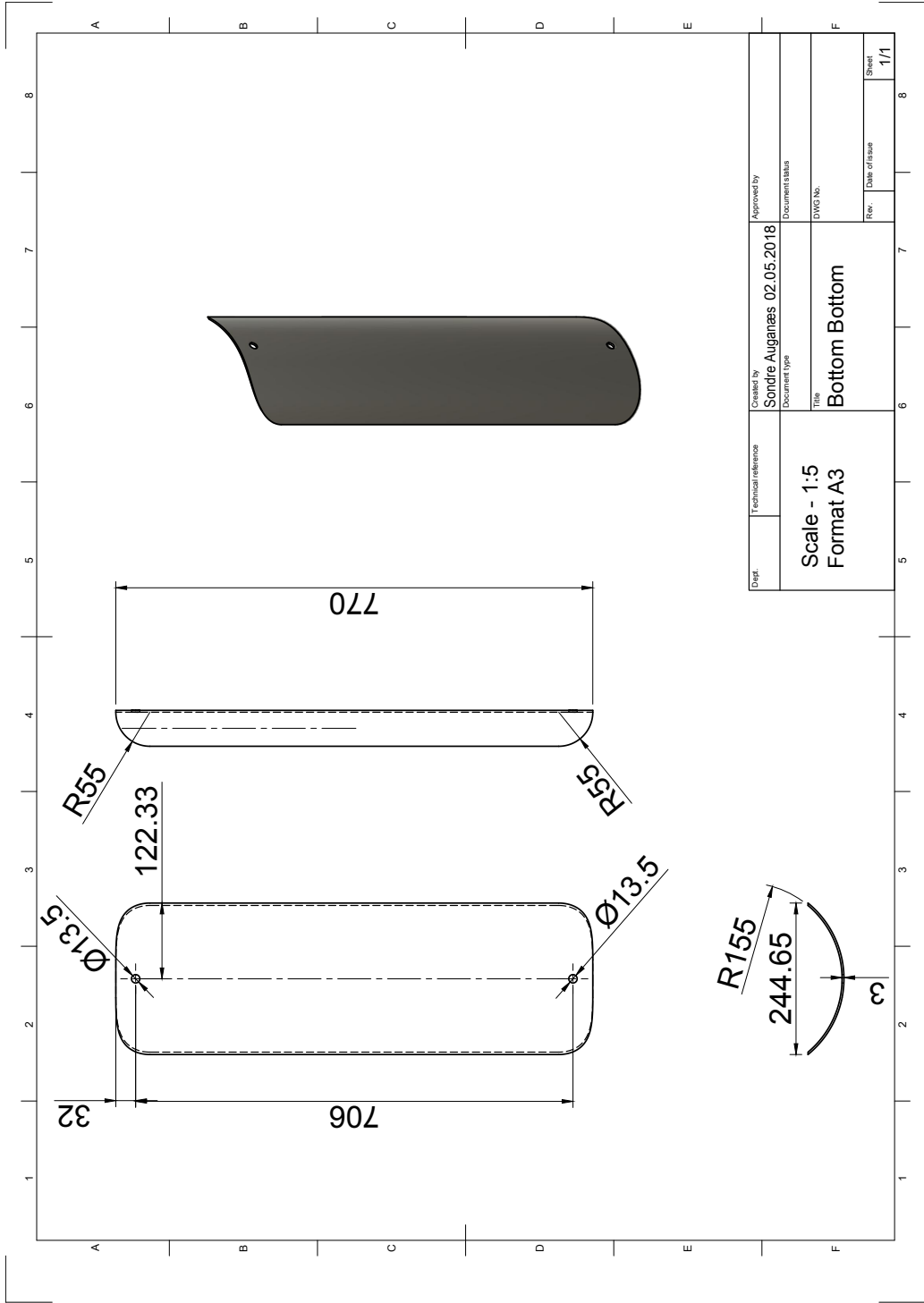
THIS PRINT CONTAINS PROPRIETARY INFORMATION WHICH MUST NOT BE USED FOR REPRODUCTION WITHOUT THE WRITTEN PERMISSION OF BETE FOG NOZZLE, INC. PRINT MUST BE RETURNED UPON REQUEST © BETE FOG NOZZLE, INC.

TOLERANCES: (EXCEPT AS NOTED)

MACHINED DIMENSIONS: ANGLES.....±10°  
FRACTIONAL.....±.002"  
TWO PLACE DECIMAL.....±.01"  
THREE PLACE DECIMAL.....±.005"  
CAST DIMENSIONS: UP TO 1".....±.010"  
FOR EACH INCH AFTER ADD ±.003" PER IN.  
METRIC: WHOLE NUMBER.....±.1mm  
ONE PLACE DECIMAL.....±.1mm  
TWO PLACE DECIMAL.....±.1mm

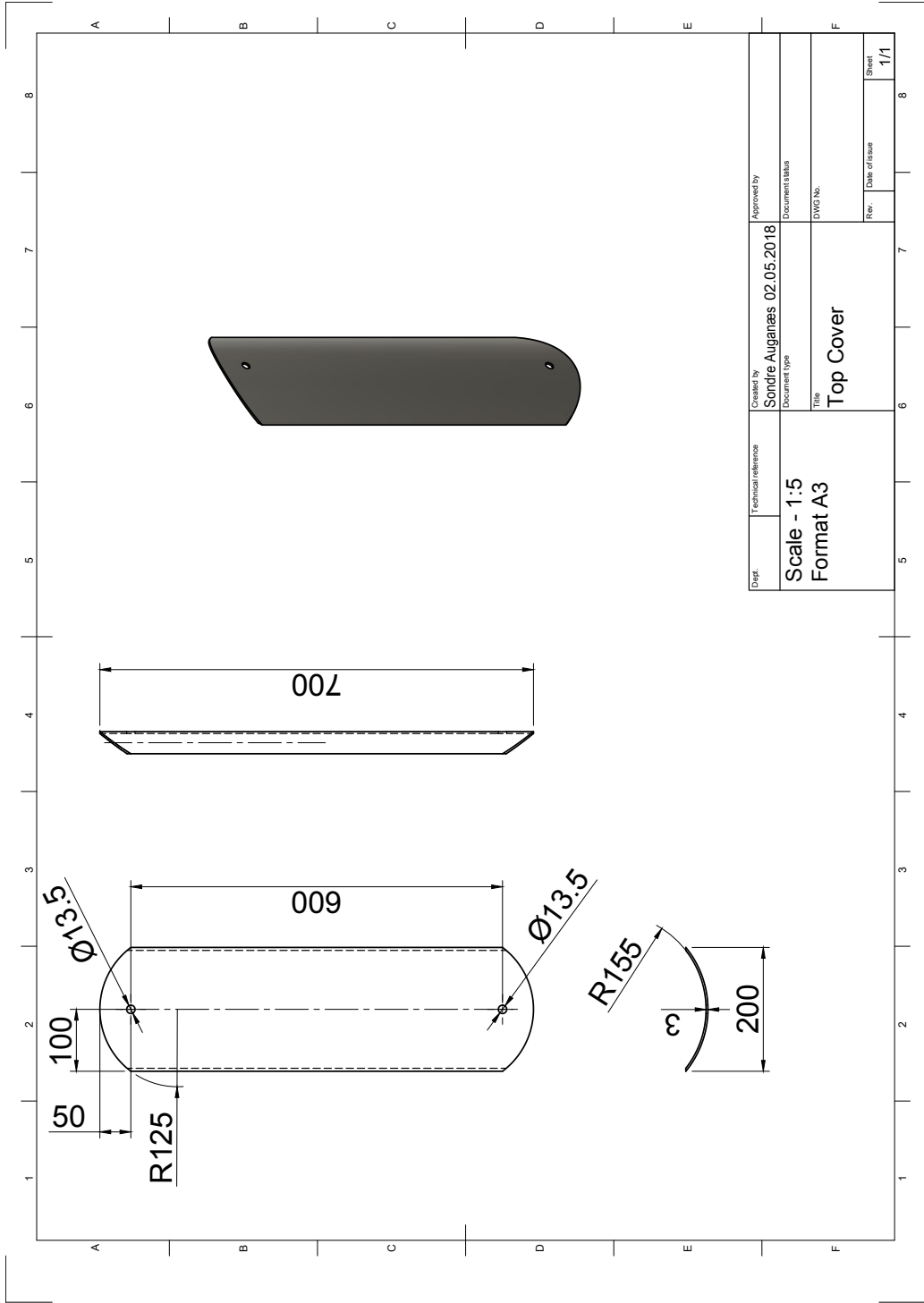


Dept.	Technical reference	Created by Sondre Auganæs 11.04.2018	Approved by
		Document type	Document status
		Title Multifunctional unit	DWG No.
		Rev.	Date of issue
			Sheet 1/1



Dept.	Technical reference	Created by <b>Sondre Auganaas 02.05.2018</b>	Approved by
		Document type	Document status
		Title <b>Bottom Bottom</b>	DWG No.
			Rev.
			Date of issue
			Sheet
			1/1

Scale - 1:5  
Format A3



Dept.	Technical reference	Created by	Approved by
	Scale - 1:5 Format A3	Sondre Auganæs 02.05.2018	Sondre Auganæs 02.05.2018
		Document type	Document status
		Title	DWG No.
		Top Cover	
		Rev.	Date of issue
			Sheet
			1/1





# H Light Armature from LADELYS



RoHS

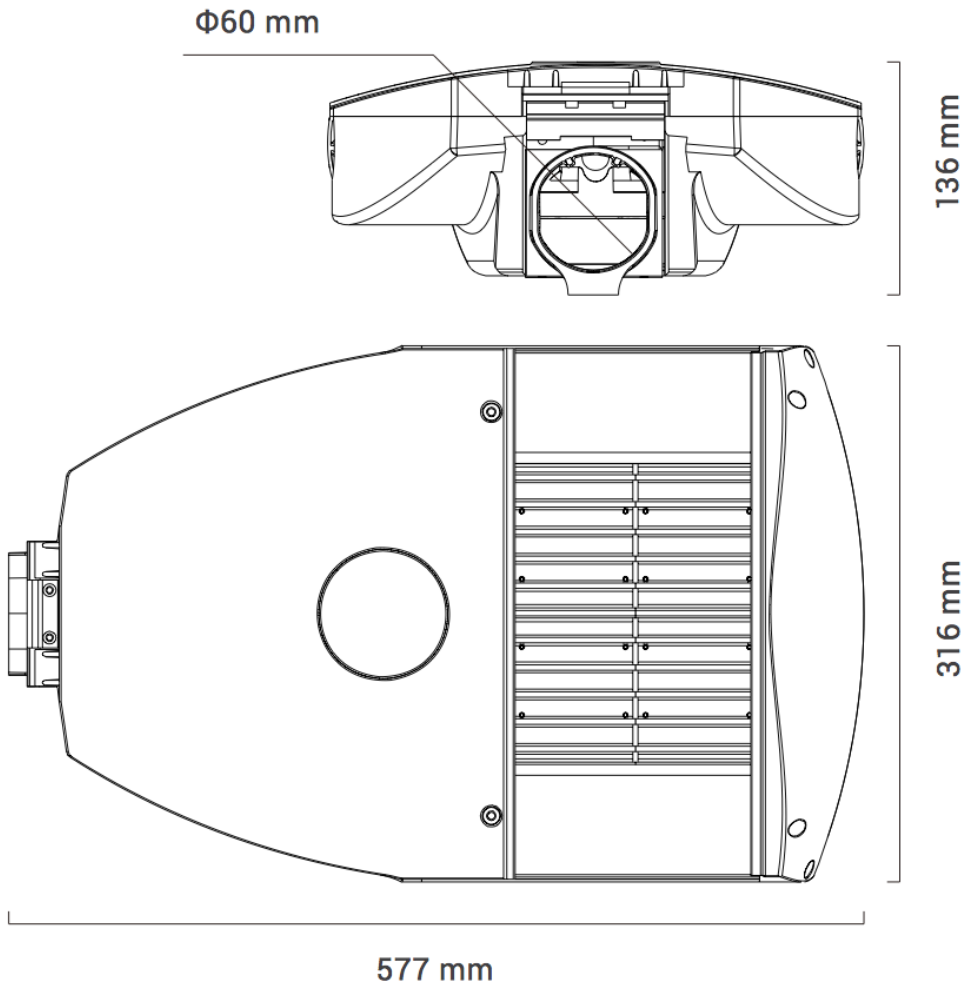


CB

RAL 9005

RAL 7042

RAL 9016



**5** ÅRS  
GARANTI

**IK08**

**IP  
66**

**DIMBAR**

**SENSOR**

**3000-  
3500k**

**4000-  
4500k**

**5000-  
5500k**

**6000-  
6500k**

### El-tekniske spesifikasjoner

Effekt LED	240W
Spenning	100-240V AC, 50/60Hz
Strøm	0.41A
Driftstemperatur	-40 oC til +50 oC

### Mekaniske spesifikasjoner

Levetid	100.000 Timer - L70, ved 25C
Armaturhus	Støpt aluminium
Kjøleribbe	Anodisert aluminium
Linse	Herdet glass
Dimenesjon	504 x316 x136 mm
Vekt	6.1 kg

### Lystekniske spesifikasjoner

Lysfluks	328400 lm
Lysutbytte	155 lm/W
Fargegjengivelse	Ra $\geq$ 75